A CLIMATOLOGY OF SOUTHWEST INDIAN OCEAN TROPICAL CYCLONES (1962-63 TO 1986-87)

by

JEFFREY SCOTT SITES, B.A.

A THESIS

IN

ATMOSPHERIC SCIENCE

Submitted to the Graduate Faculty
of Texas Tech University in
Partial Fulfillment of
the Requirements for
the Degree of

MASTER OF SCIENCE

Approved

Accepted

December 1989

ACKNOWLEDGEMENTS

I would like to thank Dr. Richard E. Peterson for his guidance and support during my stay at Texas Tech and in my research. My sincere thanks to Dr. Chia-Bo Chang and Dr. Kishor Mehta for taking the time to serve on my committee. I can not thank JoAnna Green enough for her help in getting data off of the magnetic tape. Thanks to Debbie Kerr for all the little things that she did to help get this thesis ready. I would also like to recognize my wife Sheila, for her love and encouragement during my time here, along with her help in typing this thesis. To my parents: Thank you for your years of support, which have allowed me to pursue my dreams. Finally, many thanks to all my friends who made my time at Texas Tech enjoyable.

TABLE OF CONTENTS

ABSTRACT

The objective for my thesis is to investigate the characteristics of tropical cyclones in the Southwest Indian Ocean. The region studied encompasses the area south of the equator, from 110°E west to the East African coast (about 25°E longitude).

Within the paths of Southwest Indian Ocean tropical storms are the islands of Mauritius, Reunion, and Madagascar, as well as the coast of East Africa, particularly Mozambique. Although little is heard of storms in this area, the frequency seems comparable to that in the Western Atlantic and many millions of lives are at risk; within this decade over 1000 people have been killed. Storms in this region have been noted since the early 1600's. With polar orbiting and, more recently, geosynchronous satellites providing imagery, the tracking of such tropical storms has become more reliable. The Indian Ocean has had many active sea routes over the centuries; in the present day, there is a large strategic importance for the area. Moreover, some of the developing countries affected by these storms have quite dense populations.

This thesis was carried out using data obtained on magnetic tape from the National Climatic Center (for activity through 1980) and from the Mariners Weather Log (particularly for the present decade). Additional data was requested from the very active national weather services of the regions. (The prior literature for storms in the area is rather meager, but French and British sources were identified.)

The Southwest Indian Ocean was subdivided into 2½° latitude by 2½° longitude blocks for the mapping of the storm characteristics. The frequency, tracks , stages of development and intensity changes were delineated. Particular attention was paid to the identification of preferred paths and to landfall statistics.

LIST OF TABLES

LIST OF FIGURES

CHAPTER 1

INTRODUCTION

Tropical cyclones in the Southwest Indian Ocean are not usually as big newsmakers as their cousins in other ocean basins throughout the world. Tropical cyclones in the North Indian Ocean are known for causing great flooding in Bangladesh, while tropical cyclones in the Northeast Pacific are known because of their large number per year and sometimes their great strength. Despite their relatively low profile, it appears that cyclones of the Southwest Indian Ocean have about the same frequency as hurricanes in the Northwest Atlantic. The Southwest Indian Ocean is generally considered to be the area south of the equator, from 110°E west to the East African coast (about 35°E longitude). Figure 1.1 shows the geography of the South Indian Ocean. The majority of the islands are scattered throughout the western half of the basin, the biggest being Madagascar. Madagascar, which has peaks over 2000 ft., sits just to the east of the African Mainland which protects it from many tropical cyclones. Other significant islands include Mauritius, Reunion, and Diego Garcia. The currents in the South Indian Ocean are shown in Figure 1.2. Some important features of Figure 1.2 are the split in the South Equatorial Current around Madagascar and the gyre just to the west of Australia. As will be seen in Chapter Three, the typical tropical cyclone tracks seem follow the basin's warm currents.

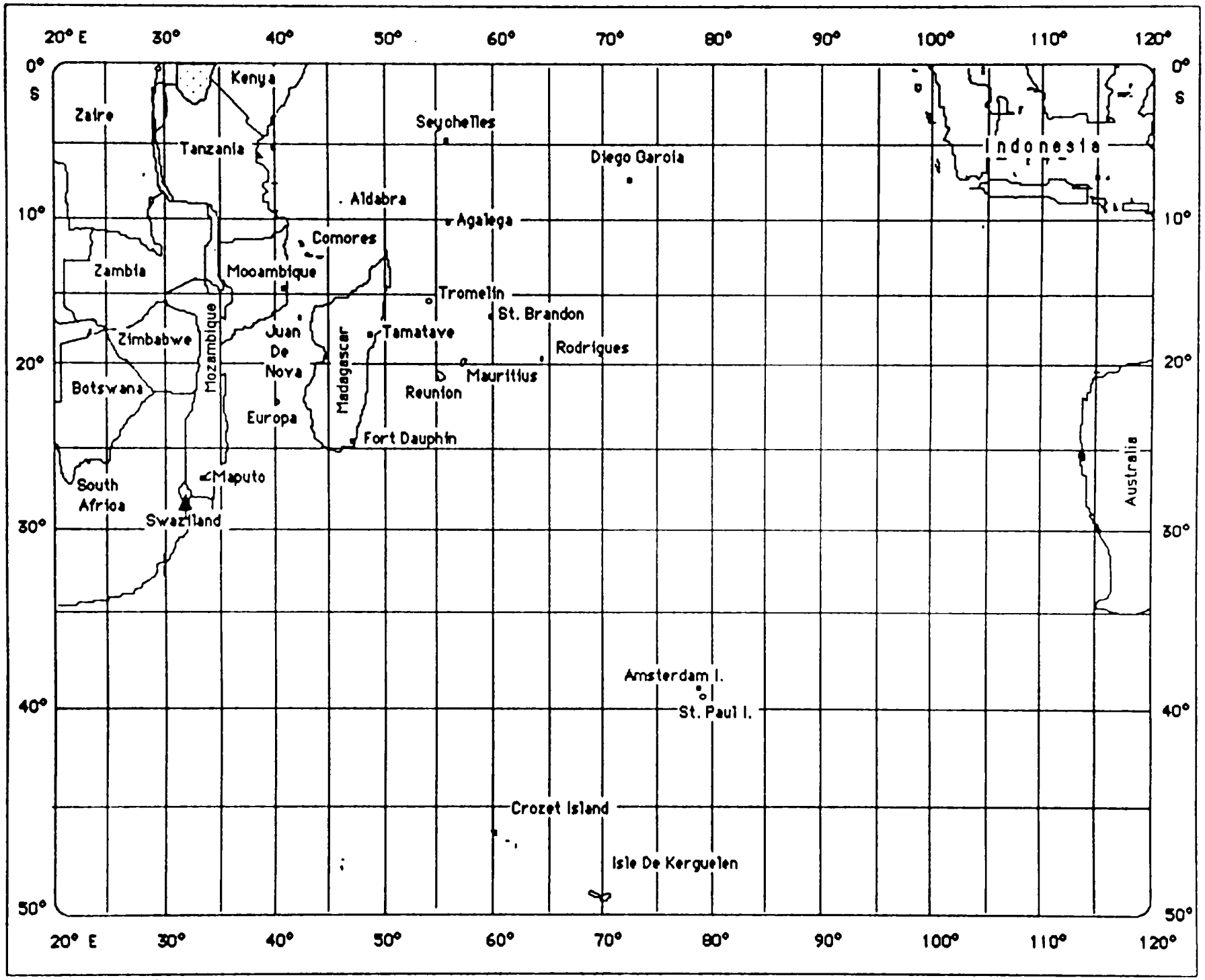

Figure 1.1. A geographical look at the Southwest Indian Ocean.

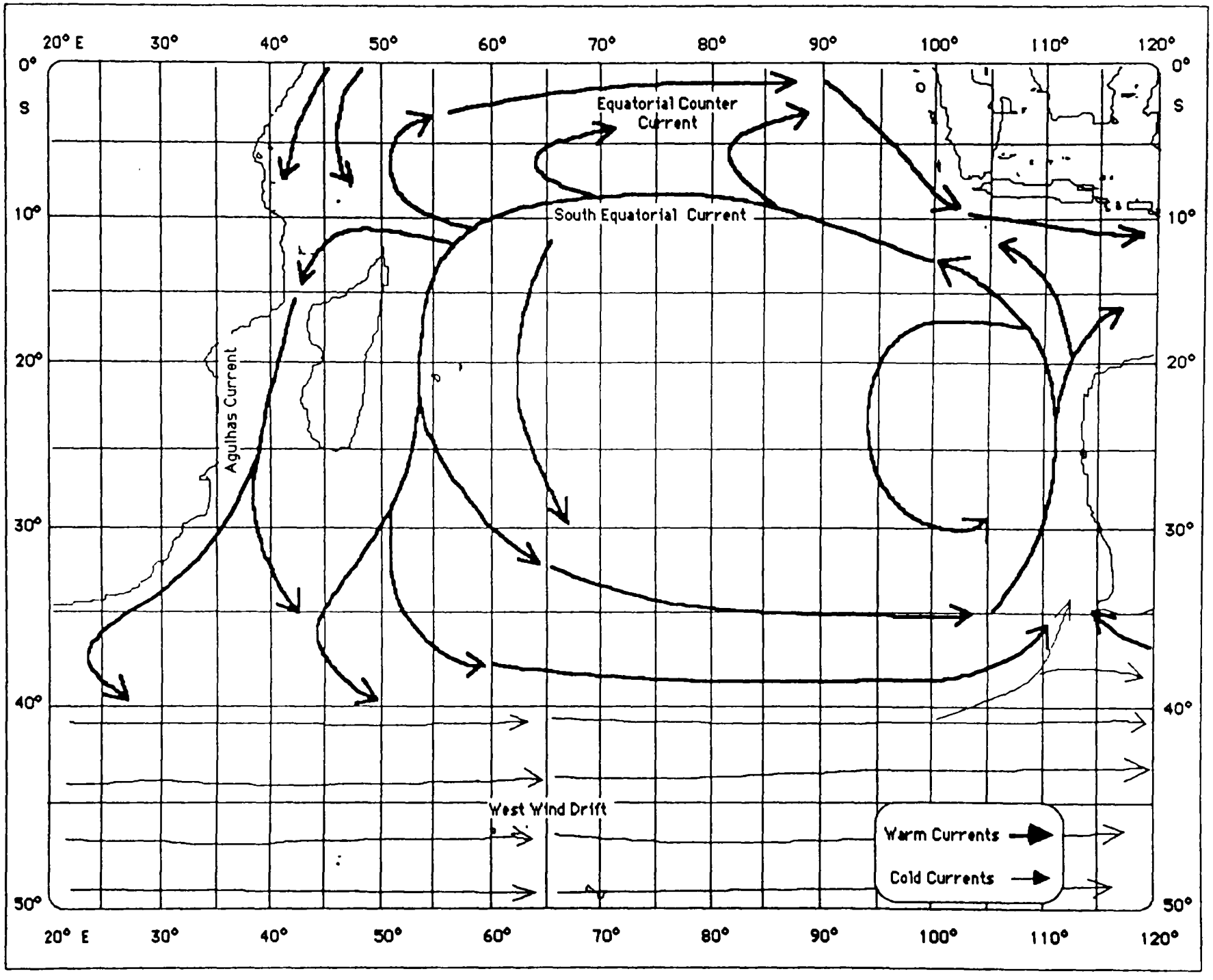

Figure 1.2. Currents in the South Indian Ocean.

1.1 Historical Background

Recognition of tropical cyclones dates back to the mariners of ancient Greece, with reference to them in both the Bible and in early Hindu writings (DeAngelis, 1970). It was not until 1831, with the publishing of William Redfield's theories, that tropical cyclones were studied scientifically (DeAngelis, 1970). Redfield upon studying trees that were blown down by the "Great September Gale of 1821," which hit the east coast of the United States, came to the conclusion that the storm had a rotary nature; this was contrary to the popular belief of the period that all storm winds were straight-line in nature. Redfield then began to study other hurricanes, using a method in which he collected and analyzed logs from ships which encountered these storms and then plotted surface maps using this data.

Redfield's writings inspired William Reid, a member of the Royal Engineers stationed at Barbados, to begin studying tropical cyclones. After studying hurricanes in the Atlantic, Reid moved his focus to the southern Indian Ocean. This study was the first scientific study of cyclones of the South Indian Ocean. After reading Reid's works, Dr. Alexander Thom, an English army surgeon living on Mauritius, wrote an analysis of the Rodrigues cyclone of April 1843. Thom was able to do an indepth analysis of the cyclone because 14 or 15 ships were caught in the storm for several days. With the ships' logs, Thom retraced the hurricane's path and analyzed the storm's characteristics. From this analysis, Thom wrote his book Nature and Course of Storms (1845).

Although scientific study of cyclones in the region began only in the 19th century, records of cyclones go well back into the early 1600's. One of the first reports was in the year 1615 from the island of Mauritius

which stated "Terrible Hurricane: the ship 'Peter's Booth' wrecked." Although a report this short and vague does not tell very much about the strength of the storm or total damage done, it does tell us about the frequency at which cyclones occurred during the pre-instrument era. One of the earliest reports with the mention of a minimum pressure was in 1818, with a recorded pressure of 950 mb, when the center of a cyclone passed very close to Mauritius; thereafter the first report of wind speed associated with a cyclone was in December 1857, as 62 mph winds were recorded (Payda, 1976).

The rest of this section will be summaries of selected Southwest Indian Ocean tropical cyclones that occurred during the past century, starting with the cyclone of April 1892. The cyclone of April 1892, which hit Mauritius on 29 Apr, was the most damaging storm to have struck Mauritius. It held this title for 68 years, until 1960. The cyclone of April 1892 took 1100 lives. The reason for the high death toll was the time of year of the storm (the cyclone season was nearing its end and the people were not expecting a storm of this magnitude), and then the storm took the island by surprise. Although the Royal Alfred Observatory had known on 27 Apr of " heavy weather to northward since the 24th," the wind and pressure remained unchanged throughout the 27th and therefore the first Assistant of the Observatory told the Acting Governor that there was no danger. On the morning of the 29th, the pressure had fallen to 29.58 inches (1001.62 mb) and was falling rapidly due to the approaching cyclone (winds at the time were from the east-northeast at 40 mph). By 11 AM the pressure had fallen to 993 mb, but the forecast still was for winds to not exceed 56 mph, but by 11:30 AM the telegraph system was knocked out of use, ending

any direct communication on the island. The center of the cyclone passed to the south of Port Louis (with a recorded pressure of 947 mb at Pamplemousses). The maximum one-hour mean wind speed was 76 mph, which would correspond to approximately a 135 mph gust, while a five-minute period saw a mean speed of 89 mph. These high speeds ended any more measurements as they knocked the anemometer out of service. Damage to Mauritius was extensive as houses had their roofs lifted off and their walls blown in, others had gaping holes exposing the inside of them to the full brunt of the rain and wind. Fires, which broke out in several parts of Port Louis due to the overturning of gas lights, hampered the efforts to free people trapped in the collapsed buildings. The trees that survived the storm were only part of their previous size, as most of their bark had been stripped away. The streets were lined with dead and dying bodies, which caused the air to be filled with the smell of human decomposition. Mauritians witnessed the extremes of damage a cyclone can accomplish (Payda, 1976).

Cyclone Carol (February 1960) surpassed the cyclone of 1892 as the most destructive cyclone to ever hit Mauritius. Its minimum pressure was measured at 942 mb as it passed over St. Brandon Island. Carol started as a low pressure area south of Diego Garcia on 20 Feb, then took a west-south-westerly track on the 21th and slowed down to begin an intensification period. As of 24 Feb Carol had become an intense cyclone and was positioned to the northwest of St. Brandon. On the morning of the 26th, the center passed over St. Brandon and then began recurving, which would take its track close to Mauritius. Carol passed directly over Mauritius on 28 Feb causing record gusts of 160 mph (there were estimates

that some locations might have had gusts up to 190 mph). Highest one-hour mean wind speeds at various locations were 83 mph at Medine, 82 mph at Pamplemousses and 78 mph at Union Flacq. Damage, other than to buildings, was to the sugar crop which was cut approximately in half, forest and fruit trees on the island were destroyed in quantities never seen before, 70,000 buildings were destroyed and 80,000 people were forced into shelters. The death toll from Carol was only 40, but this number might have been higher if not for several factors. First, Cyclone Alix had affected the west coast in January awakening the population to the destructive capability of a tropical cyclone. Second, Alix had damaged some of the weaker and older trees already, which made clean up quicker allowing help to get where it was needed. Last was the fact that it took Carol a full 48 hours to travel the distance from St. Brandon to Mauritius, which gave Mauritians time to prepare for the coming on-slaught (the fact that Carol had set a record pressure reading made many Mauritians take this storm seriously). Amongst all the destruction, Carol also left behind a beneficial aspect: the view that Mauritians could not continue to live in wooden-based structures in a cyclone-prone area; they realized that buildings needed to be of concrete base. With this in mind wooden structures still standing have slowly been replaced by concrete-based structures (Payda, 1976).

Severe Tropical Depression Domoina (January 1984) is an example that a tropical cyclone does not have to do its damage via strong winds, but that damage can be caused by its rainfall; some have called Domoina the most devastating tropical cyclone to have struck East Africa this century (Note: an explanation of the classifacation scheme is given in Chapter 2).

Domoina began as a mass of convective activity positioned east of Agalega on 11 Jan and by the 18th she had intensified to a moderate tropical depression. Domoina traveled southwest and crossed the east coast of Madagascar on the 21st, entering the waters of the Mozambique Channel on the 24th. She reintensified over the channel reaching her highest classification of severe tropical depression on the 26th. On the 29th Domoina again moved over land, as she entered Mozambique north of Maputo with a central pressure of 987 mb and winds gusting up to 67 mph. Domoina's remnants remained over land from the 29th through the 31th, then moved back over the waters of the Mozambique channel early on 1 Feb.

As Domoina moved over the African continent she caused heavy rains and flooding in Mozambique, Swaziland, and the Natal province of South Africa, killing 200 people. Figure 1.3 shows rainfall amounts for the area most affected by Domoina's landfall. Some of the most severe flooding was seen on the Mfolozi floodplain in South Africa and on the Maputo River in Mozambique. The flooding by the Mfolozi River cost farmers heavily, R150 million in damage and 420,000 tons of sugar cane were destroyed as large quantities of sand were deposited on top of their sugar cane fields, which were growing in the river's floodplain. A few miles upriver from St. Lucia the developed Mfolzi swamp was under seven to ten feet of sand (Greig, 1984). The flooding started a heated debate over the agricultural development of the river catchment. Areas of the catchment, which had been converted from low rolling floodplains and swamps to sugar cane fields were in some people's opinion overpopulated by peasant farmers and

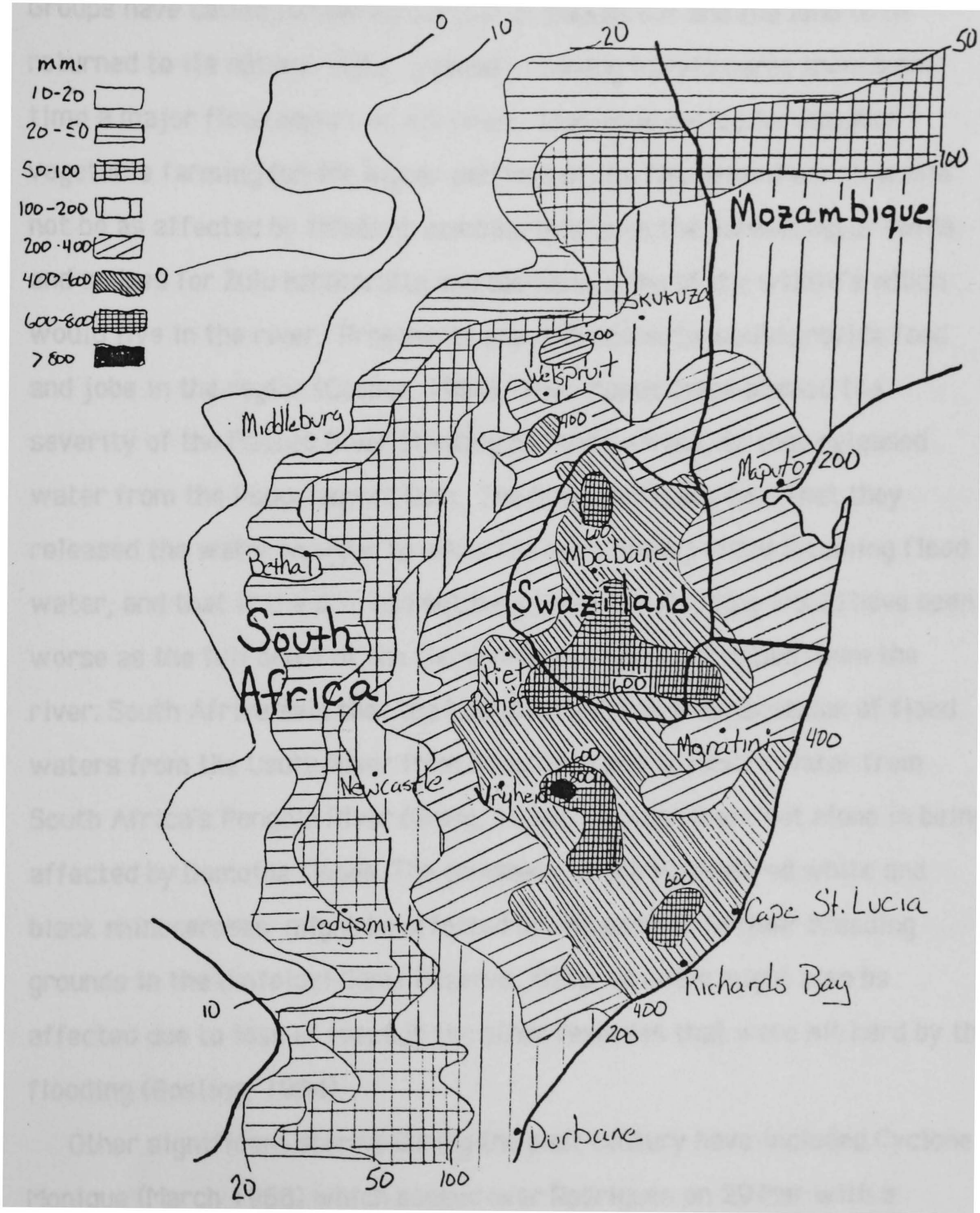

Figure 1.3. Rainfall amounts due to Domoina from 28 Jan to 1 Feb 1984.(After South African Weather Bureau Newsletter, 1984)

had a lack of surface vegetation, which added to the severity of the damage. Groups have called for the farmers to be bought out and the land to be returned to its natural state, instead of having to reimburse them every time a major flood occurs on the river. They have called for limited vegetable farming (on the higher portions of the floodplain) which would not be as affected by flooding, combine this with the harvesting of reeds and sedges for Zulu handicrafts and the harvesting of the wildlife which would live in the river. Proponents say this scenario would provide food and jobs in the region (Cooper, 1984). Then Mozambique blamed the severity of the Maputo River flooding on South Africa, as they released water from the Pongolapoort Dam. The South Africans said that they released the water in order to allow for more room to hold incoming flood water, and that if the dam had not been there the flooding would have been worse as the full brunt of the floodwaters would have rolled down the river. South Africa said that the Maputo flood was a combination of flood waters from the Usutu River from Swaziland and the extra water from South Africa's Pongolo River (Greig, 1984). Humans were not alone in being affected by Domoina floods. The comeback of the endangered white and black rhinoceroses might be affected by the damage to their breeding grounds in the Umfolozi Game Reserve. Other animals might also be affected due to loss of trees in the other reserves that were hit hard by the flooding (Gosling, 1984).

Other significant storms during the past century have included Cyclone Monique (March 1968) which passed over Rodrigues on 29 Mar with a minimum pressure recorded at 933 mb, which made her the strongest storm on record in the basin. Marechal, Rodrigues, experienced one-hour sustained

winds of 92 mph and gusts up to 173 mph. Monique's center did not, however, cross directly over Rodrigues, so estimates have put her actual lowest pressure below 930 mb. On 8 Mar, 1973, Cyclone Lydie passed over Tromelin with a pressure of 932 mb, putting her just behind Monique as the second most intense storm.

Cyclone Maud (April 1962) was one of the largest storms areawise ever in any basin as she had gales extending out 300 miles and cyclone strength winds out 150 miles. Southwest Indian Ocean cyclones have also caused world record rainfall amounts. The 12- and 24-hour rainfall records have both been set on Reunion Island. Reunion's steep mountainous terrain (it has peaks over 10,000 ft. on a 40 x 30 mile island) causes good orographic precipitation to occur, thus cyclones are especially prolific rainmakers. The effects of Southwest Indian Ocean cyclones are not all deleterious, however, as they supply many areas with the majority of their annual rainfall; thus a lack of cyclone activity in a certain region might translate into a drought for that region. So the effects of tropical cyclones in the South Indian Ocean have ranged from giving beneficial rainfall to stirring up debates on sensitive issues. Finally a Southwest Indian Ocean cyclone was captured in the first complete view of the world's weather (see Figure 1.4) from TIROS IX on 13 Feb 1965.

1.2 Data and Data Sources

Tropical cyclone activity in the Southwest Indian Ocean reaches a peak in the months of December, January, and February with the down period occurring during the months of June, July, and August. Because of this "wrap around" of the cyclone season, the cyclone year will be considered to

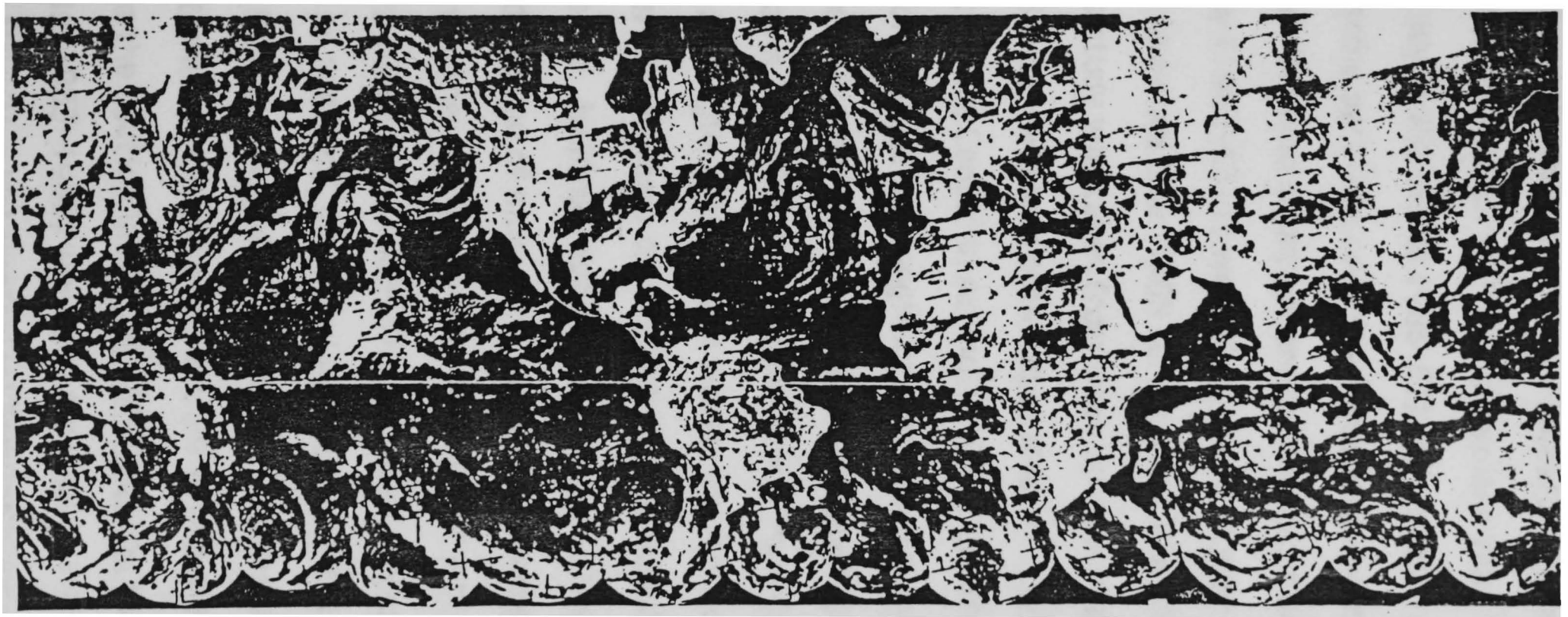

Figure 1.4. First complete view of the world's weather taken from TIROS IX on Feb 1965. This mosaic captured a Southwest Indian Ocean tropical cyclone. (From NOAA, 1985)

start in July and end the following June. Therefore, years in this thesis are named with hyphenation; such as Tropical Cyclone Year 1962-63. The years in this study (1962-63 to 1986-87) were chosen so that they all coincided with some satellite coverage. This will overcome any bias towards areas around land areas and around any major sea lanes. The first year of the study (1962-63) is well after the first year in which weather satellites were launched (the TIROS series, first launched in April 1960).

Data for this study was taken from three sources. For the years 1962-63 to 1981-82, data was obtained on magnetic tape from the National Climatic Data Center in Asheville, North Carolina. Data on this tape consisted of latitude and longitude positions for every 12 hours of the storm's lifetime. Also included was the storm's position within a 5° x 5° square as well as a 2½° x 2½° sub-square. Other important data included were the stage (strength of the storm within a certain catagory) of the storm, direction of movement on an eight-point compass heading, movement mode (i.e., looping, recurvature, etc.), maximum winds (given for some storms), direction of movement in degrees, average speed of movement, and whether the storm was over land or water.

For the years 1982-83 to 1986-87, two data sources were used. For the years 1982-83 to 1984-85, Technical Reports from the Mauritius Meteorological Service (Technical Report-CS7, 1984 and Yan, 1986) were used to track storms which had most of their effect west of 80°E longitude, while the section in Mariners Weather Log entitled Hurricane Alley (DeAngelis, 1983-1985) was used for storms from 80°E to 100°E. On 1 Jul 1985, the Mauritius Meteorological Service's zone of responsibility was extended to 90°E. Therefore for the last two years of the study, the

Mauritius Technical Reports (Yan, 1987 and Appadu, 1987) were used for storms west of 90°E and Hurricane Alley (DeAngelis, 1986-1987) was used for storms only between 90°E and 100°E.

The Mauritius Technical Reports contained data on named storms within the Mauritius-Madagascar regions. This data included: names, dates, maximum sustained winds, lowest pressure, storm track (with strength given every 12 hours) and a discussion about each storm. Also included was a synoptic discussion for each month of the storm season.

Data from Mariners Weather Log included only the name of the storm, date of lifetime, whether its highest intensity was of tropical storm (maximum sustained winds between 34 and 63 knots) or hurricane strength (maximum sustained winds greater or equal to 64 knots), and the storm track (with intensity given every 12 hours).

CHAPTER 2

TRACKING AND INTENSITY DETERMINATION

The World Meteorological Organization (WMO) has catagorized tropical cyclones in the Southwest Indian Ocean into the following stages depending on their maximum sustained winds:

Tropical depression : 15 to 33 knots
Moderate tropical depression : 34 to 47 knots
Severe tropical depression : 48 to 63 knots
Tropical cyclone : 63 to 90 knots
Intense tropical cyclone : 91 to 115 knots
Very intense tropical cyclone : 116 knots and above

Notice that these catagories are more specific than those of the North Atlantic which are as follows:

Tropical depression : less than 34 knots
Tropical storm : 34 to 63 knots
Hurricane : 64 knots and greater

2.1 Tracking Responsibility

The Cyclone Season in the Southwest Indian Ocean officially begins on 1 Nov and ends on 15 May, however, tropical depressions form during all months of the year. Responsibility for naming and tracking these storms is divided among three weather services in the region: Madagascar, Mauritius, and Australia. The areas of responsibility are shown in Figure 2.1. The Mauritius Meteorological Service has the largest area of responsibility (55°E to 90°E), while the Australian Weather Bureau takes care of all

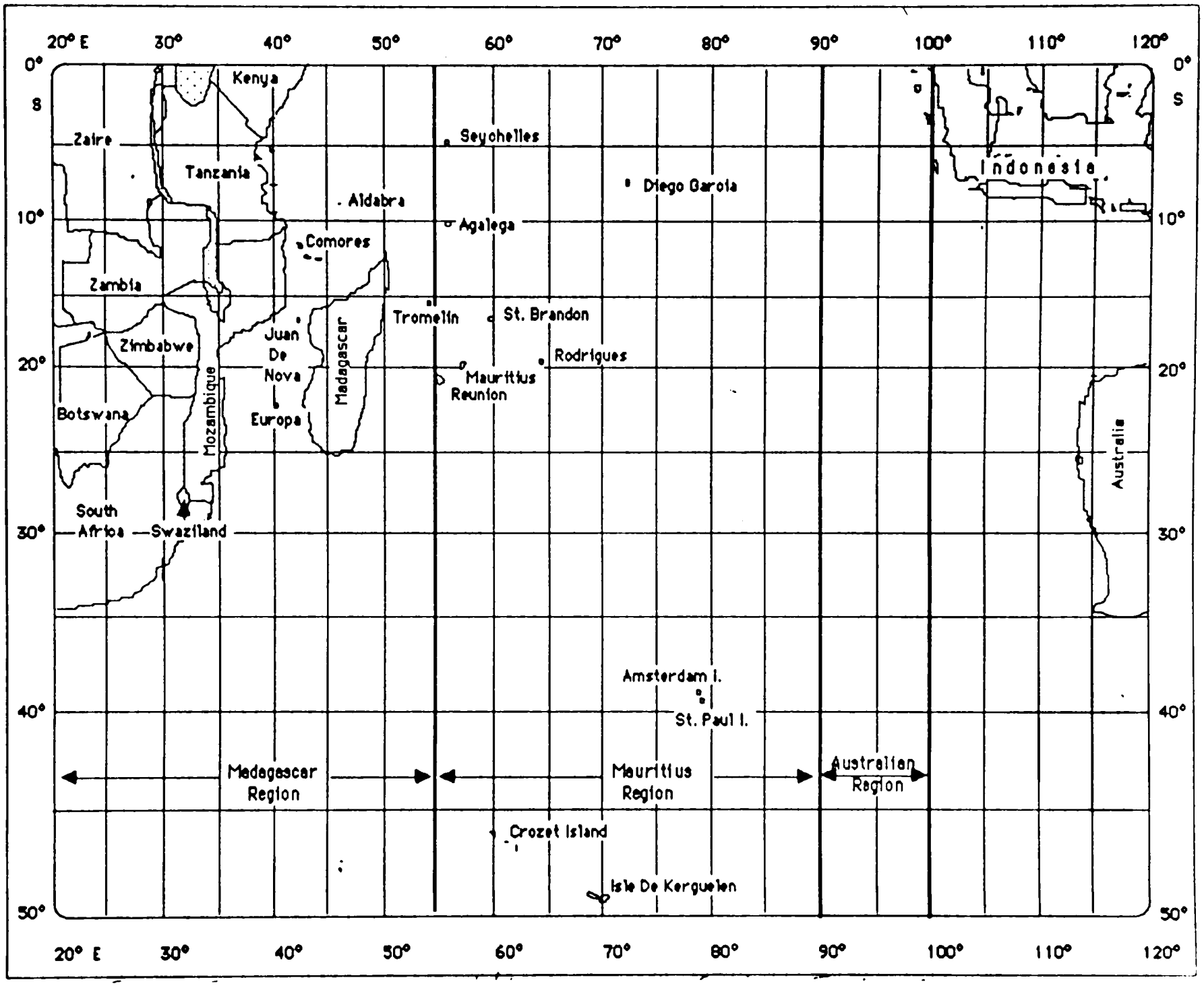

Figure 2.1. Tropical cyclone responsibility areas in the Southwest Indian Ocean.

storms east of 90°E and Madagascar's Weather Service tracks storms west of 55°E. In Figure 2.2 a cyclone report from Reunion is shown (both the English and French versions) . The statement is broken down into two parts. Part 1 gives the current condition of the storm (its position, movement, central pressure, wind speed, wind distribution, and any synoptic analysis). Part 2 gives the storm's T-number information (see section 2.3, The Dvorak Cyclone Intensity Technique) and a forecast of the cyclone's future position. Part 2A gives the satellite from which the satellite image is taken. 2B is the T-number code describing the storm. The first number is the storm's current T-number, followed by the number which is forecast by the T-number forecast by Dvorak's model (called the current intensity or C.I. number), the current state of the storm (weakening, same, or developing) and the amount of change since the last analysis, and the time since the last analysis. So Tropical Depression Hanitra has a T-number of 3.5 and C.I. number of 4.0; it is weakening and has dropped 1 T-number since the last analysis which was 24 hours ago.

In naming of the storms Mauritius and Madagascar use a common list, whereas Australia uses a different list of names. A tropical cyclone is given a name when it reaches the moderate tropical depression stage. When a cyclone moves from the Australian region of responsibility to that of Mauritius, it is given a hyphenated name comprising the names from both regions for a 24-hour period. Thereafter, it is known by the Mauritius-Madagascar name only. When a storm travels from the Mauritius zone to the Australian zone a hyphenated name is again used, but the period of use of the hyphenated name is not well defined.

```
WHI020 FMEE 271000 CCC
BMS CMRS/CYCLONE REUNION
PART 1
1. ORDER NUMBER        : 113/1989
2. BEGINNING OF VALID: MONDAY 89/02/27  TIME :1000 UTC
3. PHENOMENON          : STRONG TROPICAL DEPRESSION HANITRA .
4. POSITION            : WITHIN 30 NM RADIUS OF POINT 27.5S AND 71.0E
                         (TWENTY SEVEN DECIMAL FIVE DEGREES SOUTH AND
                         SEVENTY ONE DECIMAL ZERO DEGREES EAST) AT
                         08H34 UTC.
5. MOVEMENT            :SOUTHSOUTHWESTWARD 15/20 KT
6. ESTIMATED CENTRAL PRESSURE    : 976 HPA
7. ESTIMATED MAX SUSTAINED WIND : 65 KT
8. WINDS DISTRIBUTION : MEAN WINDS 50/60 KT WITHIN 30NM OF THE CENTER
                         35/45 KT WITHIN 120 NM, BUT 200 NM IN SOUTHERN
                         SEMI-CIRCLE.
9. SYNOPTIC ANALYSIS   :HIGH 1033 HPA NEAR 42S/80E MOVING ENE-WARD
                        ABOUT 20 KT.
PART 2 :
A. SATELLITE     : NOAA 11   REVOLUTION NUMBER 2199
B. CODE T        : T3.5/4.0/W 1.0/24HRS
C. ORGANIZATION :HYBRID PATTERN WITH CLEAR-CUT NORTHWESTERLY
                  SHEARING.
D. FORECAST EVOLUTION : 12 H : 30.7S/70.5E
                      : 24 H : NOT SPECIFIED
E. OTHER INFORMATIONS : THE SYSTEM WILL CONTINUE TO PAY ITS TOLL TO
                    THE SHEARING AND RAPID WEAKENING IS EXPECTED.
BMS CMRS/CYCLONE REUNION
PARTIE 1
1. NUMERO              : 113/1989
2. DEBUT VALIDITE      : LUNDI 27/02/89 HEURE:1000 UTC
3. PHENOMENE           : FORTE DEPRESSION TROPICALE HANITRA
4. POSITION            : DANS UN RAYON DE 30 MN AUTOUR DU POINT 27.5S
                         ET 71.0E (VINGT SEPT DEGRES CINQ SUD ET
                         SOIXANTE ET ONZE DEGRES ZERO EST) A 08H34 UTC
5. DEPLACEMENT         : SUD-SUD-OUEST 15/20 KT
6. PRESSION ESTIMEE AU CENTRE : 976 HPA.
7. VENT MAX SOUTENU ESTIME  : 65 KT
8. DISTRIBUTION DES VENTS   : VENT MOYEN 50/60 KT DANS UN RAYON DE
                         30 MN, 35/45 KT DANS UN RAYON DE 120 MN MAIS
                         JUSQUE 200 MN DANS DEMI-CERCLE SUD.
9. ANALYSE SYNOPTIQUE: ANTICYCLONE 1033 HPA VERS 42S/80E DEPLACEMENT
                       ENE 20 KT .
PARTIE 2
A. SATELLITE     : NOAA 11  ORBITE NO : 2199
B. CODE T        : T 3.5/4.0/W 1.0/24HRS .
C. ORGANISATION : CONFIGURATION HYBRIDE AVEC CISAILLEMENT DE NORD-
                  OUEST DE PLUS EN PLUS NET.
D. EVOLUTION PREVUE : 12 H :30.7S/70.5E
                    : 24 H :NON PRECISEE
E. INDICATIONS COMPLEMENTAIRES: POURSUITE DE L'ATTENUATION DU SYSTEME
```

Figure 2.2. A cyclone report from Reunion Island.

2.2 Tracking the Storms

When the tropical cyclones are in the western Australian zone they have little effect on any land masses, therefore the Australian tracking techniques will not be discussed in this thesis. Meteorologists in the Mauritius Meteorological Service have a network of stations throughout the south central Indian Ocean on the islands of Tromelin, St. Brandon, Agalega, Rodrigues, and Diego Garcia. These islands are all dependencies of Mauritius and therefore provide good cyclone lookout posts. Mauritius also receives reports from its island neighbor to the southwest, Reunion, the Weather Service on Madagascar, and reports from ships that come under the infuence of a tropical cyclone. Although Mauritius uses satellite imagery to determine intensity (by the Dvorak Method), it still uses a combination of synoptic data along with satellite pictures to determine location. This is because of the error that arises from the placement of the latitude-longitude lines on the picture (Padya,1976). When attempting to forecast the movement, the Mauritius office uses mainly subjective and simple semi-objective techniques. The subjective techniques include synoptic reasoning, evaluation of expected changes in the large-scale, surrounding flow fields, and subjective evaluation of the cyclone's steering current. Simple semi-objective techniques are forecasts based on persistence, maintaining of acceleration, and simple climatological forecasts based on long-term mean movements at that location and time of the year (McBride and Holland, 1987).

The Madagascar Mereorological Service also relies on satellite images, synoptic observations (from across Madagascar, their region, and from the Mauritius Region), and radar to determine the location and strength of a

storm (Saison Cyclonique 1987-88 à Madagascar, 1988). Then they use subjective and simple semi-objective techniques to forecast a storm's movement (McBride and Holland, 1987).

2.3 Dvorak Cyclone Intensity Technique

Most tropical cyclones when viewed by satellite can be described as having "a comma or a rotated comma pattern." This pattern usually contains clusters of convective cloud lines and cirrus clouds. Cirrus clouds may add or subtract from the apparent organization of the cyclone's cloud pattern. At the head of the comma pattern a central core of clouds might be found. The clouds that form the hook of the comma might either hook inwards towards these clouds or almost wrap around the core clouds. As the cyclone increases its intensity, the comma pattern is observed to become more circular, and the core clouds increase their amount and density (Dvorak, 1975).

The Dvorak Cyclone Intensity Technique is based on the "average cyclone" which follows a set pattern of development. The average cyclone will increase its T (for tropical) number by one each day (T1 being the lowest tropical cyclone intensity and T8 the maximum possible intensity). Table 2.1 shows the appropriate minimum sea level pressure and maximum sustained wind for each one-half T-number.

Figure 2.3 shows the Dvorak Technique model, while common developmental patterns are seen in Figure 2.4. The model consists of a set of curves depicting tropical cyclone intensity change with time. There are three sets of curves, one for a typically developing tropical cyclone, one for a rapidly developing cyclone, and one for a slowly developing cyclone.

Table 2.1. T-number scale according to Dvorak for Southwest Indian Ocean Tropical Cyclones.

T-number Minimum	Sea Level Pressure	Maximum Wind Speed	
	mb	kts	mph
1	-	25	29
1.5	-	25	29
2	1000	30	35
2.5	997	35	40
3	991	45	52
3.5	984	55	63
4	976	65	75
4.5	966	77	89
5	954	90	104
5.5	941	102	117
6	927	115	132
6.5	914	127	146
7	898	140	161
7.5	879	155	178
8	858	170	196

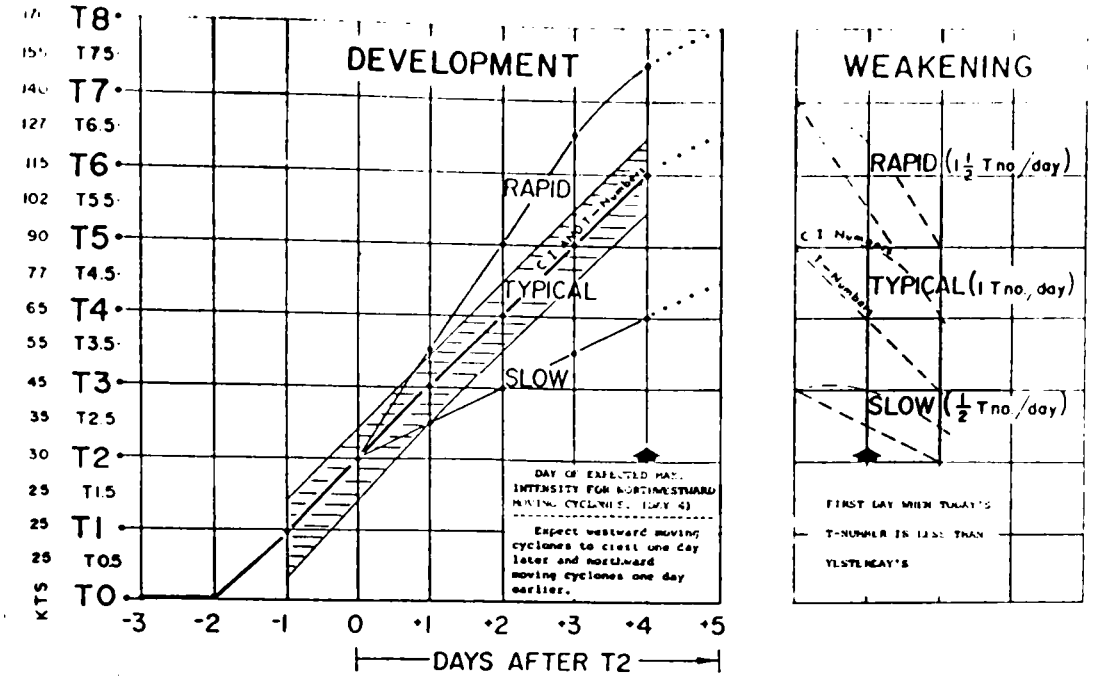

Figure 2.3. Intensity change curves from Dvorak's tropical cyclone model. (From Dvorak, 1975)

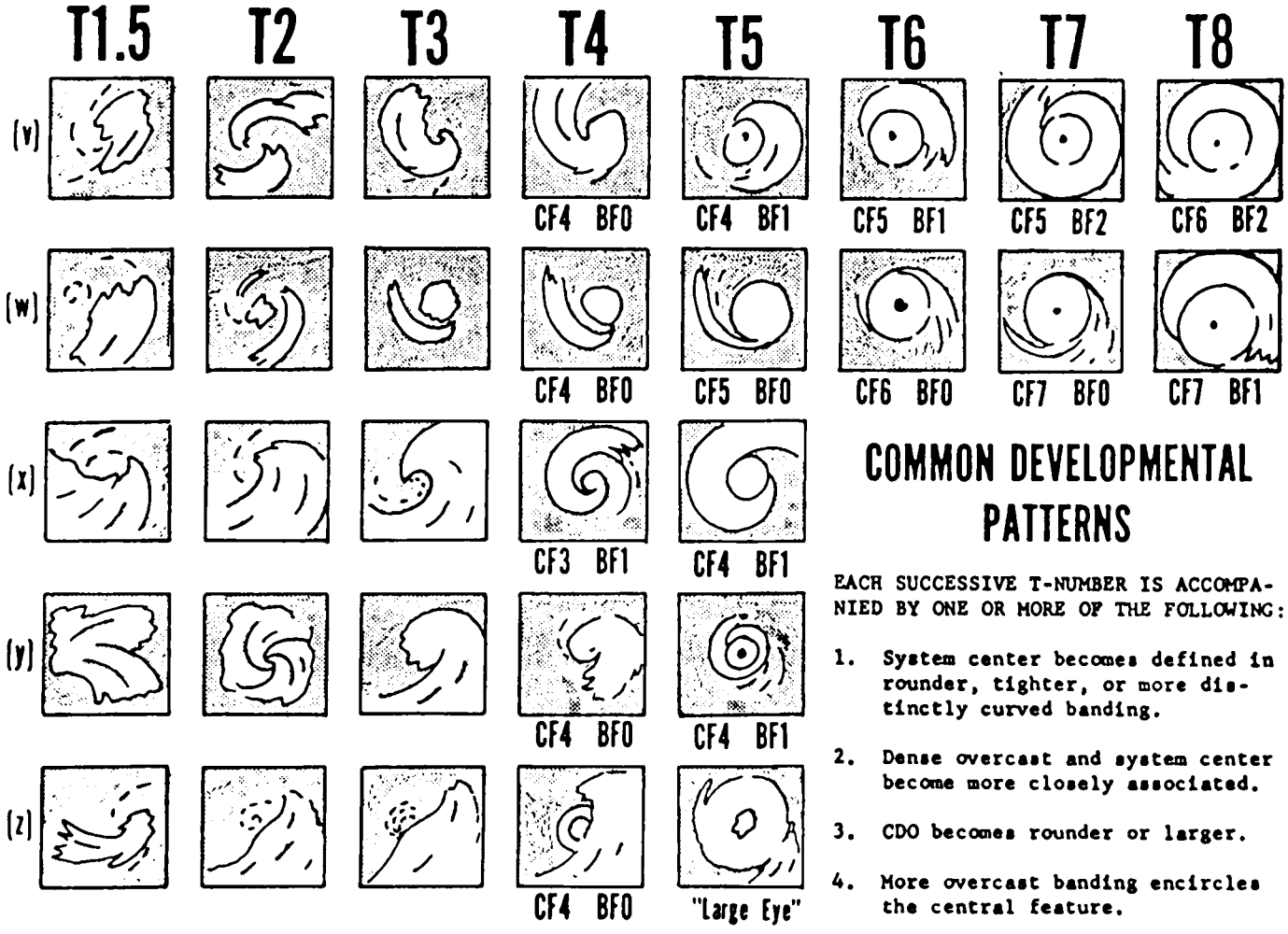

Figure 2.4 Common developmental patterns for tropical cyclones.(From Dvorak, 1975)

The typical curve applies only to cyclones developing or weakening in a more or less unchanging environment. When the cyclone encounters a different environment, a switch to either the rapid curve or the slow curve must be made, the adjustment depends on whether the new environment is beneficial or detrimental. When looking at a Dvorak forecast it is important to remember that the forecast is for only the next 24 hours. After that time a new set of pictures will be received and a new analysis and forecast will be made. The remainder of this section will be a brief look at cloud features used in the Dvorak Technique along with hints in using them for estimating a cyclone's T-number.

The cloud features that first reveal the development of a tropical cyclone are curved cloud lines that are associated with a deep convective layer or a dense overcast, either must have persisted for 12 hours or more. The average cloud system is generally organized over an area of at least 4° latitude that includes an area of convective overcast or an organization of cumulonimbus clouds of at least 3° in extent. As the lines of cumulonimbus are observed, they will merge toward or hook at, or curve around one general area. This area will generally be less than 2½° in diameter. When the center becomes defined by low cloud lines, it must be less than 1.25° from a dense overcast. Indications of intensification should also be seen in order to provide that development will continue over the next 24-hour period. The indication of development (which will be discussed below) is important during the developing stages of a tropical cyclone. Two very important factors are the presence of deep-layer convective clouds near the center of the system and the absence of strong unidirectional winds at upper levels. Dvorak has put a limit on the T-number attainable (T1.5) for

the first day of development. This is due to the fact that the disturbance's pattern during its first day may appear stronger than its surface winds or central pressure. Dvorak states that this may be a reflection of the fact that the stronger winds have not yet reached the surface. The typical disturbance is recognized at its stage about 36 hours before it attains tropical storm intensity.

As a cyclone develops, the forecaster must begin to look for features within the cyclone's cloud systems. The features used to estimate the cyclone's present intensity are broken down into two general catagories: 1) central features which are described as "those which appear within the broad curve of the comma band and either surround or cover the cloud system center" and 2) outer banding features, which refer "to only that part of the comma cloud band that is overcast and curves evenly around the central features." The central features (CF) and other banding features (BF) are combined with an "implied cloud depth parameter" to determine the cyclone's T-number. Central features are defined by Dvorak in terms of both the inner most curved cloud lines and a central dense overcast (CDO). This is because a cyclone's center may be cloud-free and located within a cloud line on one day and then be obscured by a CDO the next. Dvorak bases the CF portion of the T-number on size, shape, and definition of central features as well as the amount of CDO. When the cloud lines are visible, intensity of the cyclone is estimated from cloud features showing the definition of the system's cloud center or cloud system center (CSC), and the associated deep-convection layer. When the cyclone's central cloud lines are covered by a dense overcast, the overcast's characteristic is used to estimate the cyclone's intensity. The nature of the eye of the cyclone is

also used in determining the T-number. Dvorak defines two types of eyes: a banding type eye and an eye which is imbedded within the CDO. No matter what type of eye the storm has, the numerical value of the CF is increased when there is an increase in the amount of overcast surrounding the eye. Other indications of intensification are: the eye becoming more distinct, rounder, or more towards the center of the CDO. A decrease in the value of the CF occurs if the eye becomes ragged, large, or cirrus-covered. The value that the BF adds to the T-number is proportional to the amount and circulation of the bands that are outside the CF. Figure 2.5 (Dvorak, 1973) shows how a value for the CF and BF is evaluated and then added together to get the T-number for a cyclone.

After the current T-number is computed, the cloud features are used to determine whether the cyclone is likely to remain on its modeled curve during the next 24 hours. The cyclone's progress throughout its life cycle is analyzed by a continuous comparison of its cloud features (and cloud feature changes) to those expected from the model based on the cyclone's past. An analysis is accomplished most easily and reliably when the comparison is made between pictures from the same satellites, and 24 hours apart. This will negate any problems which might arise from the different responses that different satellite sensors might have, and from any diurnal variations in cloud characteristics or viewing conditions (Dvorak, 1975).

When trying to decide on the future intensity of a cyclone, Dvorak states that indications of the ongoing change at the time of the satellite picture can help. Things to look for in the cloud features are indications of vertical motion and inflow/outflow characteristics. When a cyclone

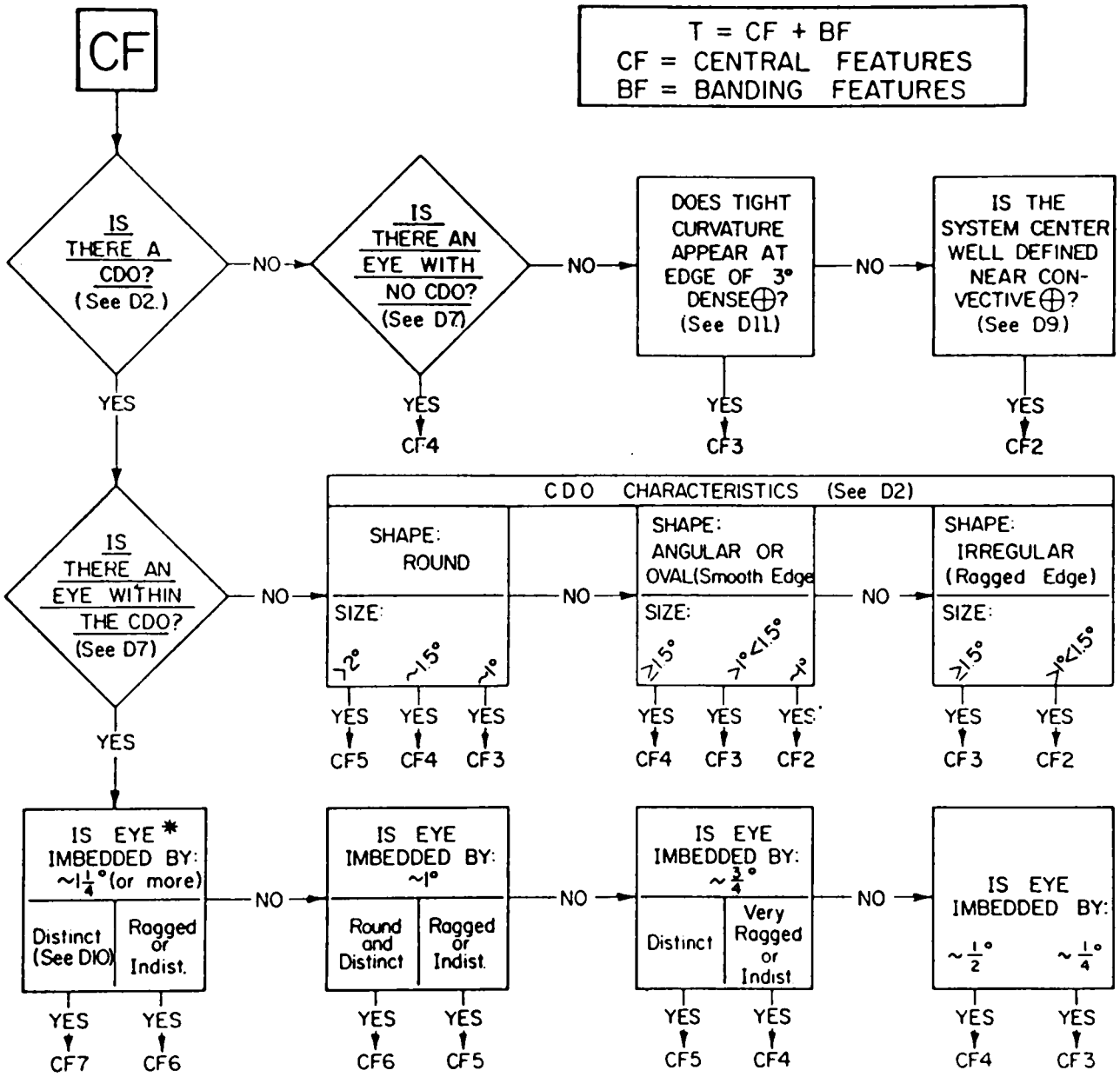

BF = A NUMBER RELATED TO THE AMOUNT OF DENSE OVERCAST IN BAND FORM THAT CURVES EVENLY AROUND THE CENTRAL FEATURE WITHIN 4° OF THE SYSTEM CENTER (See D1.)

BF = 0 when little or no quasi-circular banding is apparent.

BF = 1 when a ½° wide band completely encircles the central feature, or when a 1°, or wider, band encircles more than ½ the central feature.

BF = 2 when a ½° wide band is coiled twice around the central feature, or when a 1°, or wider, band is coiled once around the central feature.

When the above conditions are not quite met, values of ½ or 1½ may be used.

Figure 2.5 Dvorak's chart for determining the Preliminary T-number.(From Dvorak, 1973)

undergoes either typical or rapid development, it will appear on satellite as a bright, sharply defined comma shape. This is an indication of a pattern with strong vertical motions. The central features will be composed of a deep convective layer or a dense, solid overcast with some cirrus. The clouds in the outer bands will appear to spread out from the CF in three or four of the quadrants. The cirrus outflow might appear either as fuzzy-edged clouds or as cirrus bands emanating from the CF. A slowly developing or steady-state cyclone will show a lack of one of the characteristics listed above, or will show a weakness in some of them. A weakening cyclone will display little evidence of any of them.

The cyclone's environment will play a role in both its development and in its appearance on satellite. If a cyclone encounters an environment that will hinder its development, the 24-hour forecast will have to mention either an interruption or a slowdown in the development. A couple of examples that might be seen in satellite pictures are as follows. If unidirectional flow aloft is observed, it might show up as increased cirrus cloud flow across the system. If the cyclone comes into a blocking pattern, then its cloud system will become elongated perpendicular to its direction of motion. After contact with the detrimental environment has ended, development can be forecast to resume.

2.4 Satellites

Since the Dvorak Intensity Method is based on satellite imagery, this section will describe satellites (and their sensors). The longest running type of satellites from which Southwest Indian Ocean tropical cyclones have been viewed is the NOAA series. These polar orbiting satellites have

their orbits in a fixed plane with respect to space and the earth rotates underneath once every 12 hours. Typical altitudes range between 800-1500 km. The NOAA series satellites carry four primary instrument systems: the advanced very high resolution radiometer (AVHRR) which has a 1-km resolution; the TIROS operational vertical sounder (TOVS); a data collections system (DCS); and finally the space environment monitor (SEM) (Rogers, 1986).

The AVHRR has five spectral channels (See Table 2.2) from which data is collected at 0300 and 1500 local time. This data is used extensively for monitoring the earth's radiation budget although the primary purpose is for weather forecasting and analysis. Channel 1 provides albedo observations using the assumption that data is representative of the entire visible spectrum. Channel 2 distinguishes land from water. Channel 4 shows snow-covered areas and high (cold) cirrus clouds against the background of warmer land and ocean. Channel 3 shows low clouds (e.g., stratus) which allows for a comparison with Channel 4 to determine sea surface temperatures, making it possible to discern clouds from surface features. Channel 5 (and 4) is used to obtain total longwave radiative flux. The AVHRR system provides image data for real-time transmission to both Automatic Picture Transmission (APT) and High Resolution Picture Transmission (HRPT) users. This system allows observations of cloud structure detail, sea ice, snow accumulation, and ocean temperature.

TOVS provides a vertical sounding of the atmosphere. It consists of three instruments, the High Resolution Infrared Sounder (HIRS/2), the Stratospheric Sounding Unit (SSU), and the Microwave Sounding Unit (MSU). HIRS/2 produces tropospheric temperatures and moisture profiles

Table 2.2 AVHRR channels (After Rodgers, 1986).

Channel	Wavelenght Interval(μm)	Objectives
1	0.55-0.70	Recognition of clouds
2	0.70-1.10	Delineation of land, water, melting and non-melting snow
3	3.55-3.93	Sea surface temperature and atmospheric correction in partly cloudy areas
4	10.3-11.3	Sea surface temperature and atmospheric correction
5	11.5-12.5	Same as channel 4

and has 20 channels which detect radiation emitted by water vapor, ozone, and carbon dioxide. This information is then used to determine temperature at different pressure levels. Meanwhile, SSU measures temperatures in the stratosphere; and MSU produces atmospheric temperature soundings in the presence of clouds. Pictures from the NOAA series satellites (6 through 11 in particular) were received by the Mauritius Meteorological Service using the CIT-Alcatel satellite picture receiver.

The next satellite that covers the region is the geostationary satellite INSAT1B operated by India. INSAT1B was launched on 30 Aug 1983 and put in orbit above 72°E, with a VHRR Radiometer on board. The INSAT1B VHRR produces visible and infrared images. The visible channel receives 0.55-0.75 µm, with a 2.75-km resolution. The infrared channel receives 10.5-12.5 µm providing 11 km resolution. The VHRR photographs the complete disk of the earth every 30 minutes (Long, 1985).

Beginning with the 1986-87 cyclone season, the Mauritius Meteorological Service received satellite bulletins from INSAT1B via its own telex terminal. In previous years, these bulletins were received via the Indian High Commission.

The other two satellites with part of their coverage in the basin are also geostationary: METEOSAT-2 positioned above 0° longitude (operated by the European Space Agency) and GMS-3 which is located at 140°E (operated by Japan and used mainly by Australia). Both METEOSAT and GMS provide visible and infrared images.

CHAPTER 3

DATA ANALYSIS

This chapter will present the analysis of Southwest Indian Ocean tropical cyclone characteristics using combined data from the National Climatic Data Center, the Mauritius Meteorological Service, and Mariners Weather Log. In 1985, the RA 1 Tropical Cyclone Committee adopted the current tropical cyclone classifications shown at the beginning of Chapter 2. In order to retain the statistics that had accumulated it was proposed to maintain the old classifications in the keeping of these data. The relationship between the old and new classification is given below.

Old Classification	New Classification
Weak Tropical Disturbance	Tropical Depression
Moderate Tropical Depression	Moderate Tropical Depression
Severe Tropical Depression	Severe Tropical Depression
Intense Tropical Cyclone	Tropical Cyclone Intense Tropical Cyclone Very Intense Tropical Cyclone

Because the data from the National Climatic Data Center divided the storms into the stages similar to those used in the North Atlantic (see Chapter 2), this study will classify storms in the following manner:

Sites Classification	Old S.W. Indian Ocean Classification
Tropical Disturbance	Weak Tropical Disturbance
Tropical Depression	Moderate Tropical Depression Severe Tropical Depression
Cyclone	Intense Tropical Cyclone

3.1 Frequency of Southwest Indian Ocean Tropical Cyclones

During the 25-year period of this study 306 tropical cyclones formed, giving an average of 12.2 tropical cyclones per year, while 250 of these reached tropical depression stage (about 82%), and 89 reached cyclone intensity (29%). These numbers indicate that once a tropical cyclone has reached a disturbance stage, it is very likely to go ahead and intensify to tropical depression strength. Then about 35% of these tropical depressions continue to strengthen and become cyclones. Table 3.1 gives the number of storms that had their maximum intensity in each catagory for each cyclone year since 1962-63. The greatest number of storms in a single year came in 1965-66 as 19 tropical cyclones formed, with the minimum of seven occurring in 1986-87.

The 250 tropical depressions give an average of 10.0 per year, with 6.6 of these per year reaching their greatest intensity in this stage. The most depressions in one year was 14 (in 1983-84) with the minimum being 4 (in 1973-74). Over the past 25 years cyclones have averaged 3.3 per year, with a high of seven occurring in four different years (1963-64, 1969-70, 1983-84, 1985-86) and in two years no cyclones formed (1966-67 and 1986-87).

Table 3.1. Number of tropical cyclones with their maximum intensity in each stage for the years 1962-63 to 1986-87.

	Disturbances	Depressions	Cyclones	Total
1962-63	0	8	5	13
1963-64	0	5	7	12
1964-65	8	7	3	18
1965-66	7	10	2	19
1966-67	5	6	0	11
1967-68	0	7	2	9
1968-69	1	7	2	10
1969-70	2	4	7	13
1970-71	2	7	6	15
1971-72	0	7	2	9
1972-73	2	5	6	13
1973-74	4	3	1	8
1974-75	4	6	1	11
1975-76	3	3	2	8
1976-77	3	4	2	9
1977-78	3	10	2	15
1978-79	4	7	2	13
1979-80	0	4	6	10
1980-81	4	7	3	14
1981-82	1	5	6	12
1982-83	1	6	1	8
1983-84	0	7	7	14
1984-85	1	10	3	14
1985-86	1	9	7	17
1986-87	0	7	0	7
Total	56	161	89	306
Average	2.2	6.6	3.5	12.2

Tropical cyclones form in every month of the year, but the peak comes in January and February (See Table 3.2). Activity is usually sparse for July through September, and when a storm does form, it progresses no farther than tropical depression stage. In October, activity picks up with some storms progressing to the cyclone stage. Activity continues to increase in November as an average of one depression every two years occurs and one cyclone occurs every five years. December is the first month when more than one depression happen in the month (1.52), but December averages only one cyclone every two years. Both January and February average over two depressions per month (2.60 and 2.44, respectively), while January averages 0.92 cyclones and February has 0.84. In March, depression activity is about half of what it was in January and February (1.56), but cyclone activity is still rather strong as March has a monthly average of 0.76. April sees activity decrease by about half again for depressions (0.72) and cyclone activity is about a third of the activity of March at 0.28. One depression forms every five years in May with just one cyclone every 25 years. Activity is at its minimum in June as only one tropical cyclone occurred in the 25 years. Figure 3.1 shows the 10-day running total for each catagory. Each 10-day total consists of storms which have formed in the period and storms that have survived from the last period. So by looking at the 10-day running total, we can see not only where formation is the greatest, but also where storm longevity is the greatest. Disturbances are most active from the end of September through the end of May. Depressions start and end about the same time as disturbances, while cyclones begin their most active period about the middle of November and ends in mid-March.

Table 3.2. Number of tropical cyclones which formed in each month with their maximum intensity in each stage. Also included is the average for each month.

	Disturbances	Avg.	Depressions	Avg.	Cyclones	Avg.
July	1	.04	1	.04		
August	3	.12	1	.04		
September	2	.08	1	.04		
October	1	.04	5	.20	2	.08
November	4	.16	9	.36	4	.16
December	16	.64	26	1.04	12	.48
January	10	.40	42	1.68	23	.92
February	11	.44	40	1.60	21	.84
March	6	.24	20	.80	19	.76
April	2	.08	11	.44	7	.28
May			4	.16	1	.04
June			1	.04		

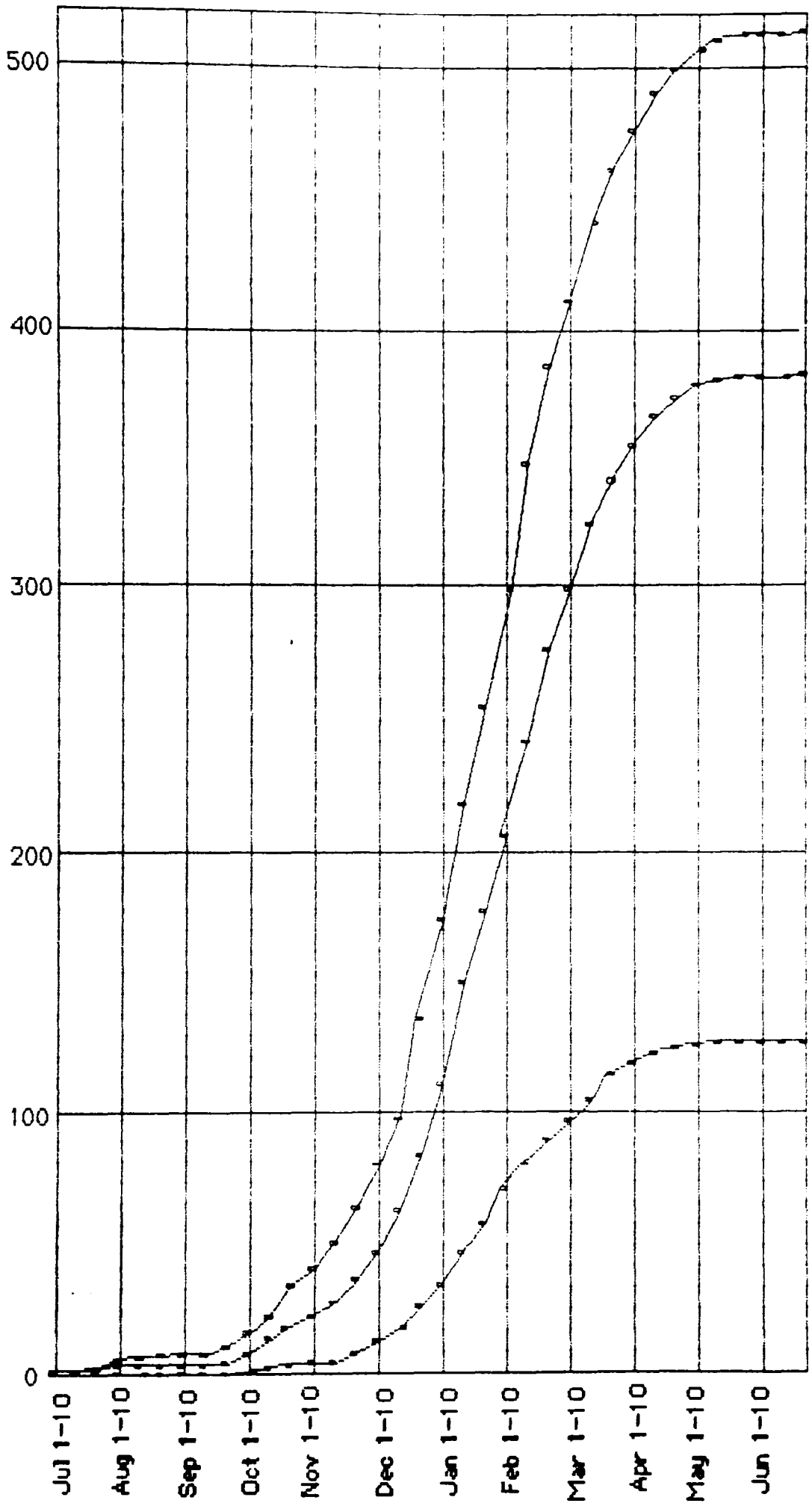

Figure 3.1. Ten-day running total for disturbances (top line), depressions (middle line), and cyclones (bottom line).

3.2 Formation Areas

Tropical cyclones in the Southwest Indian Ocean have three major formation areas (Figure 3.2). The largest of these three areas lies southeast of Diego Garcia. At 15°S to 20°S it lies from about 53°E to 70°E; the area extends to the northeast and to around 73°E at 10°S. It then lies westward to 53°E again. Imbedded in this area is one 2½°x 2½°square with an extremely high formation rate. The square bounded by 10°S to 12½°S and 70°E to 72½°E had 14 tropical cyclones form within it; this is seven more than any other 2½°x 2½°square. There is also a branch off this main formation area which has a northwest-southeast orientation; it runs from about 8°S, 76°E to 15°S, 86°E, averaging about 2½°in width.

The next formation area is in the central Mozambique Channel from 17½°S to 20°S and from 40°E to 45°E. This one area accounts for about one-third of all the tropical cylones that form in the Mozambique Channel. The final formation area is in the eastern part of the basin. It is broken into two parts, the first running north-south from 10°S to 20°S; between 90°E and about 93°E. The second half is an east-west area running from 90°E to 100°E , in between 10°S and 12½°S.

These formation areas move and expand as the cyclone year progresses (Figure 3.3). For the low activity months of June through October, formations are usually confined to the north-central part of the basin, between 5°S to 10°S and 70°E to 85°E. In November, this area begins to spread both east and west to cover an area from about 60°E to 93°E. The north-south expanse of the November area is from 8°S to 13°S in the west, to 5°S to 8°S at 75°E and 8°S to 13°S in the east. In December, the formation area has an oval shape, which is positioned between 55°E-95°E

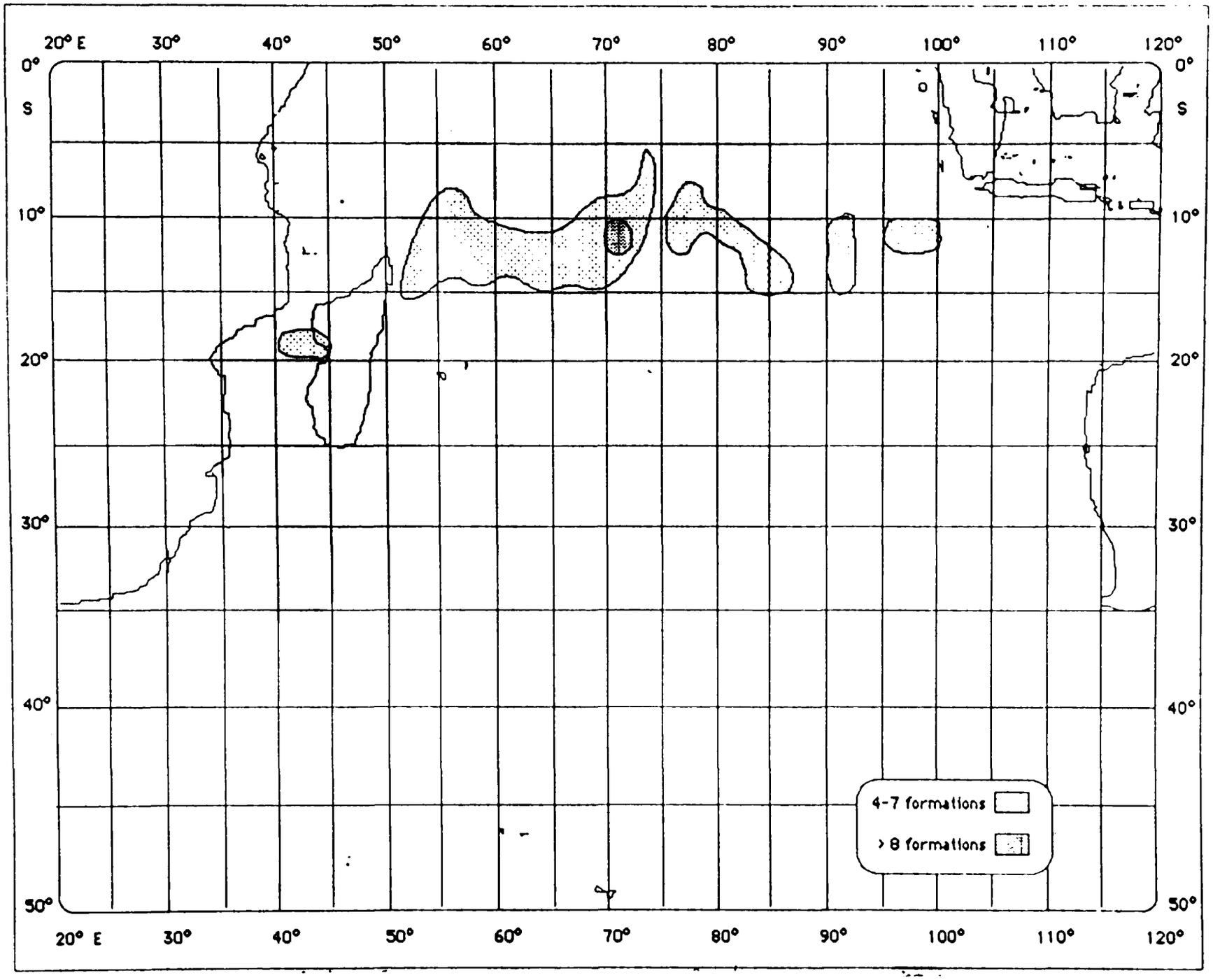

Figure 3.2. Major formation zones in the Southwest Indian Ocean. (1962-63 to 1986-87)

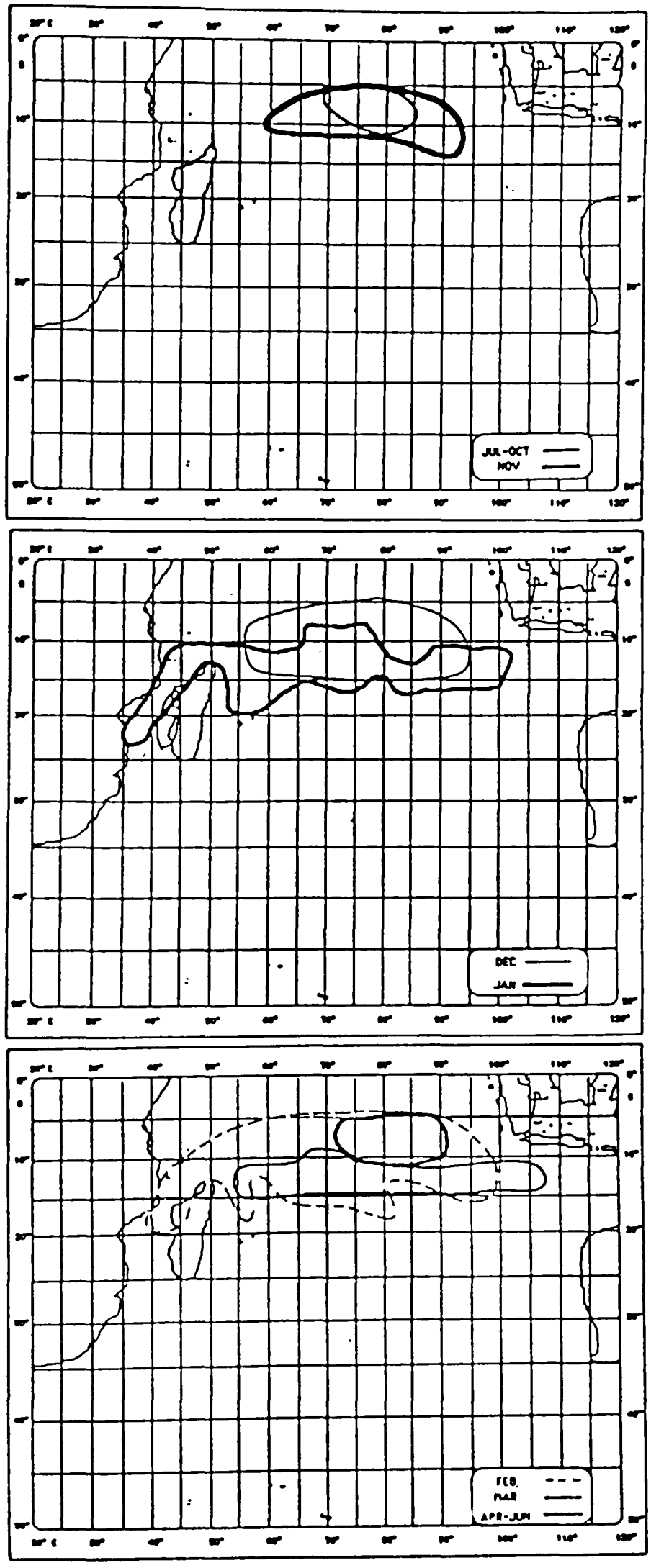

Figure 3.3. Progression of the formation areas as the cyclone year advances.

and 5°S-15°S. There is now also an area in the Mozambique Channel just to the west of Madagascar from 15°S to 22°S.

January sees the joining of these two separate areas as the main area has moved south and has continued to expand. In the Indian Ocean itself, the area is centered on 13°S with about a 5° width; this connects with an area that almost covers the entire Mozambique Channel. In Febuary, a slight northward movement is observed, but the northern part of the Mozambique Channel is still covered by the area which then extends across the entire Southwest Indian Ocean. The formation area continues to shrink in March as formations in the channel have stopped and the westward limit of the area is 55°E. The formation area does extend eastward to to 100°E and sits between 10°S and 15°S. For the rest of the cyclone year the formations retreat to about the same area as they began.

Figure 3.4 shows the average position of the 26.5°C sea surface temperature (SST) isotherm for each month of the year. This is the hypothetical minimum SST at which tropical cyclones can form. When comparing Figure 3.3 to 3.4, there appears to be about a month lag in the months of July through January between the SST reaching 26.5°C and tropical cyclones forming in that area. In February through June, this lag turns into a month advance as formation areas lead the retreat of the 26.5°C SST isotherm.

3.3 Affected Areas

Since the tropical cyclones in the basin have a general east to west movement with recurvature in the western half of the basin, it makes sense that the areas affected most by these storms are in the western half.

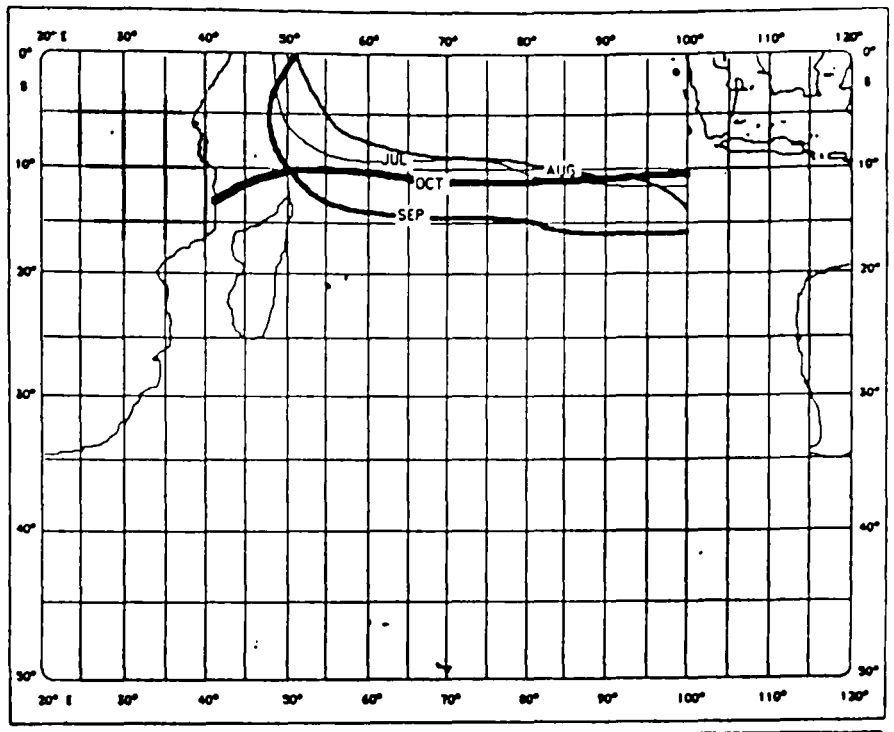

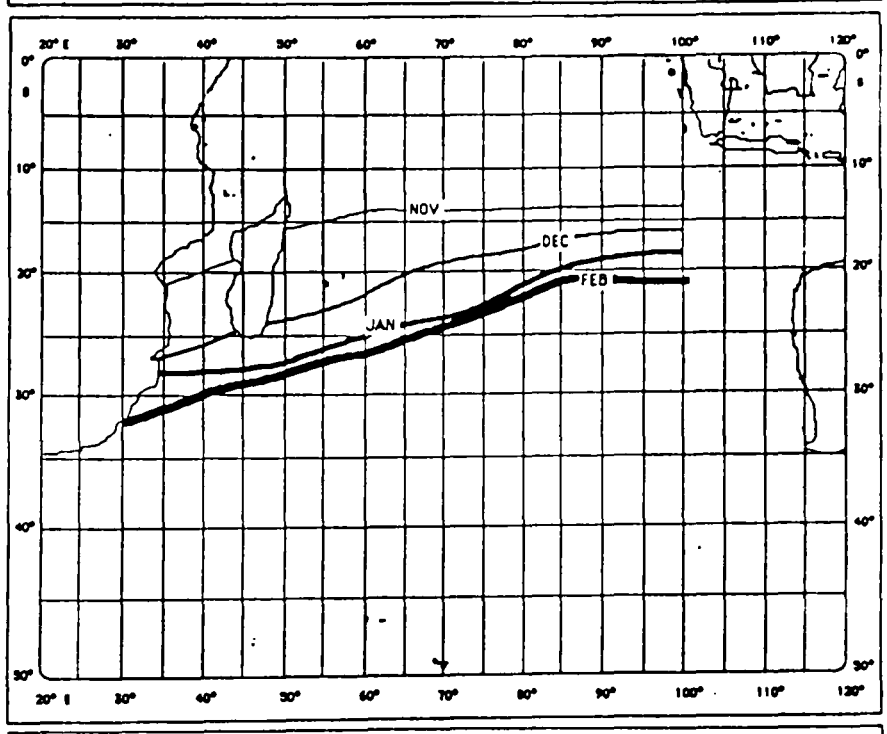

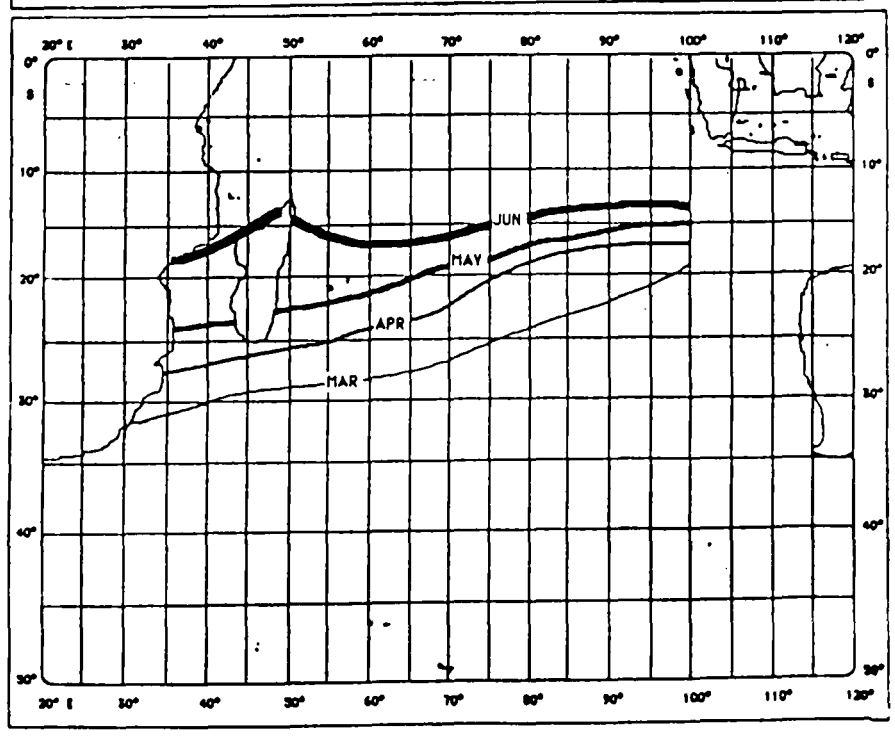

Figure 3.4 Average position of the 26½°C SST isotherm for each month of the year.

Figure 3.5 shows the Southwest Indian Ocean's most affected areas. The area with lightest shading corresponds to a cyclone occurring within a given 2½° x 2½° square once every two years; the medium shading corresponds to one every year; and the heaviest shading corresponds to 1.5 storms every year. The greater than 12 area takes on an oval shape with the major axis running from 22½ °S, 35°E to 12½ °S, 97½ °E, and the minor axis is marked by the endpoints 10°S, 62½ °E, 32½°S, 62½ °E.

The island of Madagascar divides the greater than 25 region into a main area in the Indian Ocean and a smaller one in the Mozambique Channel. The main region starts at 12½°S, 80°E and expands southward to the west. At 50°E, the area runs from 10°S to 25°S. The channel area is a circle of 2½° diameter, centered on 20°S, 40°E. The area affected by 1.5 storms per year runs northeast from 17½°S, 55°E to 12½°S, 72½°E. This swath averages about 2½° wide. Finally, there is a 2½° square, where the southwest corner touches 20°S, 40°E in the Mozambique Channel that is also affected by 1.5 storms per year.

The monthly progression of these affected areas is shown in Figure 3.6. Tropical cyclones during July through October are usually weak and short-lived, so they remain in the northern third of the basin and generally track to the west without too much recurvature taking place before dissipating. Storms begin to affect areas more south and west in November as they persist longer and begin to recurve. They still do not affect the central and southern Mozambique Channel as storms have not formed there and they cannot survive the trek across Madagascar. The months of December through February have storms at the southernmost latitudes. This southern push is about 10° to 13° farther south to the west of 80°E as

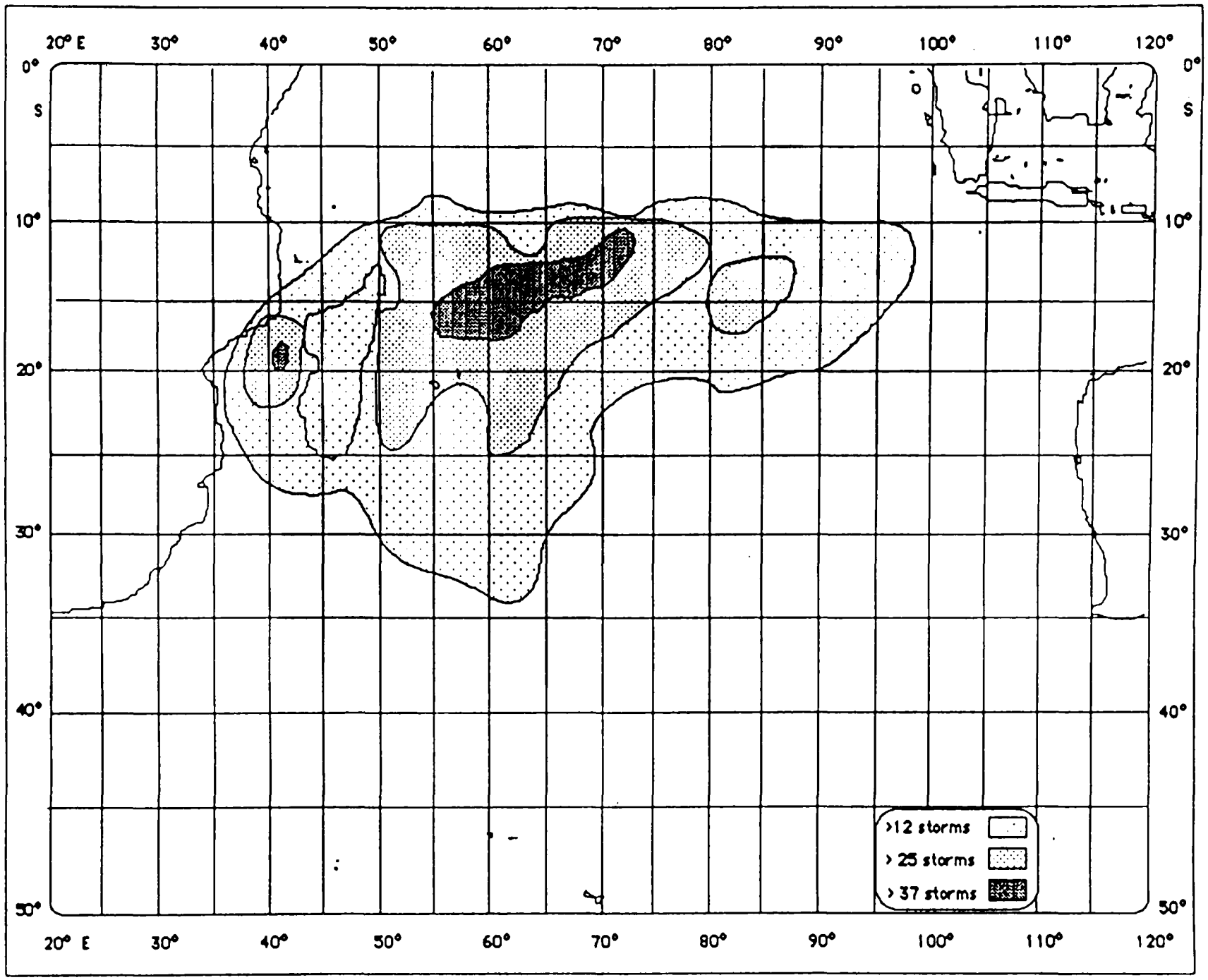

Figure 3.5. Areas most affected by Southwest Indian Ocean tropical cyclones. (1962-63 to 1986-87)

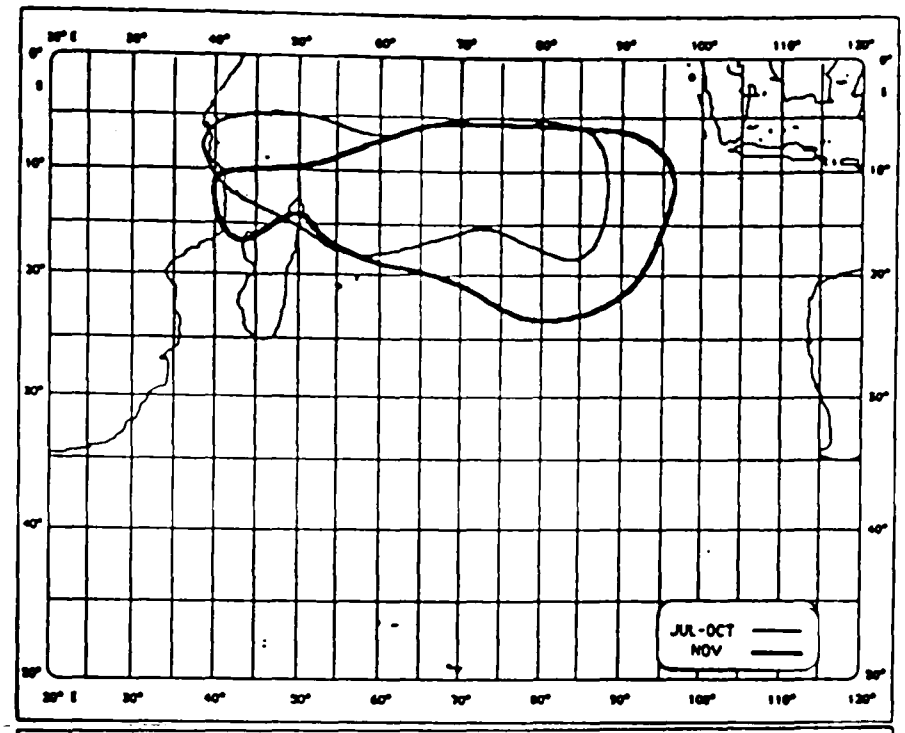

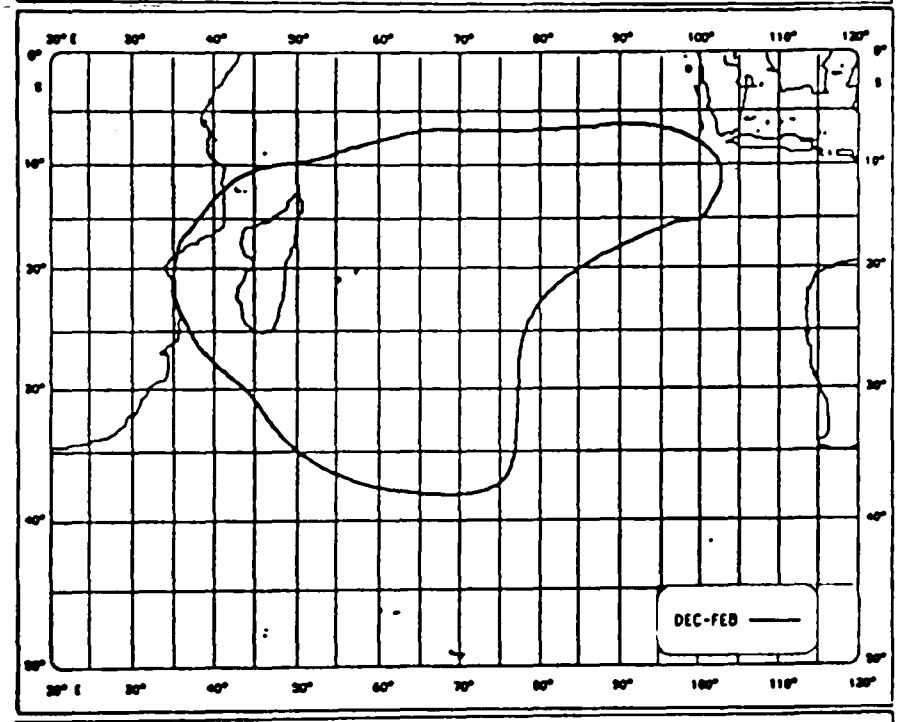

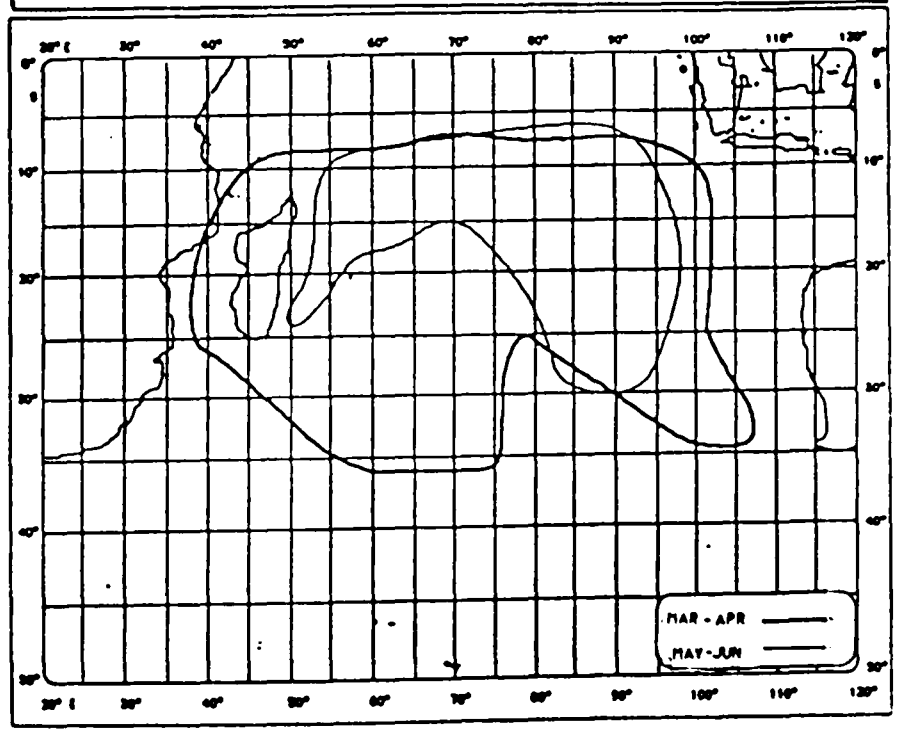

Figure 3.6 Progression of affected areas during as the cyclone year advances.

compared to east of 80°E. Storms begin to retreat to the northwest of 80°E, but east of 80°E they reach down to 35°E (the same latitude as the retreating area). This is probably due to the circulation around the developing high pressure over Australia with the onset of thermal winter (See Figure 3.7).

3.4 Dissipation

The dissipation of tropical cyclones appears to have a more random pattern when compared to either formation areas or affected areas. There are, however, two main areas in which tropical cyclones show a climatological ending (Figure 3.8). The first runs roughly parallel to the east coast of Madagascar. This is an area in which one expects to see many of storms terminate, as their circulations interact with the mountains of Madagascar. The second area is in the central Mozambique Channel. Storm endings in this area might be the result of landfall on the African continent, landfall on the west coast of Madagascar, or due to the weakening of their circulation after their journey across Madagascar. Finally, the third ending area is found southeast of Madagascar, in an area where the storms would be entering an area of higher shear and lower sea surface temperatures.

The progression of the endings during the cyclone year does not follow the smooth transition that was seen in Figures 3.3 and 3.6. Storms in July through October have an ending area off of Tanzania and northern Mozambique and also off the northeast coast of Madagascar (Figure 3.9). In November, the area off Tanzania and Mozambique disappears leaving just the area off northeastern Madagascar, which has expanded eastward.

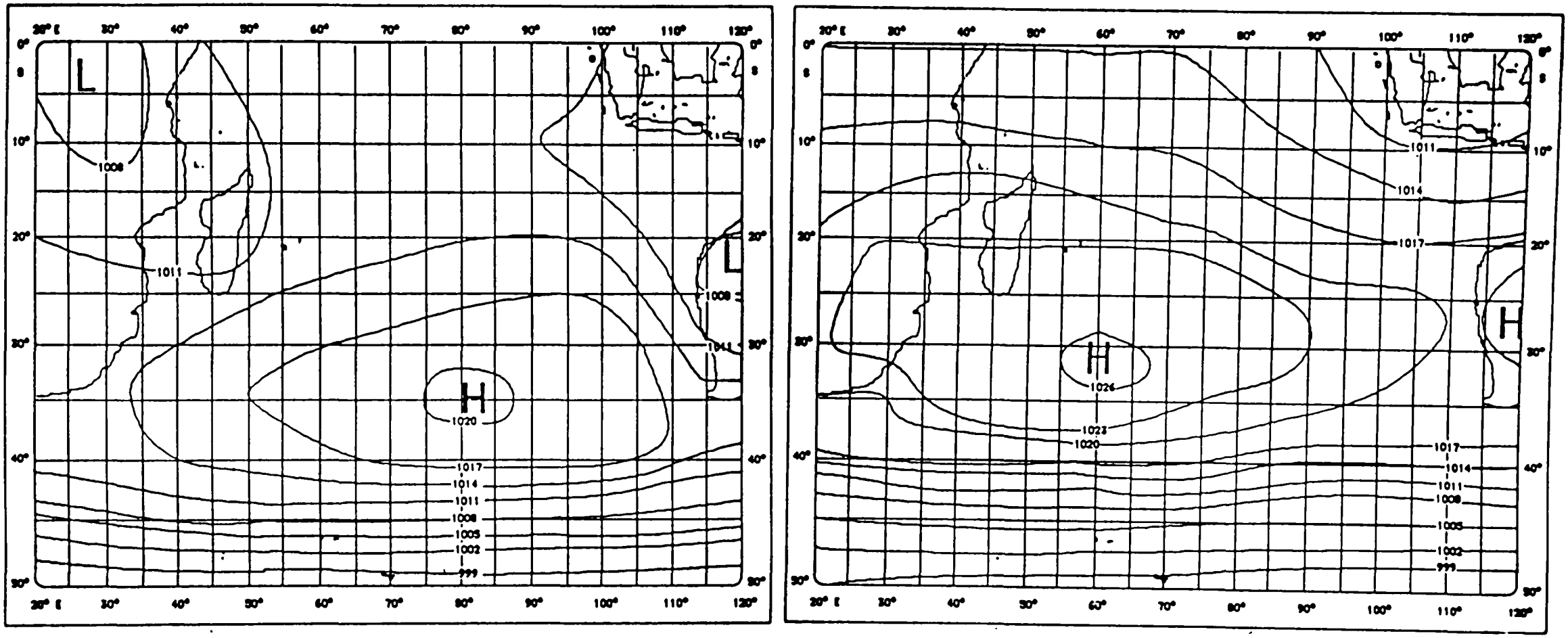

Figure 3.7. January (left) and July (right) mean sea level pressure in millibars. (After Fairbridge, 1966)

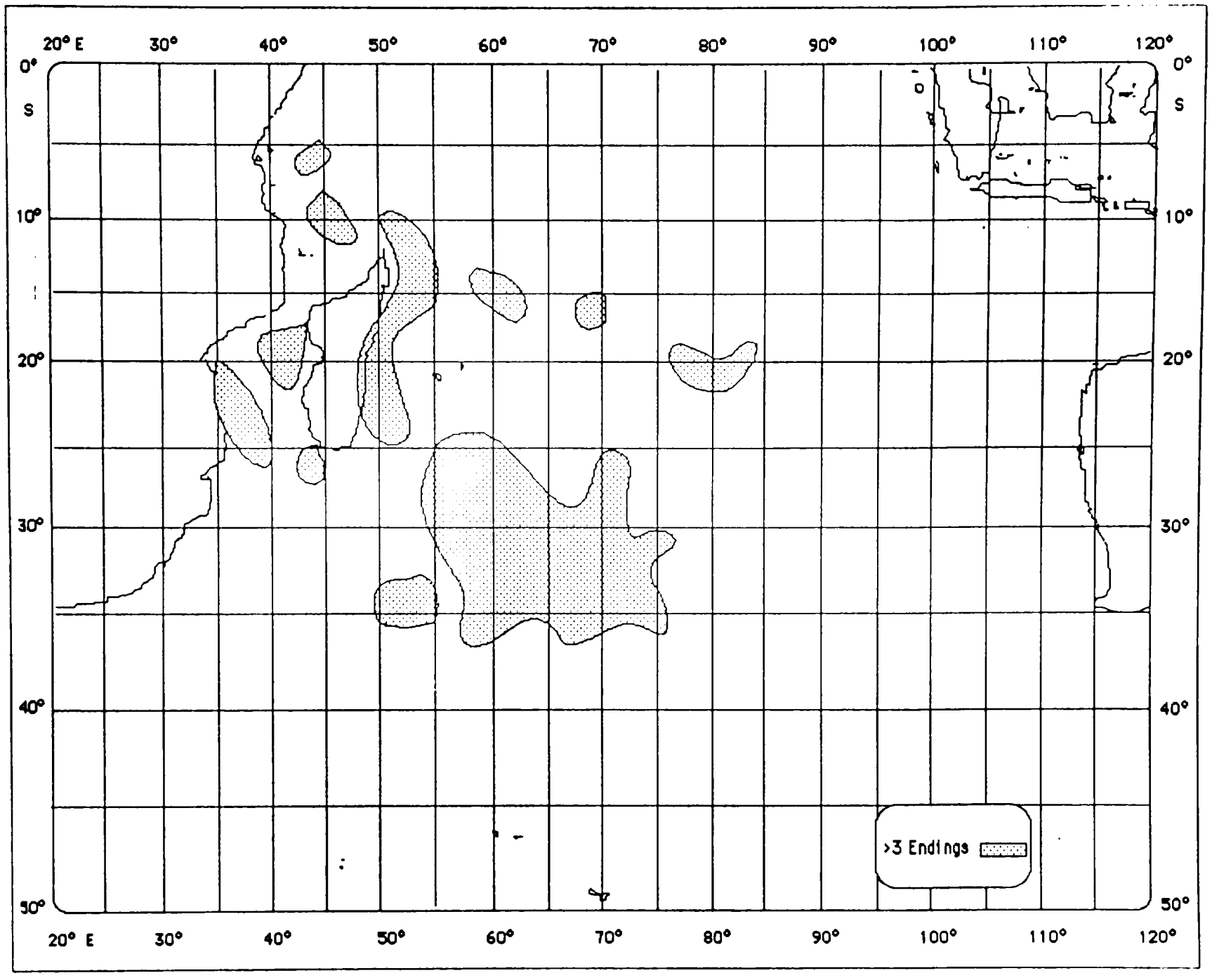

Figure 3.8. Most common places for tropical cyclones to dissipate. (1962-63 to 1986-87)

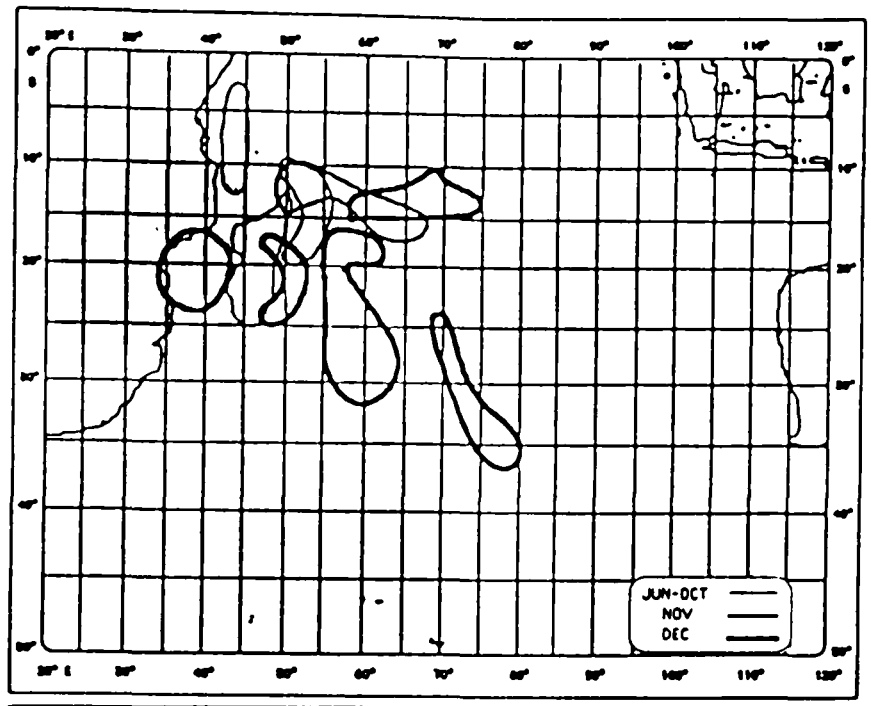

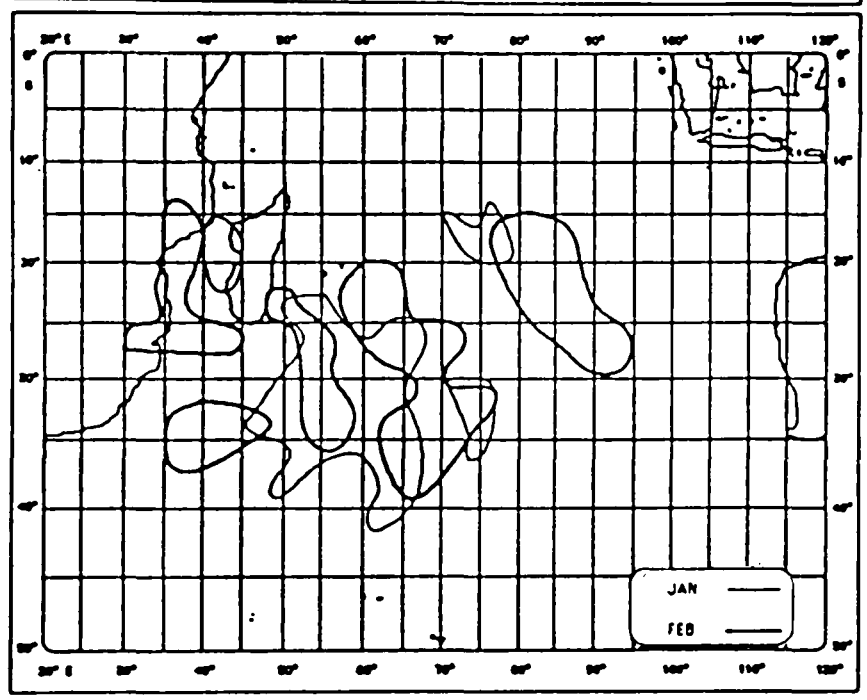

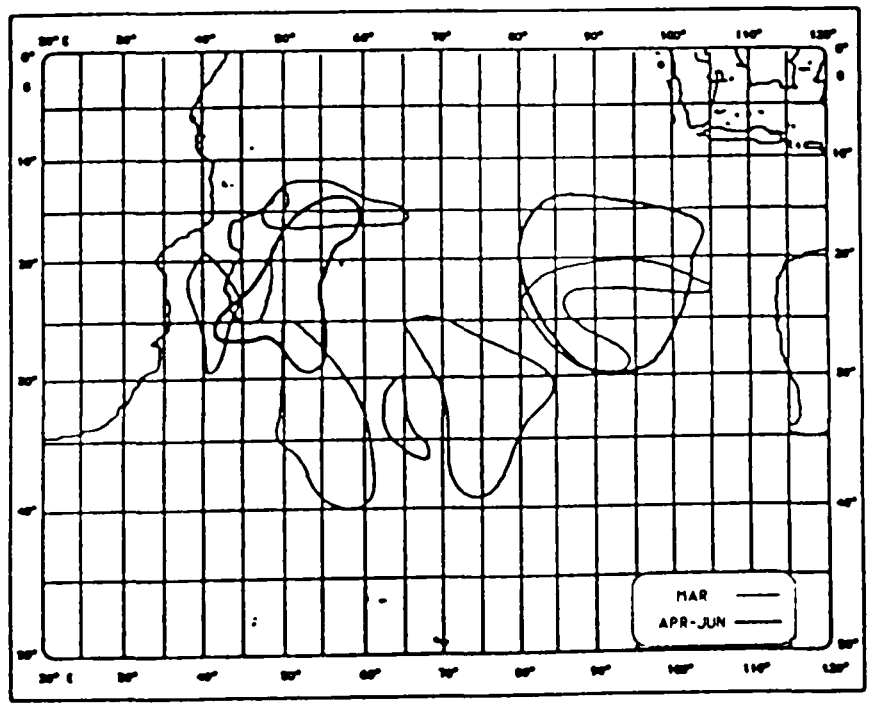

Figure 3.9 Progression of tropical cyclone dissipations as the cyclone year advances.

December sees a southward movement of the endings but there are as many as five different areas. Endings then consolidate into three areas in January as they continue to move southward.

In February, the areas remains pretty much in the same locations as in January. Movement is not to the north in March as we have seen with formations and affected areas, but to the east, which is in response to the affected areas eastern push. Finally, in April through June, a split in the endings is seen. One area is off of the east coast of Madagascar, while the other is in the extreme eastern third of the Indian basin.

3.5 Depressions

This section analyzes where storms of tropical depression strength occur, with Figure 3.10 showing the areas most affected by tropical depressions. The 12-storm isoline that was used in Figure 3.5 does not give a very good sense of where tropical depressions occur, so the eight-storm isoline is used. (This line corresponds to one depression every three years.) Using this isoline the same general shape and position as Figure 3.5 is observed. The one exception is the lack of tropical depressions over the southern four-fifths of Madagascar. There are several areas that see greater than one depression every two years. The main region being situated just off the east coast of Madagascar and running east to 85°E. Two other smaller regions are found north of 15°S between 90°E and 95°E, and in the Mozambique Channel just northeast of 20°S, 40°E.

Progression of the areas affected by depression follows the pattern seen before with the affected areas (Figure 3.11). For July through October the main depression areas are found in the north central to the

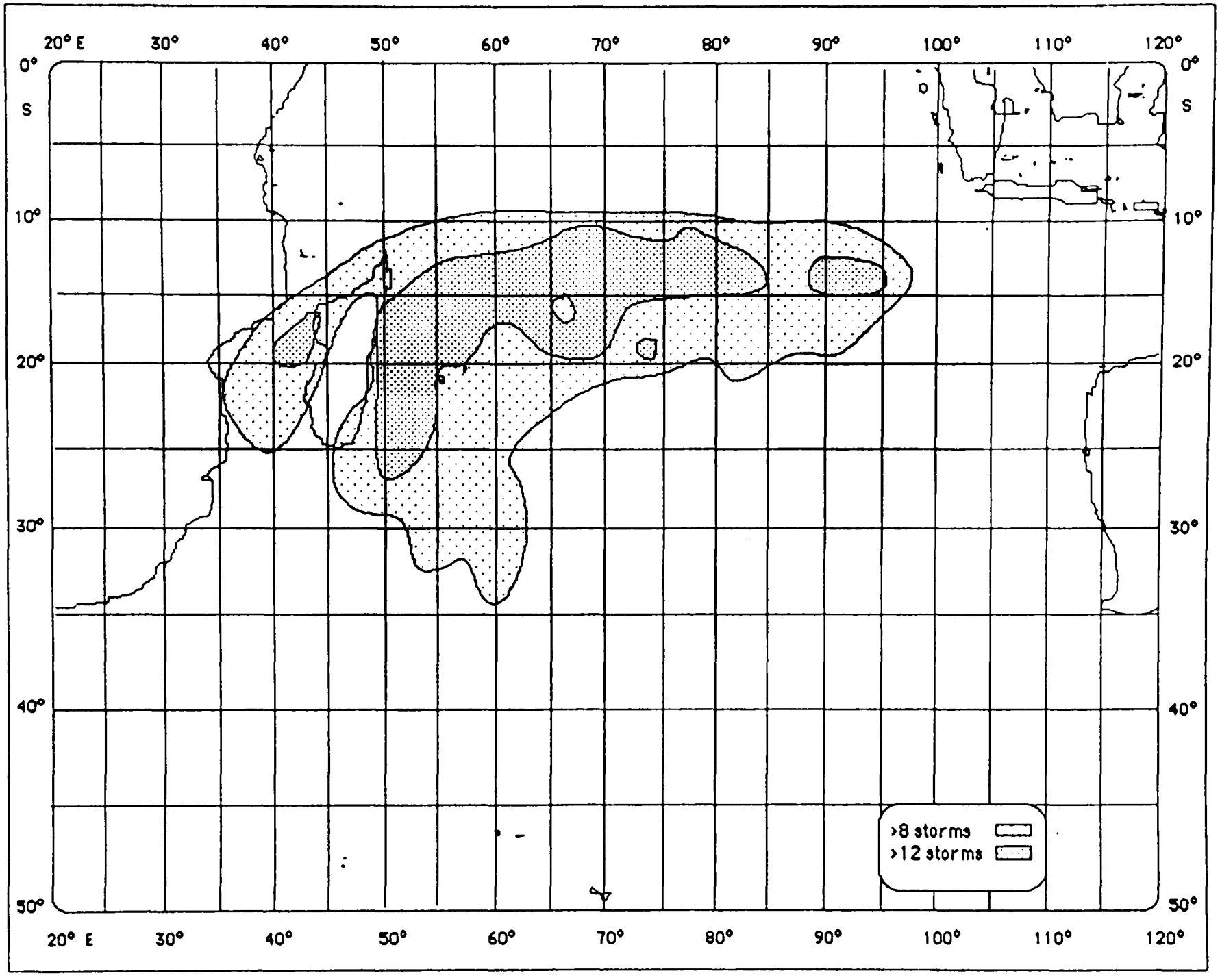

Figure 3.10. Areas most affected by tropical depressions.
(1962-63 to 1986-87)

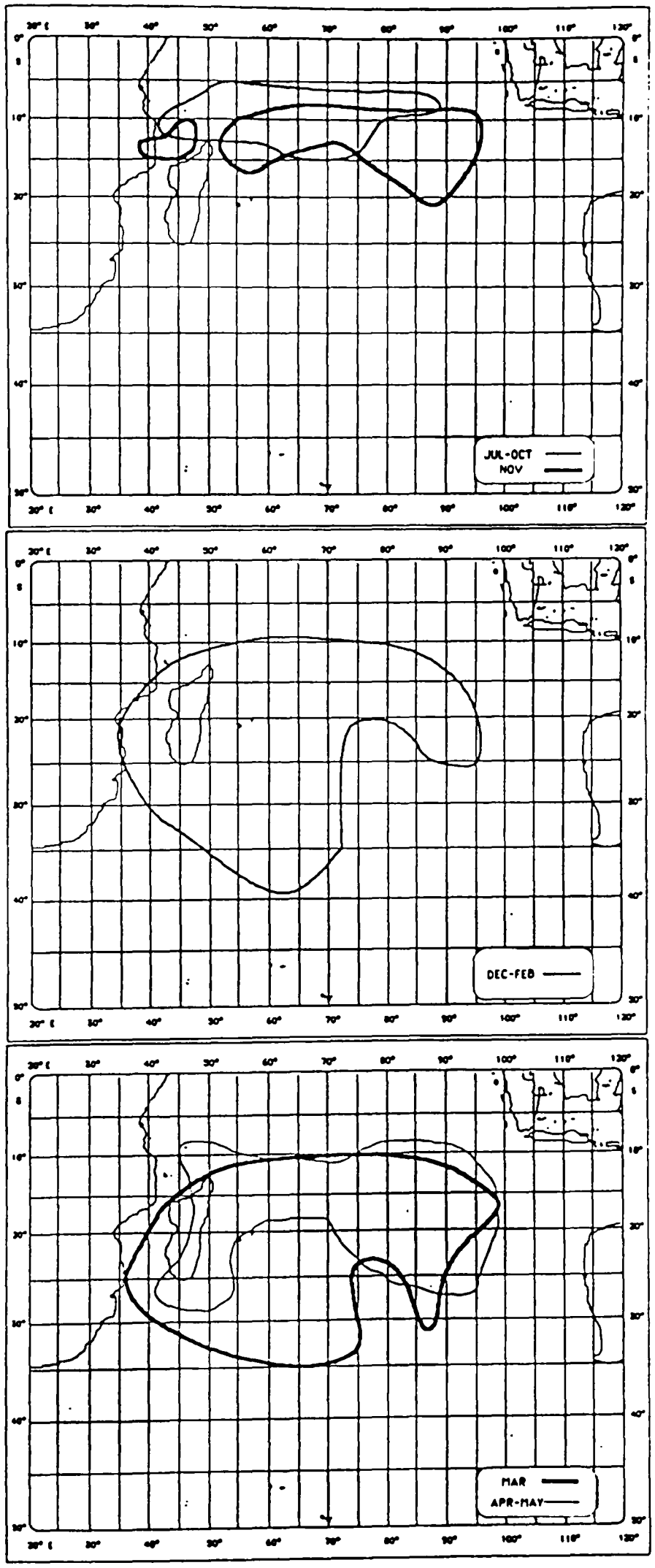

Figure 3.11 Progression of affected areas by tropical cyclones of tropical depression strength.

northwestern sections of the basin as the storms usually track to the west, without much southerly movement. In November, depressions can survive farther south so the areas move south and they spread back to the east as well. For December through February, depressions affect the greatest areas as approximately the western two-thirds of the basin are affected by depressions. With March comes the northward retreat of depressions in the west, but in the east they continue to advance southward. Depressions are limited in the northern part of the Mozambique Channel as they generally cannot maintain their strength as they cross Madagascar, but the southern third of the channel is affected by the storms which form there. In April and May, depressions usually do not affect any area west of Madagascar, but instead they recurve and stay in the eastern two-thirds of the basin.

3.6 Cyclones

Cyclones in the Southwest Indian Ocean have two main areas of effect: one is east of Madagascar, while the other is in the Mozambique Channel (Figure 3.12). The area in the Indian Ocean can be thought of as an inverted triangle. As in Figure 3.10, the initial isoline value had to be lowered in order to get a better sense for when cyclones occur. Four cyclones in 25 years corresponds to roughly one cyclone every six years. The base of the triangle is situated at about 15°S and extends from 50°E to around 90°E. The peak of the triangle is located at 30°S, 60°E. Inside this triangle is an area that has experienced greater than 12 cyclones during the last 25 years. This region is located between 60°E and 67 °E, and straddles the 20th parallel by 2½° on each side. The cyclone area in the Mozambique

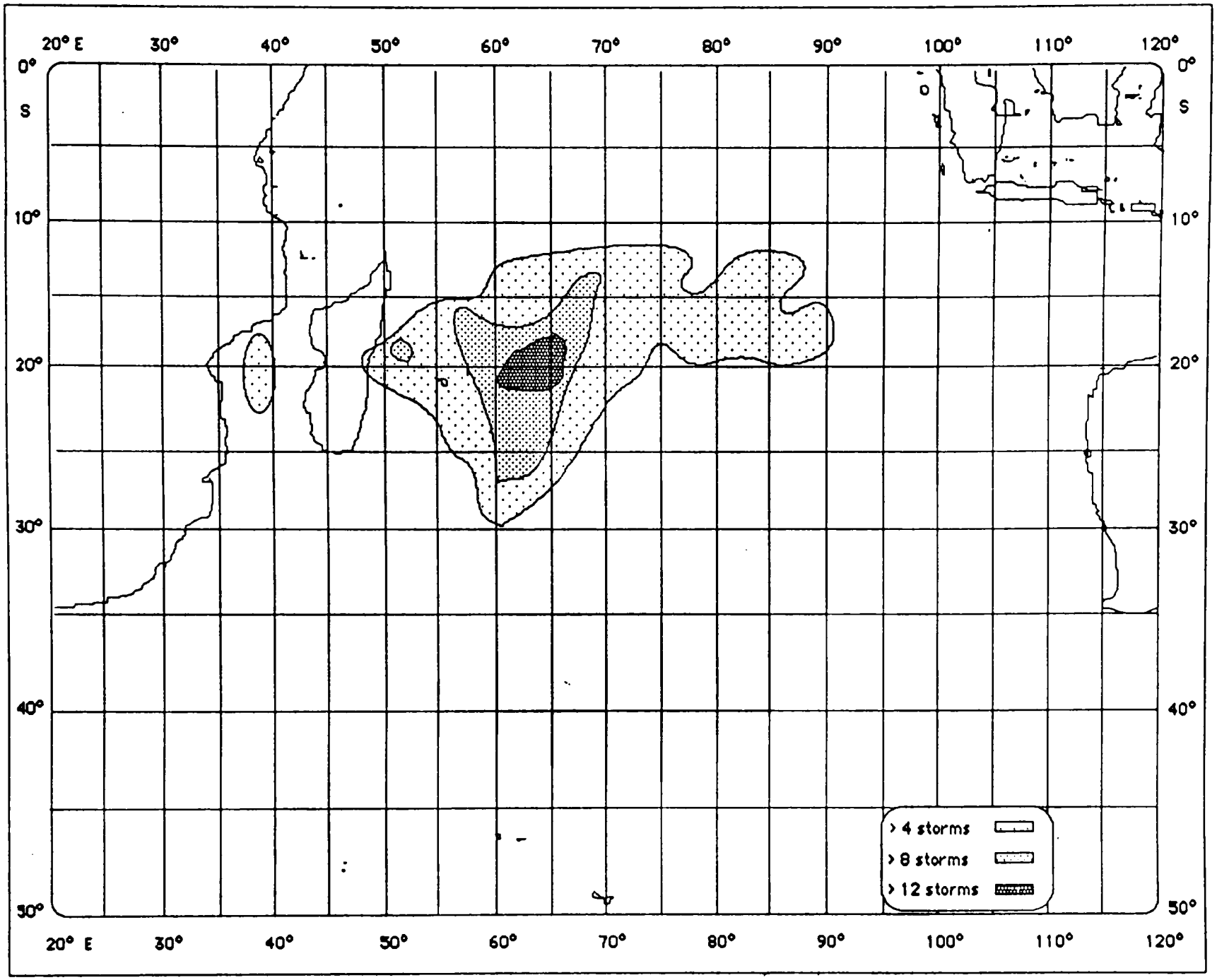

Figure 3.12. Areas most affected by tropical cyclones of cyclone intensity. (1962-63 to 1986-87)

Channel is located roughly in the middle of the channel, running from 17½°S to 22½°S.

No cyclones formed in July, August, or September so discussion of cyclone-affected areas must begin in October. Cyclones in October and November generally affect only the north central part of the South Indian Ocean (Figure 3.13). This area is usually found between 60°E and 85°E in the east-west direction and 5°S and 15°S north-south. In the month of December, cyclones have moved both south and west in their coverage. They only affect areas north of 20°S in the Mozambique Channel, while they extend as far south as 30°S in the Indian Ocean proper. The lack of cyclones in the southern Mozambique Channel is probably due to the fact that the cyclones are recurving across Madagascar and are losing their strength, or they continue their westward path and make landfall over Mozambique.

In January cyclones start to become more prevalent in the western two-thirds of the basin, as they leave a swath from 85°E all the way the African mainland. There is a hole in the cyclone swath over Madagascar as cyclones which form in the Indian Ocean weaken over the island, having little effect on the African mainland. Continental Africa does have to worry about storms that form in the Mozambique Channel. Although these storms are generally weaker than the ones that form over the open waters of the Indian Ocean they can still reach cyclone strength. In January the area affected by cyclones in the Channel shifts from then northern half to the entire Channel. Cyclones reach their southern limit in Janaury as they affect areas as far south as 35°S.

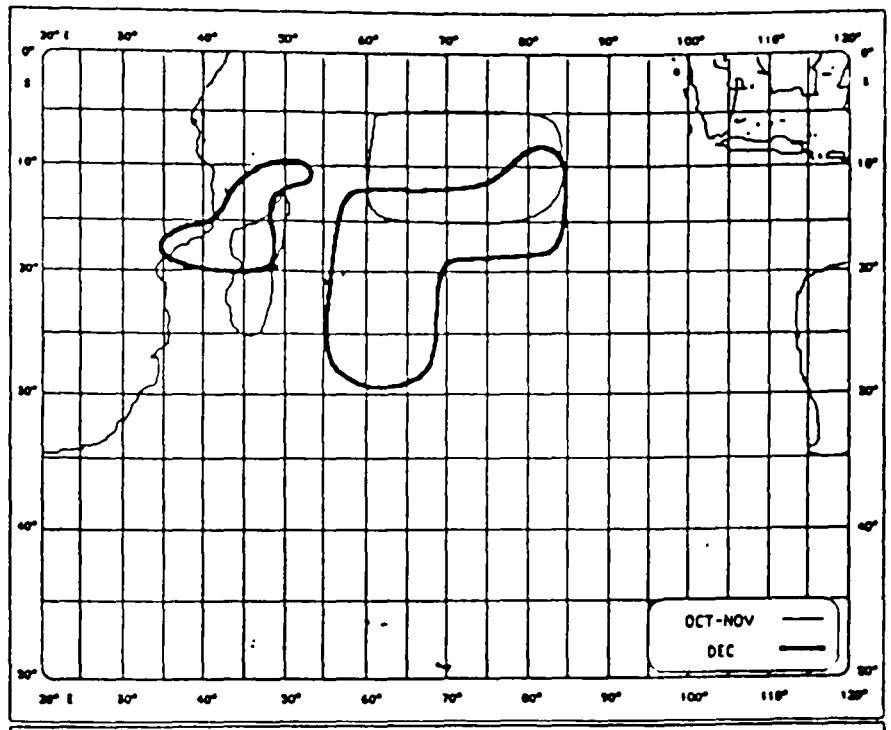

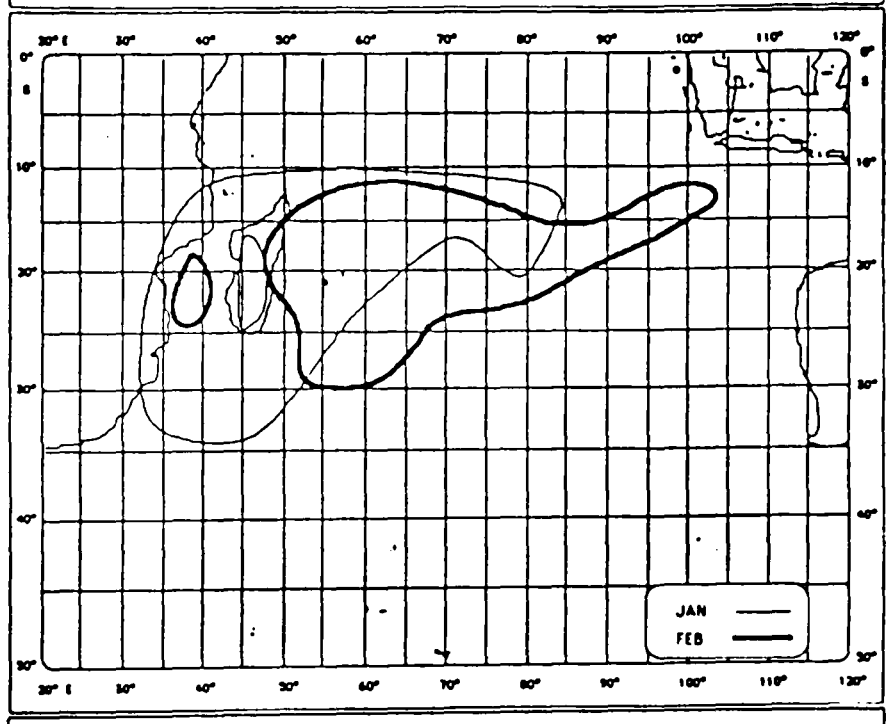

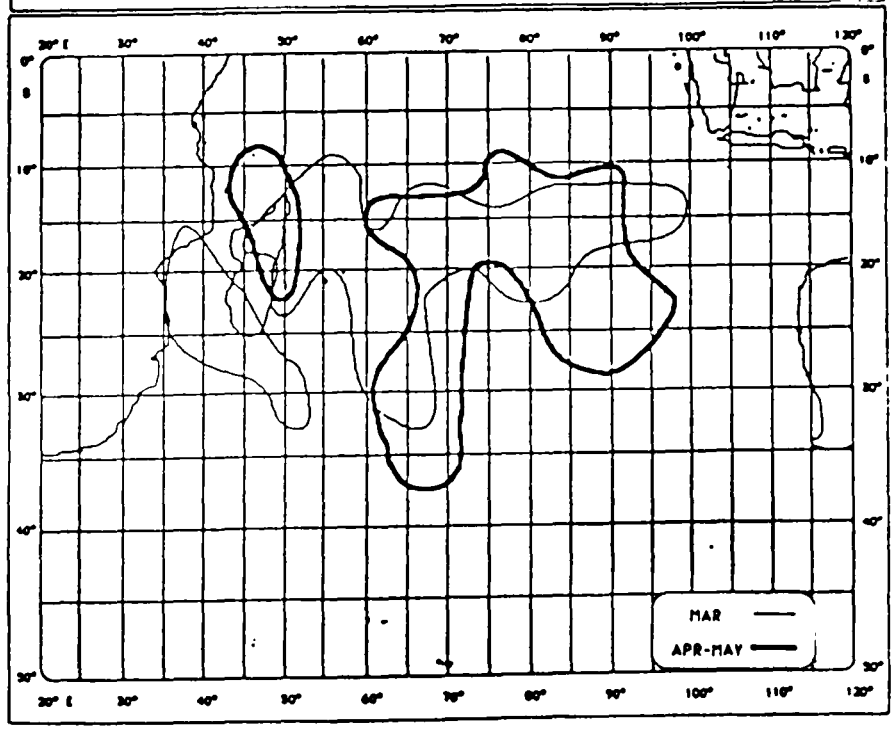

Figure 3.13 Progression of affected areas by tropical cyclones of cyclone strength.

An unusual pattern occurs in February as the cyclone area in the Mozambique Channel becomes separated from that in the Indian Ocean. This would not be peculiar if this area were not affected by cyclones again in March. Upon seeing this pattern it was thought that it might be a result of the contour interval, but upon further study of the data it turned out that no cyclones had been plotted in this empty area. This pattern then might result from one of three situations. 1) The cyclones had a westward movement and made landfall over Africa. 2) the cyclones were following an eastward path and they deteriorated over Madagascar, and 3) the cyclones weakened to below-cyclone intensity as they passed below the 25°S latitude line. As mentioned before, March cyclones again show an almost joined pattern between the southern Mozambique Channel and the Indian Ocean. The overall pattern is similar to that of Janauary except that cyclones in March extend farther east; and farther south in the eastern part of the basin. This is expected, however, after what has been seen with affected areas and depressions in the eastern sections. Cyclones in April and May are usually found east of 60°E as they either recurve quickly or have an eastward track to begin with, the exception being a smaller region just to the north and over northern Madagascar.

3.7 Translation Vectors

Due to the abundance of data in this catagory, a discussion will not be attempted here. Instead, a brief description of how to interpret the data in Figure 3.14, which is a plot of the average translation vector for the entire year, will be provided. The movement of tropical cyclones has been catagorized into one of eight compass headings. In Figure 3.14 each

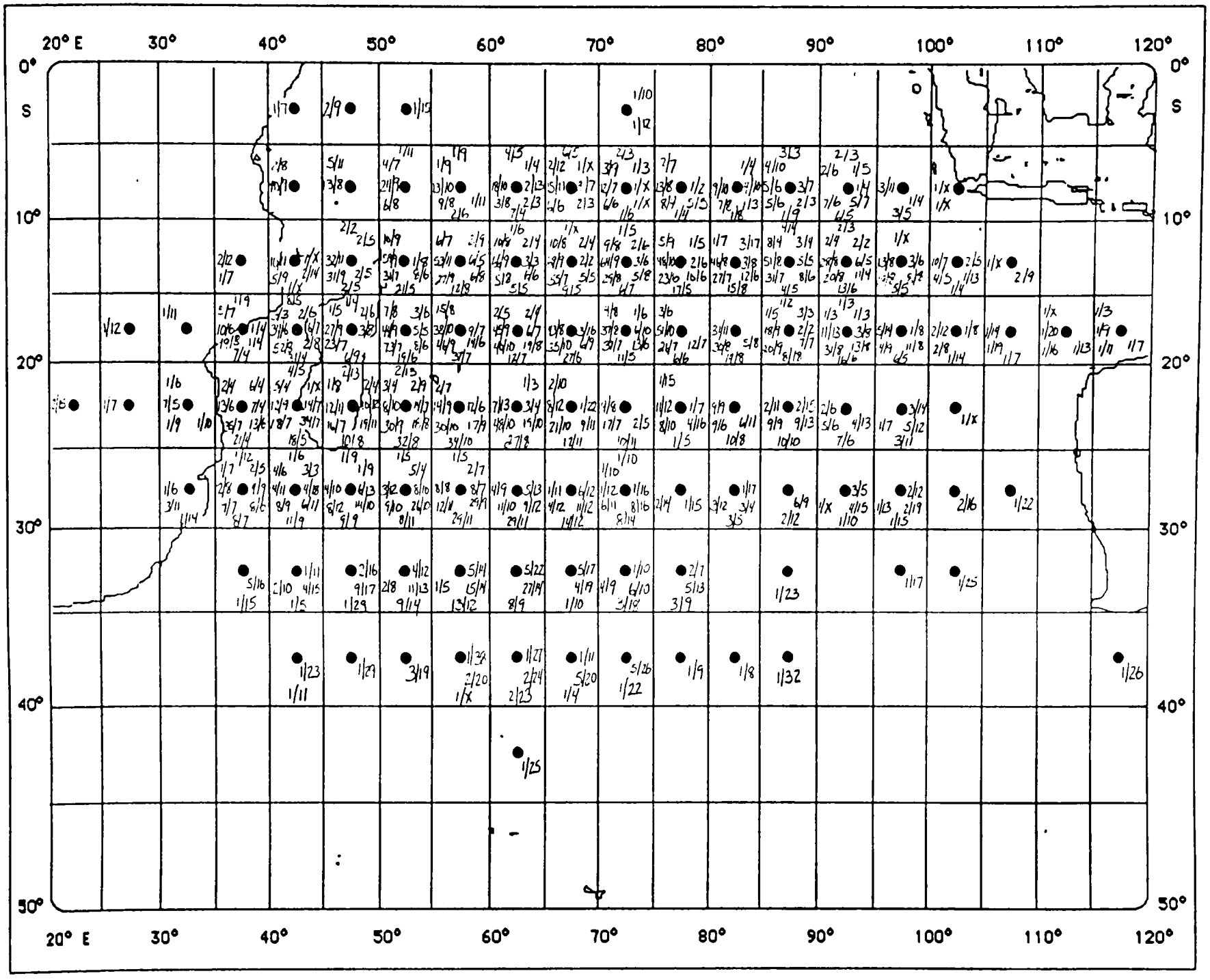

Figure 3.14. Translation vectors averaged over the entire year.

compass heading has two numbers divided by a slash. The first number is the number of storms which moved in that direction. The second number is the average speed (in knots) in that direction, rounded to the nearest whole number (Note: the translation vectors for each individual month are found in Appendix B, so that a climatologically-based forecast of a tropical cyclone's path might be made). If the speed of the storm was not able to be calculated a "x" is put in for the speed.

3.8 Recurvature

As we saw in Section 3.3 and again in 3.7, as tropical cyclones affect more southern areas, their direction of movement turns from west to east. An indication of where the direction changes from westward to eastward is recurvature. In the month of July since storms are usually weak, their course is erratic and movement toward the east is occasionally seen, but generally the movement is westward. For September through November almost all movement has a component to the west. December is the first month that storms really begin to recurve with an average latitude for the recurvature of 25°S, but there is also an area of eastward recurvature over Madagascar. This is due to the effect of Madagascar's terrain on the tropical cyclones which causes them to change their direction of travel (Figure 3.15). In Figure 3.15, a "W" is plotted if a majority of the storms in the particuar 2½° x 2½° square moved with a westerly component, while an "E" is plotted if the majority had an easterly component to their movement. If the same number of storms moved in each direction then a "-" is plotted.

Recurvature in January moves south to an average latitude of 27½°S. The recurvature over Madagascar also has moved south about 2½°. February

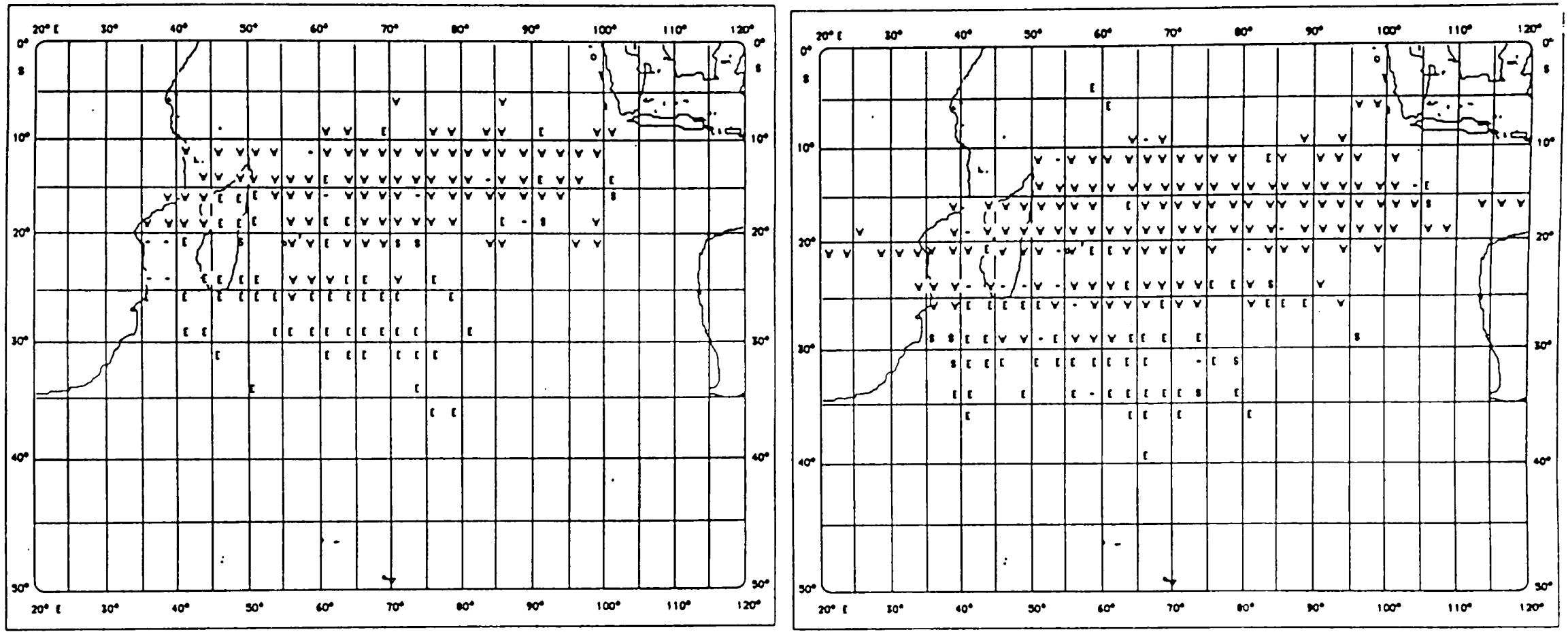

Figure 3.15. Primary direction of movement in each 2½° square for December (left) and February (right). Where the direction changes from west to east marks the point of recurvature.

recurvature has moved all the way to 30°S and the recurvature over Madagascar has disappeared (Figure 3.16). March sees a retreat to 27½°S again for the average recurvature along with an increased eastward movement of storms in the southeastern section of the basin. April and May see this trend in the east continue, although it is about 10° farther north in May. Storms in the west still continue to generally track westward, however.

3.9 Storms near Land

This section analyzes tropical cyclones which afffected selected locations. Table 3.3 shows the number of tropical cyclones which made landfall, passed over, came within 100 miles of land, or 100-200 miles of selected cities or islands. A tropical cyclone is placed in one of the four categories based on the position of its center. If a storm's path carries it to within 100 miles, it is not also listed in the 200 miles column. All the cities are shown in Figure 1.1, except Morondava which is located on the west coast of Madagascar at 20.2°S, 44.2°E. All three cities on Madagascar are quite frequently visited by tropical cyclones (all above 1.6 storms per year) with Tomatave (2.12 per year) on the east central coast leading the way.

Morondava on the west coast which was affected by eight fewer storms than Tomatave had eight landfalls; one and a half as many landfalls as Tomatave's three. Morondova's location was also good for it to be affected by four storms which were crossing Madagascar. Fort Dauphin also experienced three storms which were crossing over Madagascar, but these

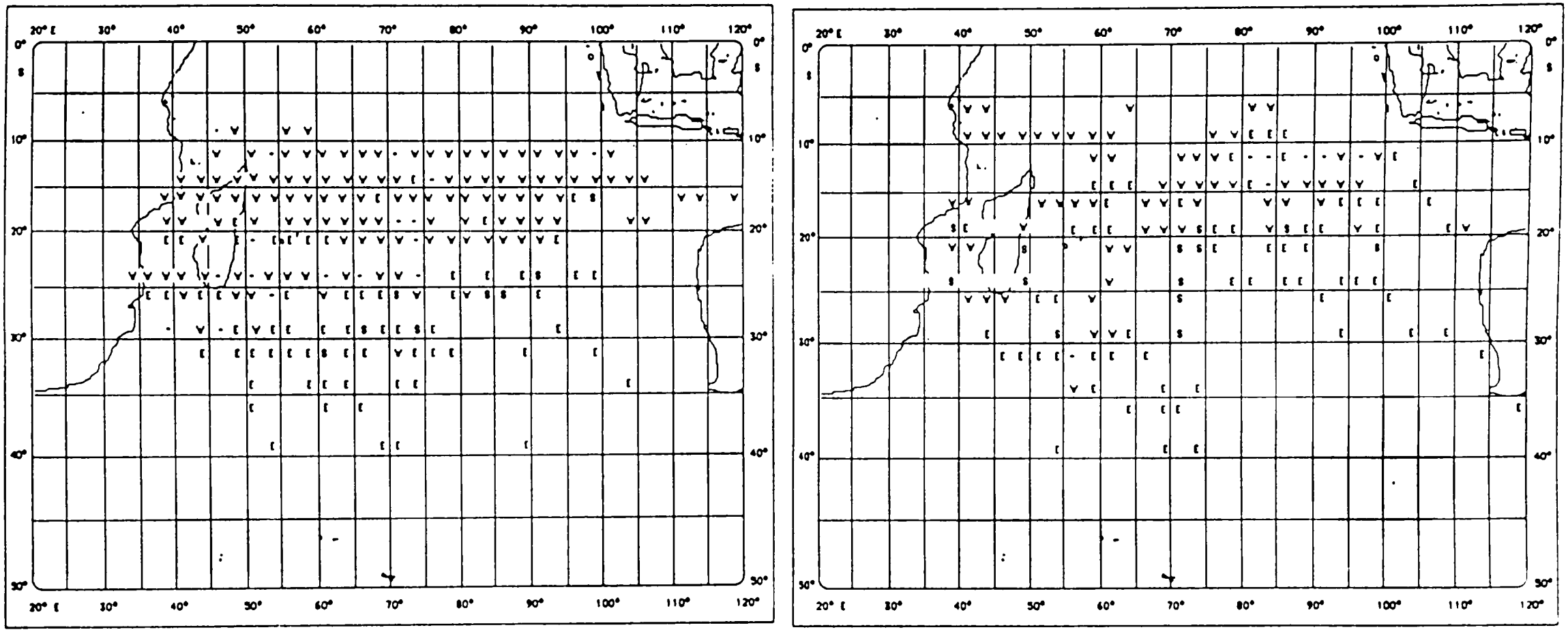

Figure 3.16. Primary direction of movement in each 2½° square for March (left) and April (right). Where the direction changes from west to east marks the point of recurvature.

Table 3.3 Number of tropical cyclones which affected selected cities and islands.

	Landfalls	Crossings	0-100 miles	100-200 miles	Total
Tamatave	3	1	22	27	53
Fort Dauphin	0	3	19	17	39
Morondava	5	4	17	22	45
Mocambique	1	0	9	18	28
Maputo	2	0	4	7	13
Mauritius	6	-	18	33	57
Reunion	6	-	15	26	47
West Coast Madagascar	38	28	25	5	68
East Coast Madagascar	43	24	16	14	73
East African Coast	15	4	24	16	55

tropical cyclones were west to east moving storms. It also had 19 storms (second only to Tomatave) pass within 100 miles.

On the African mainland the city of Mocambique, in northern Mozambique, was affected by a total of 28 storms (with only 10 coming closer than 100 miles), twice as many storms as its southern counterpart Maputo. While Mocambique can expect to have about one tropical cyclone per year (1.1) pass within 200 miles, Maputo averages only one storm every two years within the 200-mile range. At the bottom of the table is the total count for all tropical cyclones affecting either the east or west coast of Madagascar or over Africa. As expected, the east coast of Madagascar has the most storms making landfall (43) and affecting it (2.9 storms per year). The west coast of Madagascar follows with 38 landfalls and 2.7 tropical cyclones per year affecting it, and the east African coast has 15 landfalls and an average of 2.2 storms per year within 200 miles.

The figures for the islands of Reunion and Mauritius show that these islands can expect to have at least two storms per year pass within 200 miles of them (2.3 and 1.9, respectively). Both islands also average a tropical cyclone landfall about once every five years.

3.10 Looping Paths

Figure 3.17 shows all the looping paths of tropical cyclones during the 25-year period of this study. In all, 24 storms crossed their own paths, 10 of these were in the Mozambique Channel alone. An additional four were also located within 400 miles of Madagascar's eastern coast (three of these where within 200 miles of Reunion). These numbers indicate that interaction with land might cause tropical storms to have looping or

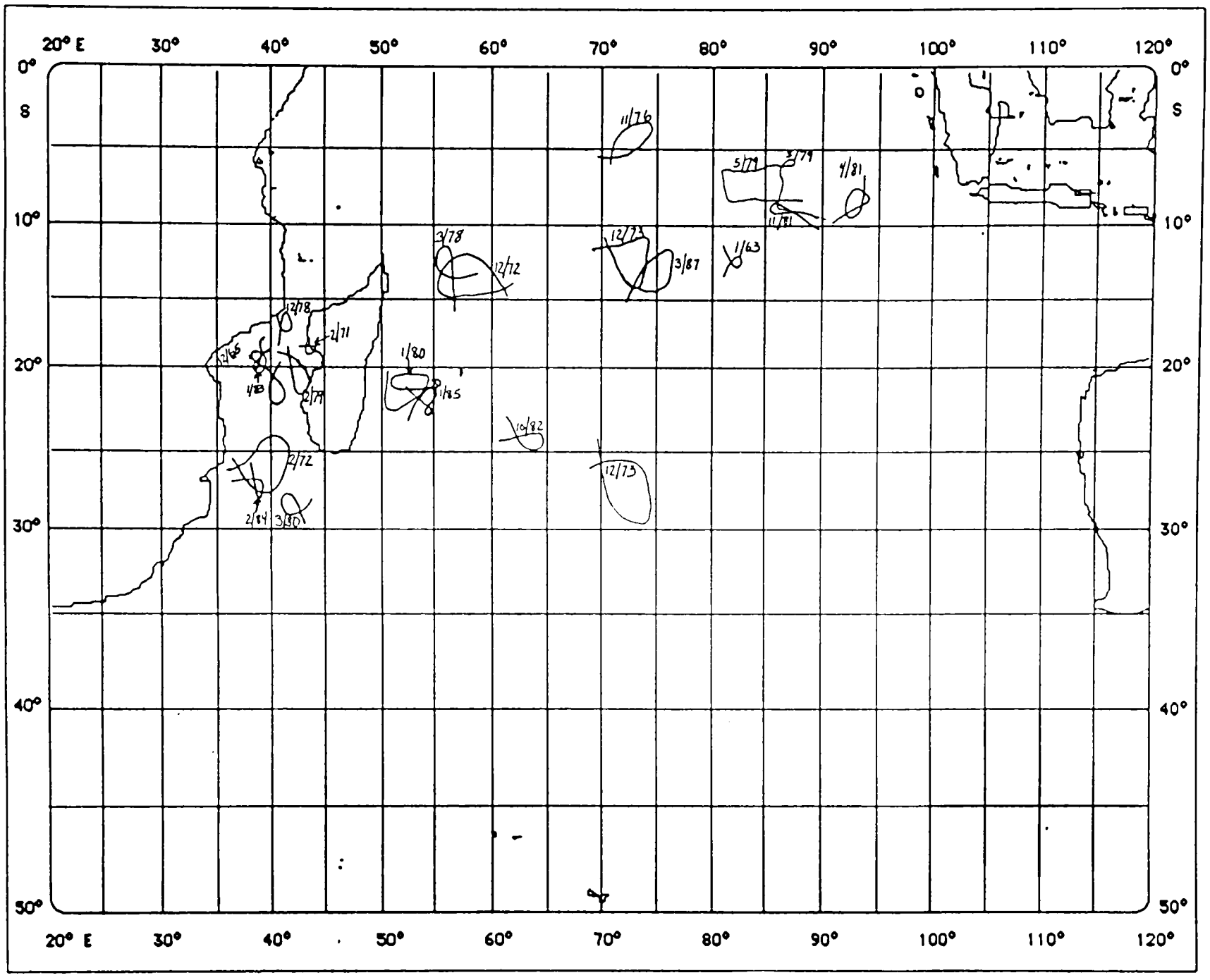

Figure 3.17. Locations of looping paths for Southwest Indian Ocean tropical cyclones. (1962-63 to 1986-87)

erratic paths. This could be due to the fact that the storm's circulation is interfered with and therefore it moves erratically, or it might be because the storm weakens.

CHAPTER 4

CONCLUSIONS

In the Southwest Indian Ocean tropical cyclone formation peaks during the months of December through March, as each of these months averages above 1.8 formations. The tropical cyclones usually form in the north central part of the basin and track west to southwest until they make landfall on the island of Madagascar or recurve to the southeast. A smaller number form in the Mozambique Channel and affect the African continent. These tropical cyclones are usually weaker than the ones which form in the Indian Ocean proper. The areas affected most by Indian Ocean proper storms are usually found between 10°S and 20°S when east of 70°E, but this area expands to around 32½°S, when west of 70°E. During the 25-year period of this study, an average of 10.1 tropical depressions and 3.5 cyclones occurred annually. Compare this to the Atlantic Ocean which averaged 11.0 tropical storms and 4.6 hurricanes (1887-1958). Although all months of the year have had tropical cyclones, January was the peak month with an average of almost three tropical cyclones, while June was the calmest seeing only one tropical cyclone in 25 years. Cyclone intensity storms occurred most often (one cyclone every two years) in a 2½° circle, centered on the island of Rodrigues (19.7°S, 63°E). Cyclones also saw their monthly peak in January (0.92 per year). The average latitude of recurvature for Southwest Indian Ocean tropical cyclones shifts between 20°S and 30°S. Finally, it appears that land has an influence on the

stability of tropical cyclone paths, as the majority of storms with looping paths were within 400 miles of land when their paths looped.

Southwest Indian Ocean tropical cyclones show similiarities to tropical cyclones in other basins. Their general westward movement with recurvature in the western part of the basin is also observed in the North Atlantic and the Northwest Pacific. Both basins also have islands (Hispaniola and Taiwan, respectively, for example) in their western areas which act as barriers to tropical cylones, although none are as effective as the island of Madagascar, which is probably due to Madagascar's greater size. Although all three islands have mountain peaks over 5000 feet, Madagascar's land area of 226,658 sq. miles (1000 miles in the north-south extent) is approximately 10 times greater than that of either Hispaniola or Taiwan (29,418 and 13,895 sq. miles, respectively). The other basins also do not show such a high frequency of tropical cyclone effect on the eastern basin areas. The Northeast Pacific tropical storms show recurvatures over Mexico, but the North Pacific is so broad that it actually consists of two cyclone basins. The Southwest Indian Ocean stands alone as the only cyclone basin with this characteristic.

It is hoped that this thesis will help to bring attention to this lightly studied basin, and that it may act as starting point for further studies. Although each storm in this study was categorized into an intensity stage, an improvement in the data that the author recommends is the inclusion of the maxium sustained wind at each 12-hour time. This type of data could be used for a better evaluation of the intensity of landfall wind speed, and would allow for more study into the effects of Southwest Indian Ocean tropical cyclones on the inhabitants and their environment. With the

definition of activity portrayed in this thesis, a topic for a future thesis might be the causes of tropical cyclogenesis in the Southwest Indian Ocean. Finally, it is the author's hope that since climatology of previous storm tracks is an important factor in the forecasting of tropical cyclones in the basin (McBride and Holland, 1987), that data in this thesis will aid in the forecasting and tracking of these storms, and help lessen the damages and injuries in the region.

REFERENCES

Appadu, S.N. Sok, 1987: Technical report-CS10: Cyclone season of the southwest Indian Ocean 1986-1987. Port Louis, Mauritius: Mauritius Government Printing Office, 34 pages.

Cooper, Keith H., 1984: The three tragedies of the Mfolozi floodplain, Wildlife, 38, 104-105.

Cyclones interessant Madagascar 1958-1973 [Cyclones affecting Madagascar 1958-1973], 1974: Antanarivo, Madagascar, 22 pages.

DeAngelis, Dick, 1970: Tropical cyclones around the world. 1. The early pioneers, Mariners Weather Log, 14, 16-19.

_____, 1973,1975-1987: Hurricane Alley, Mariners Weather Log, 17, 227-230; 19, 225-228, 351-352; 20, 17-18, 210-211; 21, 16-19; 22, 21, 96-97, 182-183, 265-266, 337; 23, 91-93; 24, 24-28, 107-110, 198-201, 282-285, 353-357, 424-429; 25, 18-20, 95-96, 178-181, 257-259, 329-330, 393-396; 26, 27-29, 95-99, 154-158, 220-224; 27, 34-40, 106-109, 172-176, 240-244; 28, 38-45, 113-116, 182-185, 247-249; 29, 36-40, 103-106, 170-177, 247-249; 30, 34-39, 100-104, 164-166, 223-227; 31, 1, 38-39, 2, 38-39, 3, 122-125.

Desaux, L. Sylvio, 1982: Technical report-CS6: The cyclone season in the South-West Indian Ocean 1980-1981. Port Louis, Mauritius: Mauritius Government Printing Office, 35 pages.

Dvorak, V.F., 1973: NOAA technical memorandum NESS 45: A technique for the analysis and forecasting of tropical cyclone intensities from satellite pictures. Washington D.C.

_____, 1975: Tropical cyclone intensity analysis and forecasting from satellite imagery, Monthly Weather Review, 103, 420-430.

Fairbridge, Rhodes W., 1966: The encyclopedia of oceanography, New York, New York, 370-400.

Gosling, Melanie, 1984: Cyclone 'Domoina': The Natal Parks Board counts the cost, Wildlife, 38, 97-101.

Greig, John, 1984: The impact of the tropical cyclone 'Domoina', Wildlife, 38, 91-95.

Long, Mark, 1985: 1985 world satellite almanac. The complete guide to satellite transmission and technology. Comn Tek Publishing Company.

McBride, John L. and Holland, Greg J., 1987: Tropical cyclone forecasting: A worldwide summary of techniques and verification statistics, Bulletin of the American Meteorogical Society, 68, 1230-1238.

NOAA satellite programs briefing, 1985: Washington D.C.

Padya, B.M., 1976: Cyclones of the Mauritius region. Port Louis, Mauritius: The Mauritius Printing Cy. Ltd, 151 pages.

_____, 1984: The climate of Mauritius. Port Louis, Mauritius: The Mauritius Printing Cy. Ltd., 45-49.

Rogers, Jeffery, Spring Quarter 1986: Class notes for Geography 623.02 Synoptic meteorology : Severe storm forecasting by radar and satellite. The Ohio State University.

Saison cyclonique 1987-1988 à Madagascar [Cyclone season of Madagascar, 1987-1988], 1988: Antanarivo, Madagascar, 28 pages.

South African weather bureau newsletter, 1984: Pretoria, South Africa.

Technical report-CS7: Southwest Indian Ocean cyclone seasons: 1981-1982, 1982-83, 1983-1984, 1984: Port Louis, Mauritius: Mauritius Government Printing Office, 64 pages.

Yan, M. Lee Man, 1986: Technical report-CS8: Cyclone season of the southwest Indian Ocean 1984-1985, Port Louis, Mauritius: Mauritius Government Printing Office, 30 pages.

_____, 1987: Technical report-CS9: Cyclone season of the southwest Indian Ocean 1985-1986, Port Louis, Mauritius: Mauritius Government Printing Office, 38 pages.

APPENDIX A

STORM TRACKS FOR EACH OF THE 25 CYCLONE SEASONS

Table A.1. Listing of all tropical cyclones in this study. Table A.1 is set up as follows: Storm number as plotted on Figures A.1 through A.25, date of storm, and name if applicable. Note: Mauritius-Madagascar names are typed normally, while the Australian names are typed in capital letters.

	1962-63	
1	OCT 9-16	Amy
2	DEC 2-6	Bertha
3	DEC 16-29	Cecile
4	JAN 11-19	Delia
5	JAN 1-11	-----
6	JAN 29-FEB 4	-----
7	FEB 3-9	Emma
8	FEB 13-22	Grace
9	FEB 10-19	Fanny
10	FEB 27-MAR 2	Hilda
11	MAR 4-5	Irene
12	MAR 5-11	Julie
13	MAR 15-24	-----

	1963-64	
1	DEC 6-14	Amada
2	DEC 23-28	Betty
3	JAN 11-16	Christine
4	JAN 15-22	Danille
5	JAN 29-FEB 10	Eillen
6	FEB 20-24	Francine
7	FEB 23-MAR 4	Gisele
8	FEB 25-MAR 1	-----
9	MAR 4-17	Harriet
10	MAR 7-16	-----
11	MAR 30-APR 3	Ingrid
12	APR 29-MAY 3	-----
13	MAY 3-10	-----

	1964-65	
1	DEC 4-8	Arlette
2	DEC 7-10	Bessie
3	DEC 19-21	Connie
4	DEC 23-28	-----
5	DEC 24-25	Doreen
6	JAN 5-10	Freda
7	JAN 6-8	Ginette
8	JAN 15-16	Hazel
9	JAN 18-28	Iris
10	FEB 6-9	Judy
11	FEB 10-18	Kathleen
12	FEB 14-26	-----
13	FEB 18-21	-----
14	FEB 20-26	Lesley
15	FEB 23-24	-----
16	FEB 24-MAR 11	Peggy
17	MAR 23-APR 3	-----
18	APR 27-MAY 5	Rose

	1965-66	
1	AUG 10-14	-----
2	AUG 17-18	Brenda
3	NOV 31-DEC 5	-----
4	DEC 25-JAN 10	Claude
5	DEC 31-JAN 2	-----
6	DEC 25-29	-----
7	DEC 30-JAN 1	-----
8	JAN 3-11	Denise
9	JAN 12-14	-----
10	JAN 17-19	-----
11	JAN 31-FEB 1	Francine
12	FEB 11-14	-----
13	FEB 25-MAR 8	-----
14	FEB 15-17	Germaine
15	FEB 21-23	Hilary
16	MAR 4-11	Ivy
17	MAR 15-29	-----
18	MAR 22-26	Kay
19	APR 23-MAY 1	-----

	1966-67	
1	SEP 28-OCT 6	Angela
2	NOV 23-30	-----
3	DEC 11-21	Colette
4	DEC 22-JAN 2	Elisa
5	DEC 23-26	-----
6	DEC 28-30	Daphne
7	DEC 28-JAN 1	-----
8	JAN 8-18	Gilberte
9	FEB 8-17	Huguette
10	APR 6-12	-----
11	MAY 5-21	-----

	1967-68	
1	DEC 8-22	-----
2	DEC 20-27	Carmen
3	DEC 29-JAN 9	Elspeth
4	DEC 30-JAN 2	Debby
5	JAN 8-14	Flossie
6	JAN 9-31	Georgette
7	JAN 17-26	Henriette
8	JAN 20-26	-----
9	FEB 11-15	Ida
10	FEB 17-26	-----
11	MAR 6-13	Karina
12	MAR 26-APR 3	Monica
13	APR 5-12	-----

Table A.1. (continued)

	1968-69	
1	OCT 29-NOV 3	Annie
2	DEC 16-24	-----
3	DEC 27-JAN 3	Berthe
4	JAN 1-4	-----
5	JAN 15-16	-----
6	JAN 27-FEB 9	Dany
7	FEB 5-13	Fanny
8	FEB 13-19	Gillette
9	MAR 20-27	Helene
10	MAR 29-APR 6	-----

	1969-70	
1	AUG 19-21	-----
2	OCT 8-14	Blanche
3	NOV 17-20	Corrine
4	JAN 4-17	Francoise
5	JAN 7-10	Genevieve
6	JAN 11-19	Hermine
7	JAN 22-27	Iseult
8	FEB 1-14	-----
9	FEB 9-19	-----
10	FEB 9-MAR 2	Jane
11	MAR 17-24	Katia
12	MAR 22-APR 1	-----
13	MAR 23-30	Louise

	1970-71	
1	OCT 5-9	Betsy
2	NOV 5-13	Claudine
3	NOV 21-30	-----
4	DEC 14-28	Domonique
5	DEC 20-23	-----
6	JAN 17-31	-----
7	JAN 17-FEB 5	Felice
8	JAN 21-31	Ginette
9	FEB 3-12	Helga
10	FEB 12-15	-----
11	FEB 15-22	Nelly
12	FEB 16-25	Kalinka
13	FEB 21-28	Lise
14	MAR 10-17	-----
15	MAR 15-24	Joelle

	1971-72	
1	JUL 9-16	-----
2	DEC 10-23	Agnes
3	JAN 2-7	Belle
4	FEB 2-7	Caroline
5	FEB 4-10	Dolly
6	FEB 7-21	Eugenie
7	FEB 10-27	Fabienne
8	FEB 23-29	-----
9	FEB 29- MAR 11	Hermione

	1972-73	
1	NOV 26-DEC 2	
2	DEC 8-25	Beatrice
3	JAN 2-12	Charlotte
4	JAN 11-15	Dorothee
5	JAN 18-21	Emmanuelle
6	JAN 19-21	Faustine
7	JAN 22-FEB 3	Gertrude
8	JAN 24-FEB 5	Hortense
9	FEB 14-19	Isis
10	FEB 14-27	Jessy
11	FEB 25-MAR 5	Kitty
12	MAR 4-15	Lydie
13	MAY 1-6	-----

	1973-74	
1	SEP 12-23	Alice
2	OCT 16-28	Bernadette
3	DEC 14-22	Christiane
4	DEC 20-JAN 3	Dadida
5	DEC 31-JAN 6	Esmeralda
6	JAN 19-20	-----
7	FEB 22-MAR 2	Ghislaine
8	APR 14-23	Honorine

	1974-75	
1	DEC 23	-----
2	JAN 8-12	Blandine
3	JAN 11-21	Camille
4	JAN 16-28	Deborah
5	JAN 25-26	-----
6	FEB 1-2	-----
7	FEB 2-9	Gervaise
8	FEB 22-26	Heloise
9	MAR 9-11	OS-16
10	MAR 13-19	Ines
11	APR 20-22	OS-22

Table A.1. (continued)

	1975-76	
1	NOV 20-29	Audirey
2	DEC 6-17	Barbara
3	JAN 7-21	Clotilde
4	JAN 11-27	Danae
5	MAR 11-12	OS-12
6	MAR 25-26	-----
7	MAR 27-APR 10	Gladys
8	APR 5-12	Heliotrope

	1976-77	
1	OCT 5-15	Agathe
2	NOV 7-29	Brigitta
3	JAN 1-16	Clarence
4	JAN 17-23	Domitile
5	JAN 25-FEB 10	Emilie
6	JAN 26-FEB 10	Fifi
7	FEB 2-8	Gilda
8	FEB 8-MAR 2	Io
9	FEB10-MAR 3	Hervea

	1977-78	
1	NOV 19-29	Aurore
2	DEC 4-10	-----
3	DEC 15-22	SAM
4	DEC 26-28	-----
5	DEC 28-JAN 2	-----
6	JAN 16-23	Fleur
7	JAN 26-31	-----
8	JAN 27-FEB 5	-----
9	FEB 10-14	-----
10	FEB 12-20	-----
11	MAR 4-9	-----
12	MAR 14-18	-----
13	MAR 15-19	-----
14	MAR 16-29	WINNIE
15	MAR 18-22	Mary Lou

	1978-79	
1	NOV 19-23	OS-22
2	DEC 13-JAN 5	OS-23
3	DEC 20-26	OS-24
4	JAN 3-13	Benjamine
5	JAN 31-FEB 12	Celine
6	FEB 4-14	Dora
7	FEB 11-18	Estelle
8	FEB 14-18	-----
9	MAR 7-13	Gelie
10	MAR 16-20	IVAN
11	MAR 23-31	Helios
12	APR 6-15	Idylle
13	APR 9-13	JANE
14	APR 28- MAY 9	KEVIN

	1979-80	
1	NOV 25-DEC 6	Albine
2	DEC 10-28	Claudette
3	DEC 15-21	Bernice
4	DEC 24- JAN 2	Danitza
5	JAN 17-29	Hyacinthe
6	FEB1-7	Jacinthe
7	FEB 20-28	FRED
8	FEB 25-MAR 13	Kolia
9	MAR 8-17	Laure
10	MAR 14-20	OS-15

	1980-81	
1	NOV 9-14	Adelaide
2	NOV 22-DEC 1	Bettina
3	DEC 2-9	Christelle
4	DEC 17-19	Diana
5	DEC 28-JAN 1	Edwige
6	JAN 4-10	Florine
7	JAN 14-18	Gaelle
8	JAN 28-FEB 4	Helyette
9	FEB 16-23	Iadine
10	MAR 1-10	Johanne
11	MAR 28-APR 6	Klara
12	APR 4-13	OLGA
13	APR 6-14	LISA
14	MAY 22-30	PADDY

Table A.1..(continued)

	1981-82	
1	JUL 25-38	-----
2	OCT 21-27	ALEX
3	NOV 3-11	Armelle
4	DEC 18-24	Benedicte
5	DEC 29-JAN 4	Clarisse
6	JAN 6-21	Damia
7	JAN 11-16	DAPHNIE
8	JAN 30-FEB 6	Electre
9	FEB 22-25	OS-12
10	MAR 15-20	OS-16
11	MAR 16-25	Justine
12	APR 23-MAY 2	Karla

	1982-83	
1	OCT 29-31	Arilisy
2	DEC 1-9	Bemany
3	DEC 19-20	Clera
4	DEC 24-31	Dadafy
5	JAN 10-17	Elinah
6	FEB 5-8	OS-12
7	APR 19-30	NAOMI
8	JUN 22-23	Feby

	1983-84	
1	NOV 13-14	PEARL
2	NOV 22-25	OS-45
3	DEC 6-15	Andry
4	DEC 21-29	Bakoly
5	JAN 5-7	Caboto
6	JAN 18-30	Domoina
7	JAN 22-25	Endoara
8	JAN 24-30	Fanja
9	JAN 29-30	Galy
10	FEB 7-22	Haja
11	FEB 11-21	Imboa
12	FEB 5-22	Jamimy
13	MAR 11-17	DARYL
14	APR 6-16	Kamisy

	1984-85	
1	NOV 20-23	Anety
2	DEC 2-10	Bobalaly
3	JAN 9-22	Celestina
4	JAN 25-FEB 2	Ditra
5	FEB 3-10	Estera
6	FEB 10-18	HUBERT
7	FEB 13-17	Felixsa
8	FEB 13-21	ISABEL
9	FEB 15-27	Gerimena
10	FEB 18-21	OS-24
11	MAR 7-14	KRISTY
12	APR 7-19	Helisaonina
13	APR 12-18	MARGOT

	1985-86	
1	DEC 22-26	Aliredy
2	JAN 5-10	Beorbia
3	JAN 7-19	Costa
4	JAN 10-18	Delifinia
5	JAN 10-13	OPHELIA
6	JAN 29-FEB 11	Erinesta
7	FEB 6-15	Filomena
8	FEB 19-MAR 1	Gista
9	MAR 8-19	Honorinia
10	MAR 11-19	Iarima
11	MAR 26- APR 4	Jefotra
12	APR 7-13	Krisostoma
13	MAY 8-13	Lila

	1986-87	
1	SEP 23-29	OS-1
2	AUG 1-3	OS-34
3	JAN 16-22	Alinina
4	FEB 6	Benazava
5	FEB 9-18	Clotilda
6	MAR 2-16	Daodo
7	APR 20-28	Elizabeta

Since the magnetic tape from the National Climatic Data Center did not report the names of the storms for the years 1962-63 to 1981-82, alternative sources had to be found (Cyclones interessant Madagascar 1958-1973, 1974; DeAngelis, 1973, 1975-1979; DeSaux, 1982; Padya, 1984 and Technical Report-CS7, 1984). The two sources used to cover the final five years of this study already had the tropical cyclone names reported.

Figures A.1 through A.25 were produced by plotting the 12-hour (00Z and 12Z) positions (as reported by the three sources stated in section 1.2). Then the assumption was made that the tropical cyclone moved in a straight line between the points.

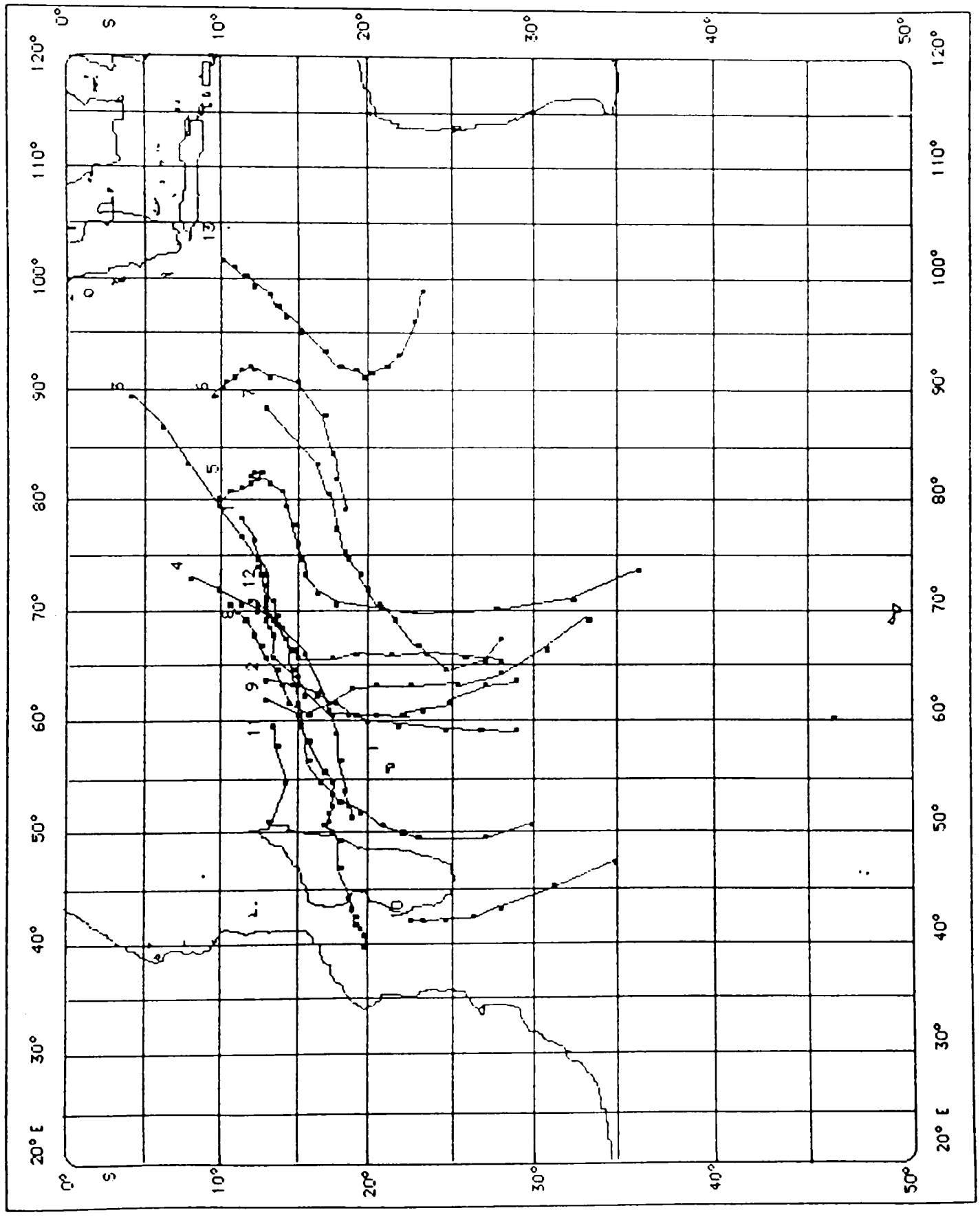

Figure A.1. Tropical cyclone tracks for season 1962-63.

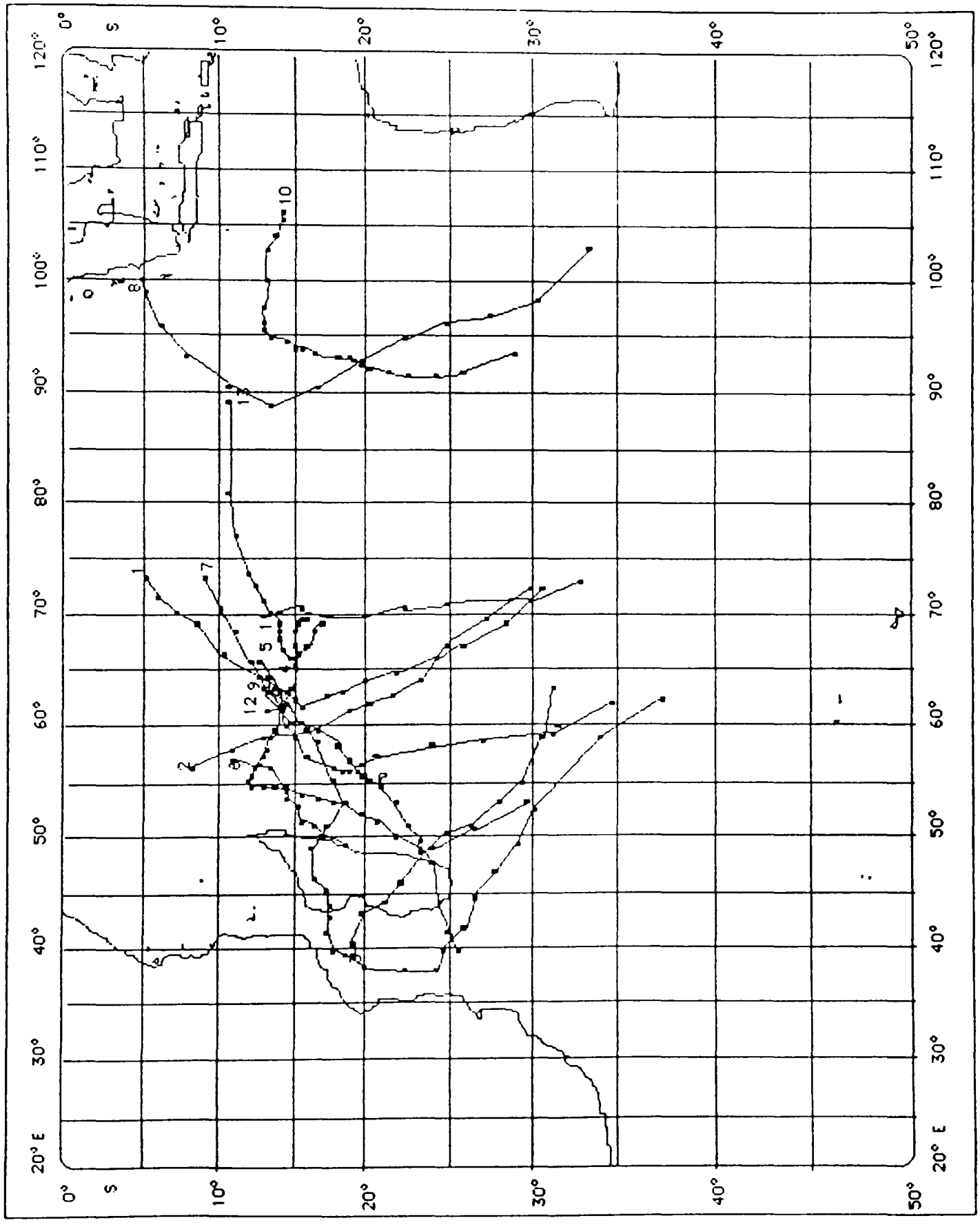

Figure A.2. Tropical cyclone tracks for season 1963-64.

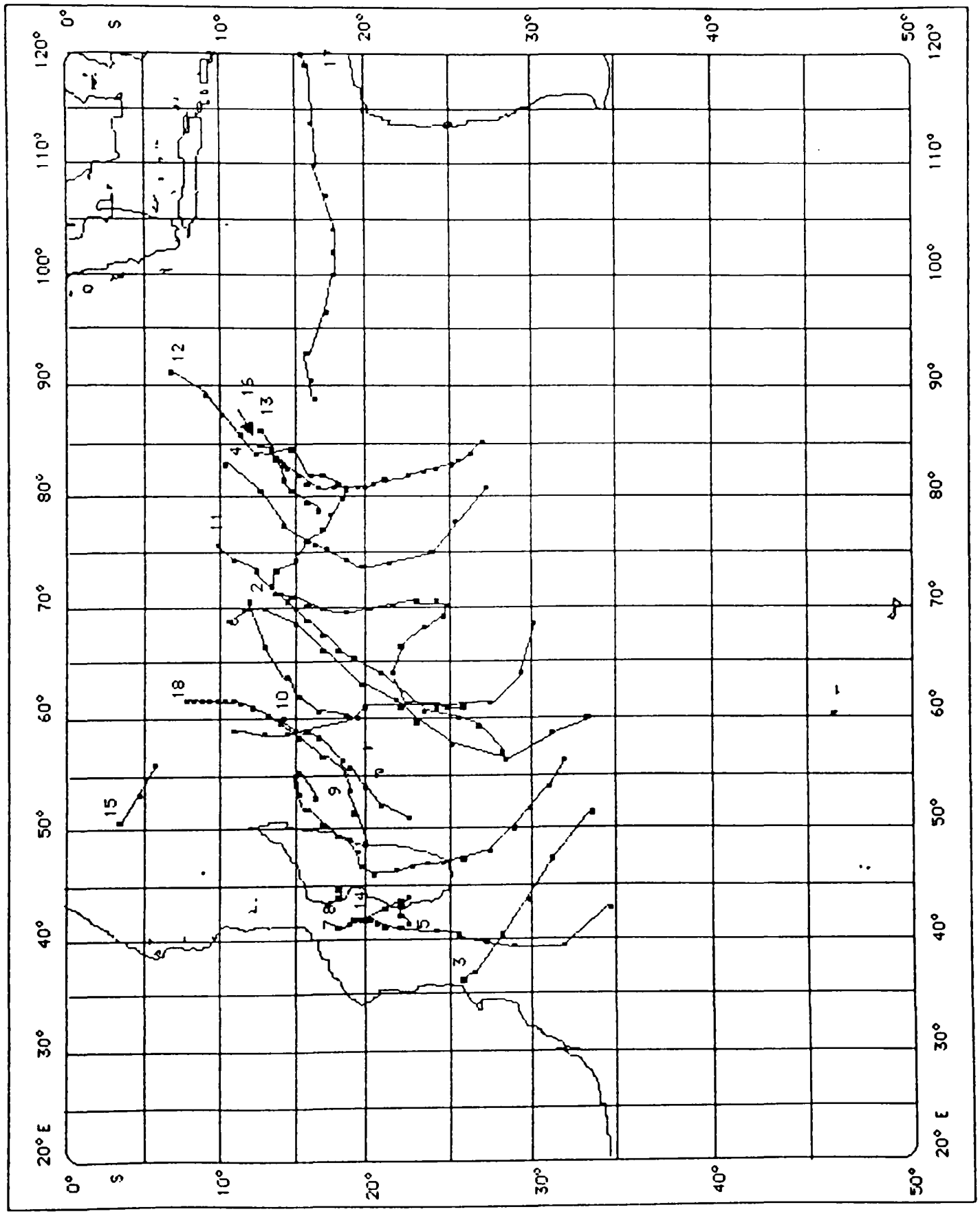

Figure A.3. Tropical cyclone tracks for season 1964-65.

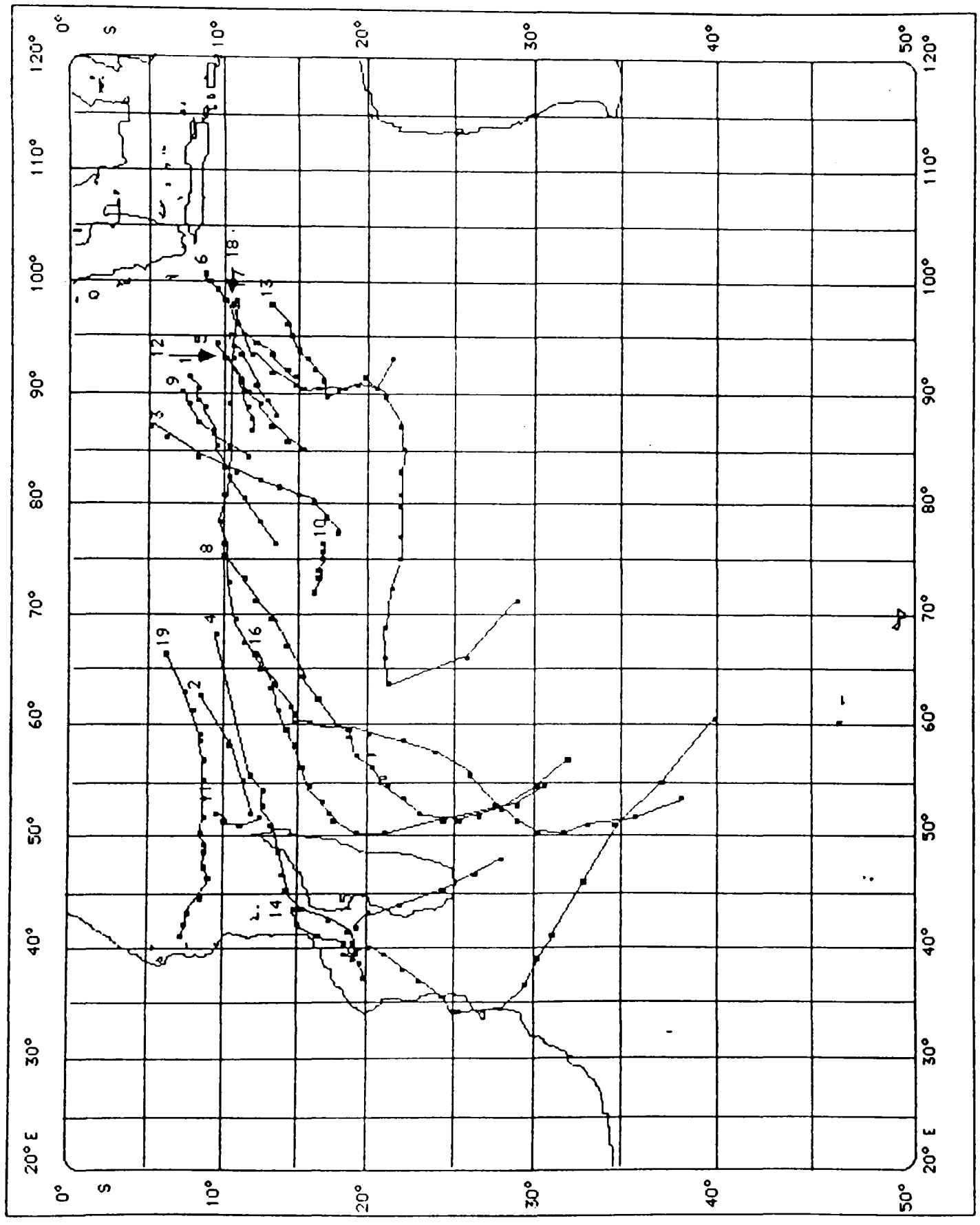

Figure A.4. Tropical cyclone tracks for season 1965-66.

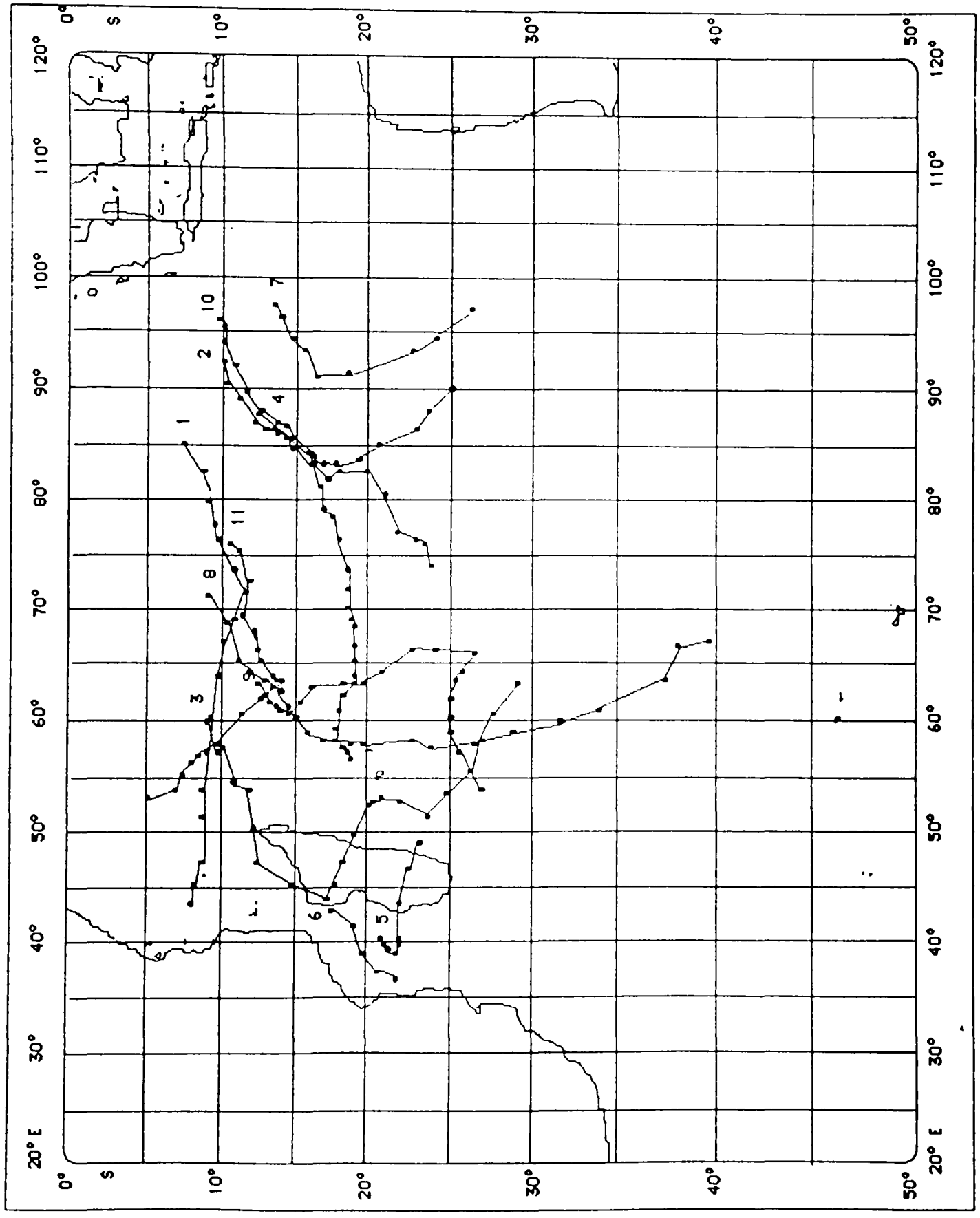

Figure A.5. Tropical cyclone tracks for season 1966-67.

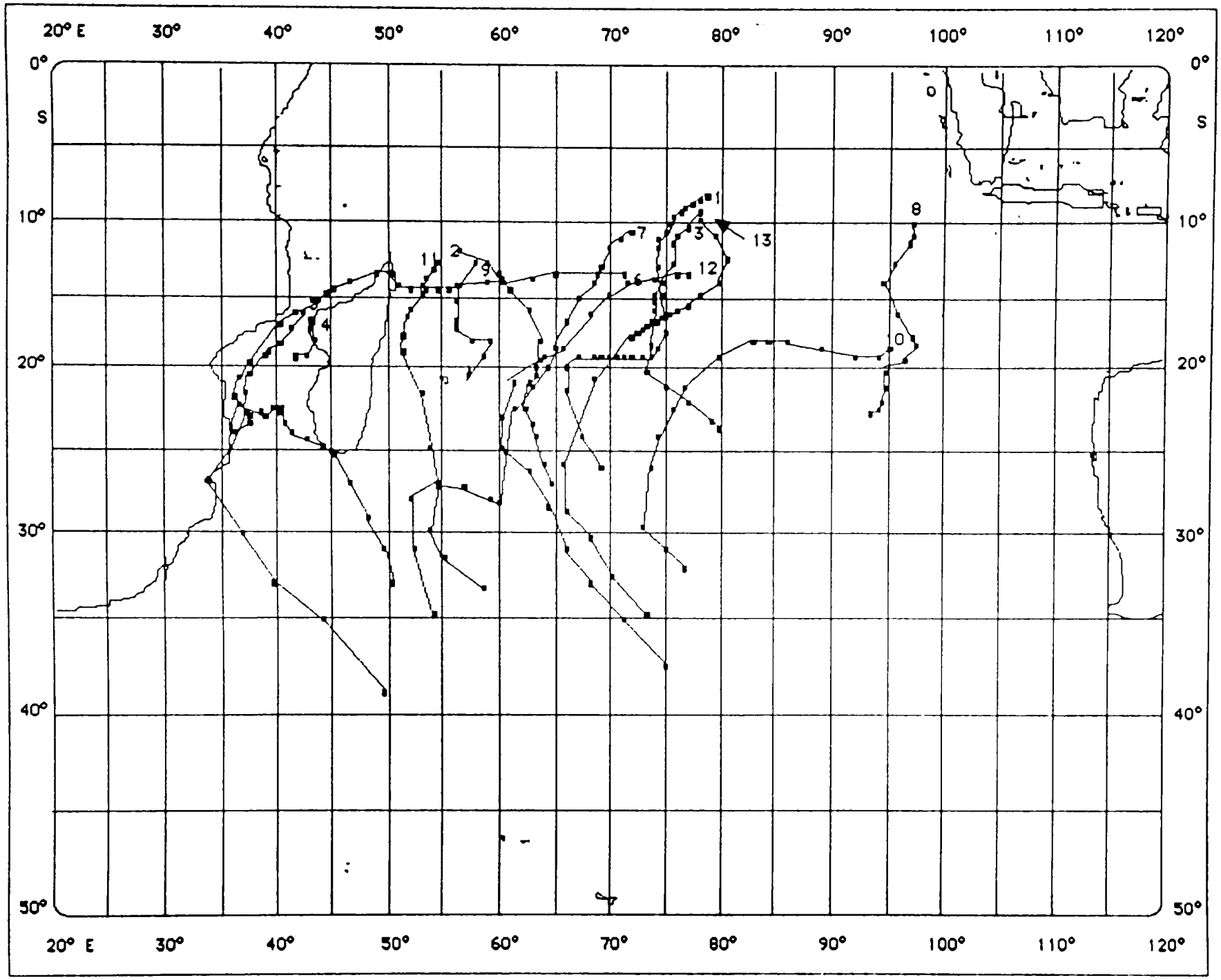

Figure A.6. Tropical cyclone tracks for season 1967-68.

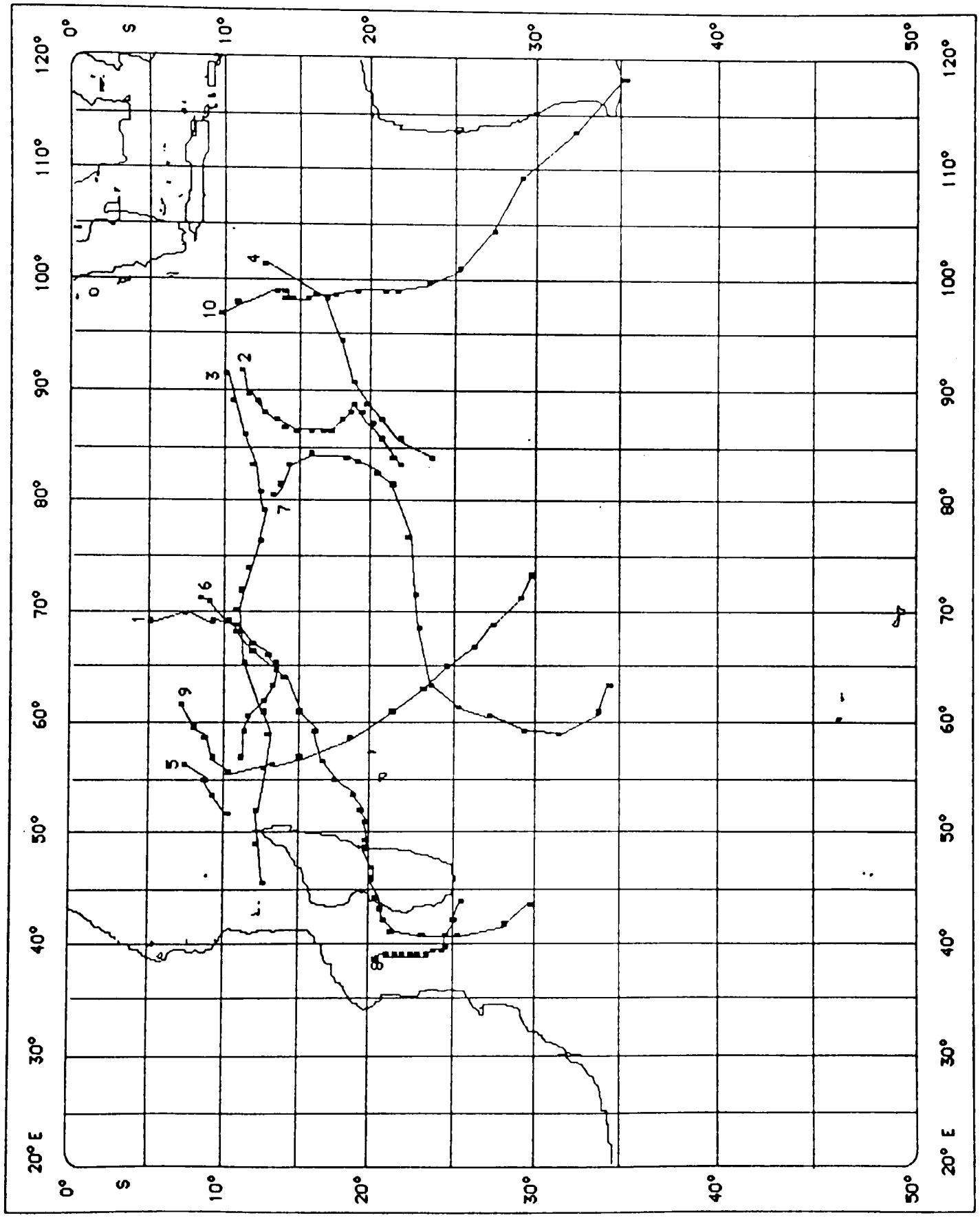

Figure A.7. Tropical cyclone tracks for season 1968-69.

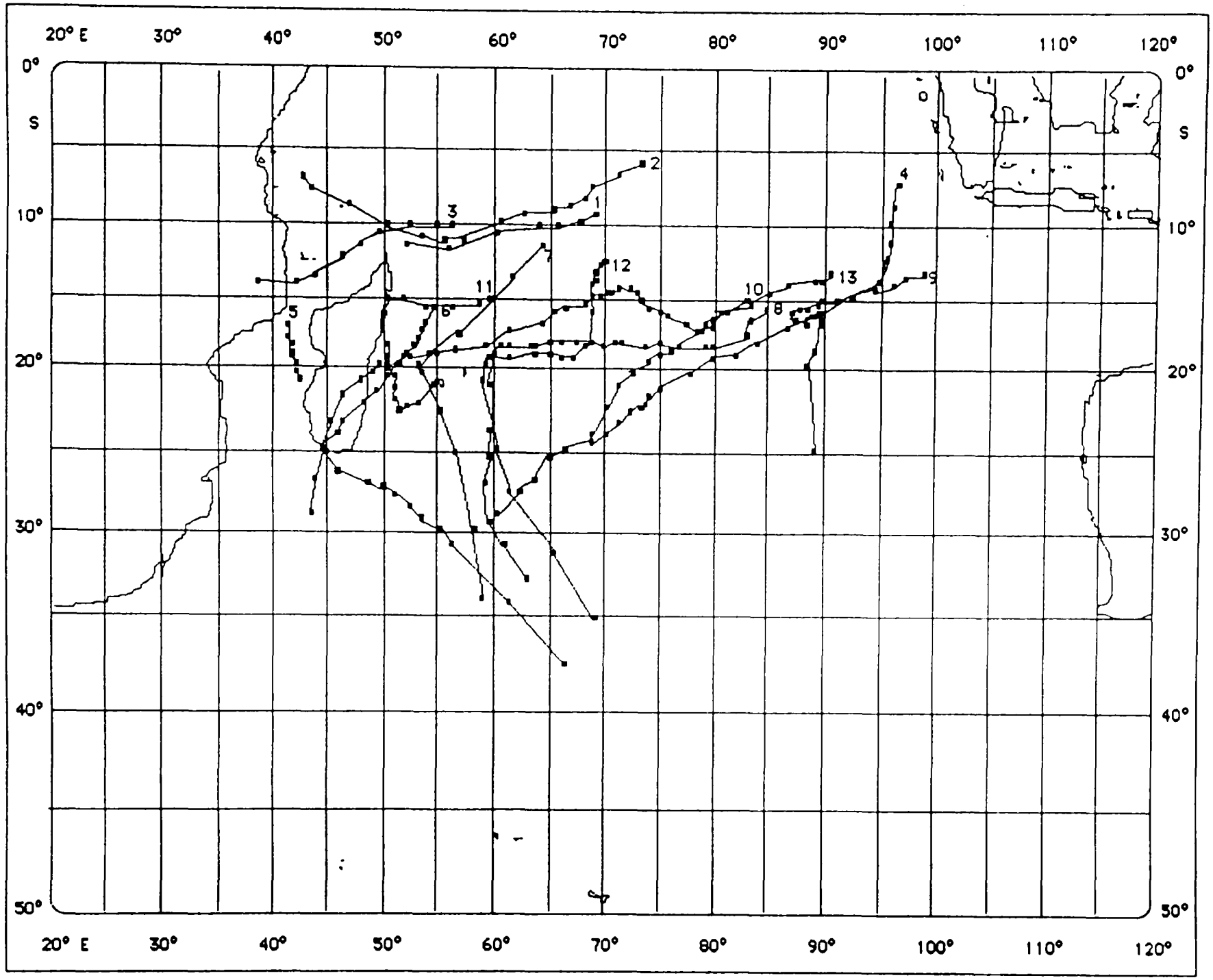

Figure A.8. Tropical cyclone tracks for season 1969-70.

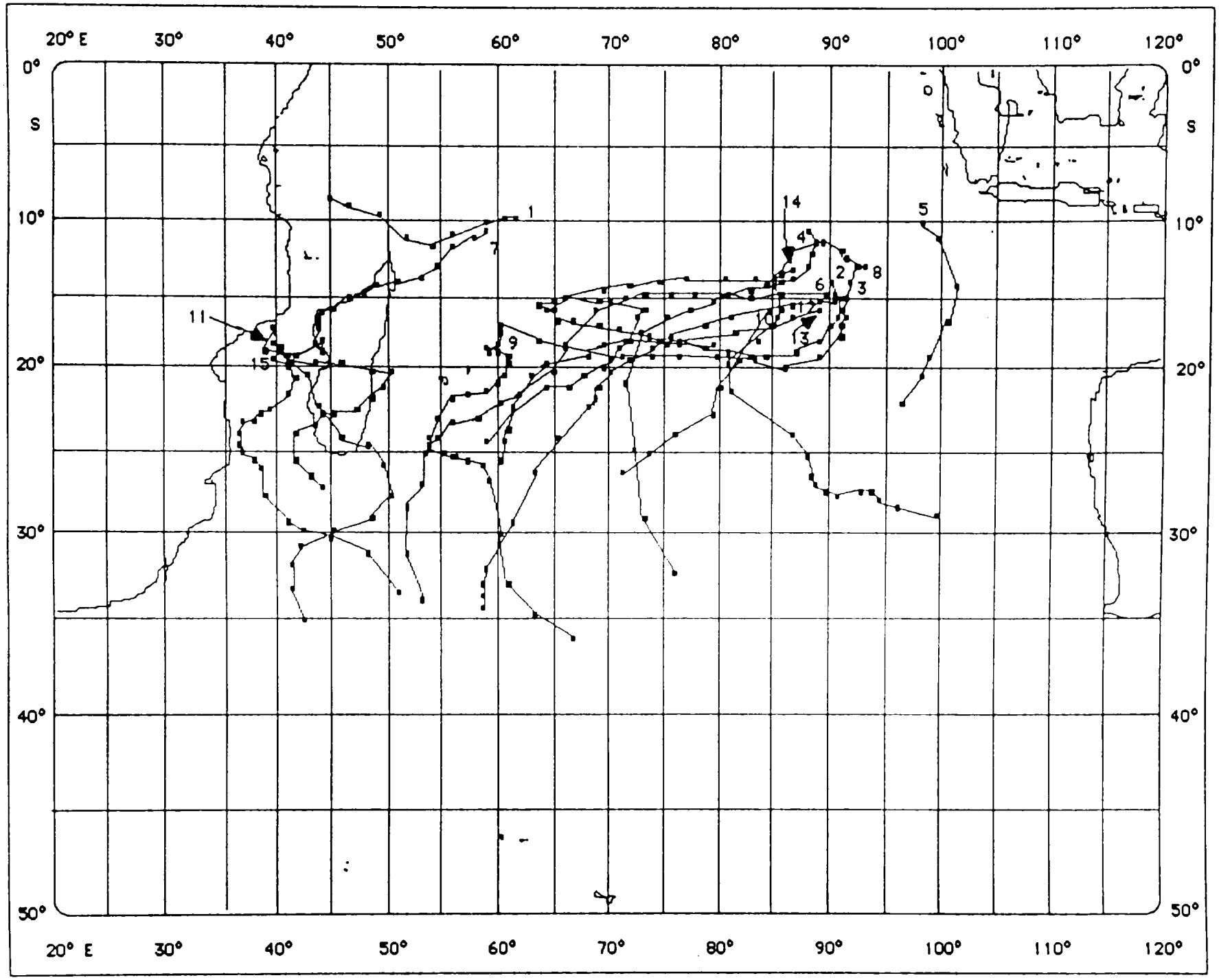

Figure A.9. Tropical cyclone tracks for season 1970-71.

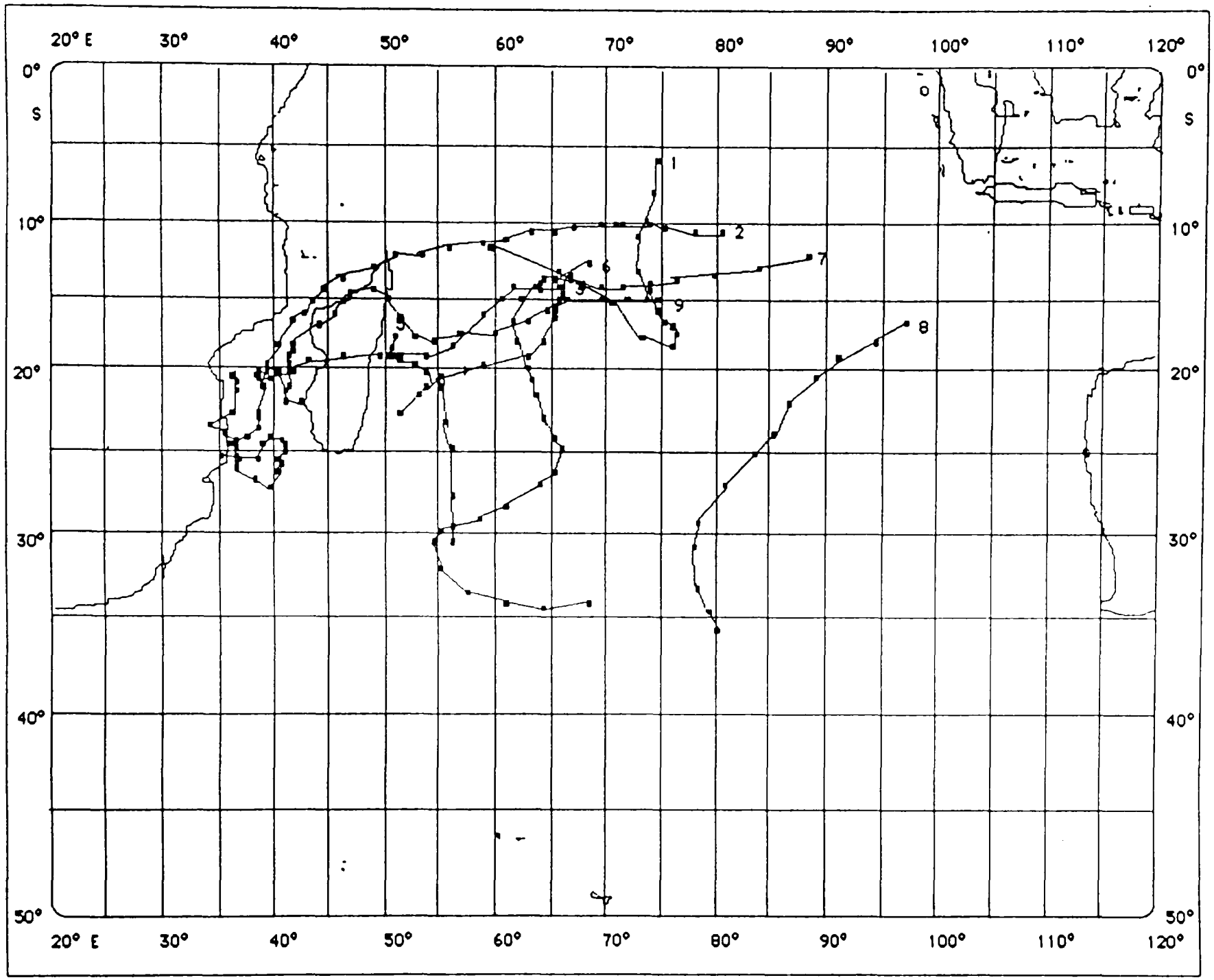

Figure A.10. Tropical cyclone tracks for season 1971-72.

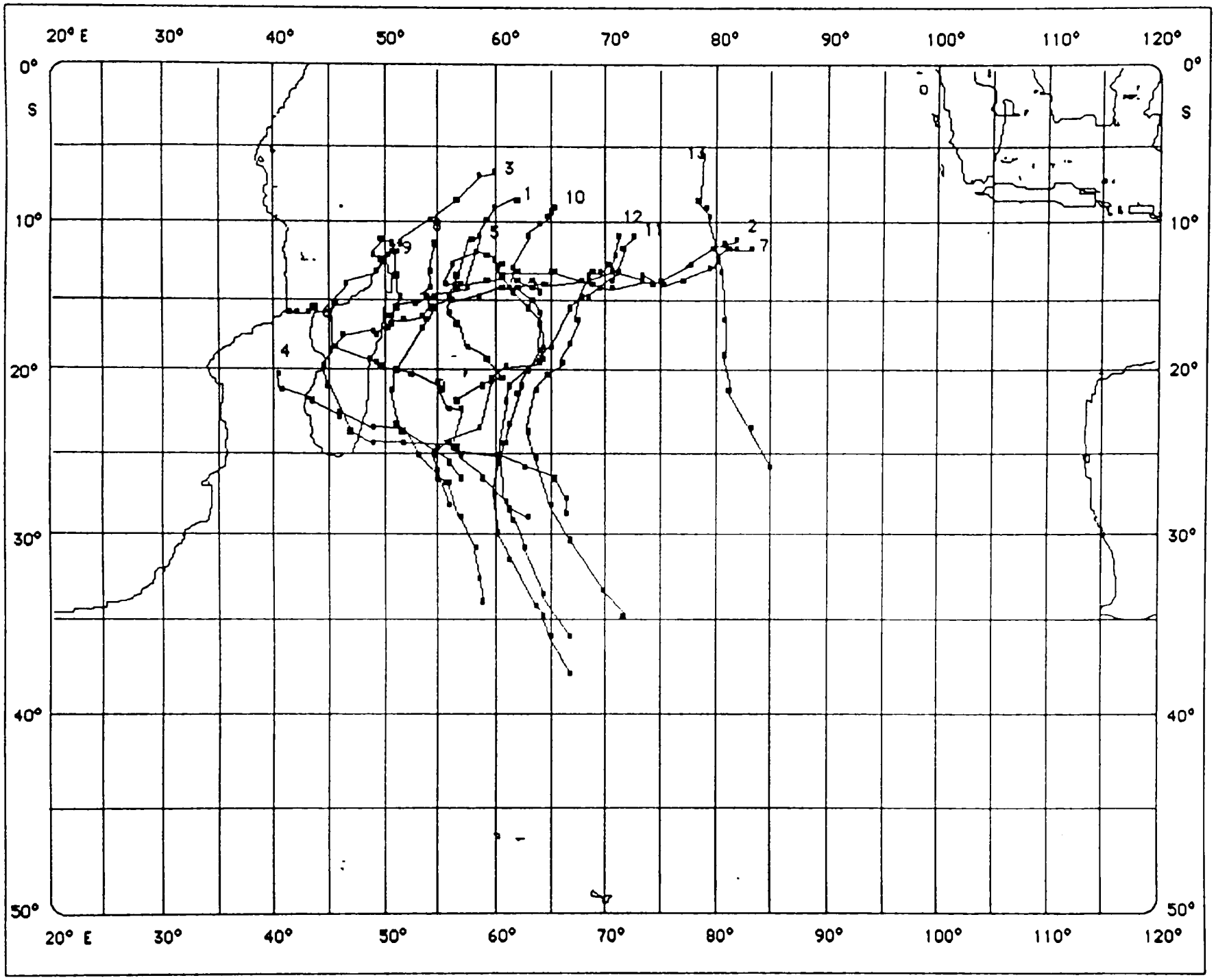

Figure A.11. Tropical cyclone tracks for season 1972-73.

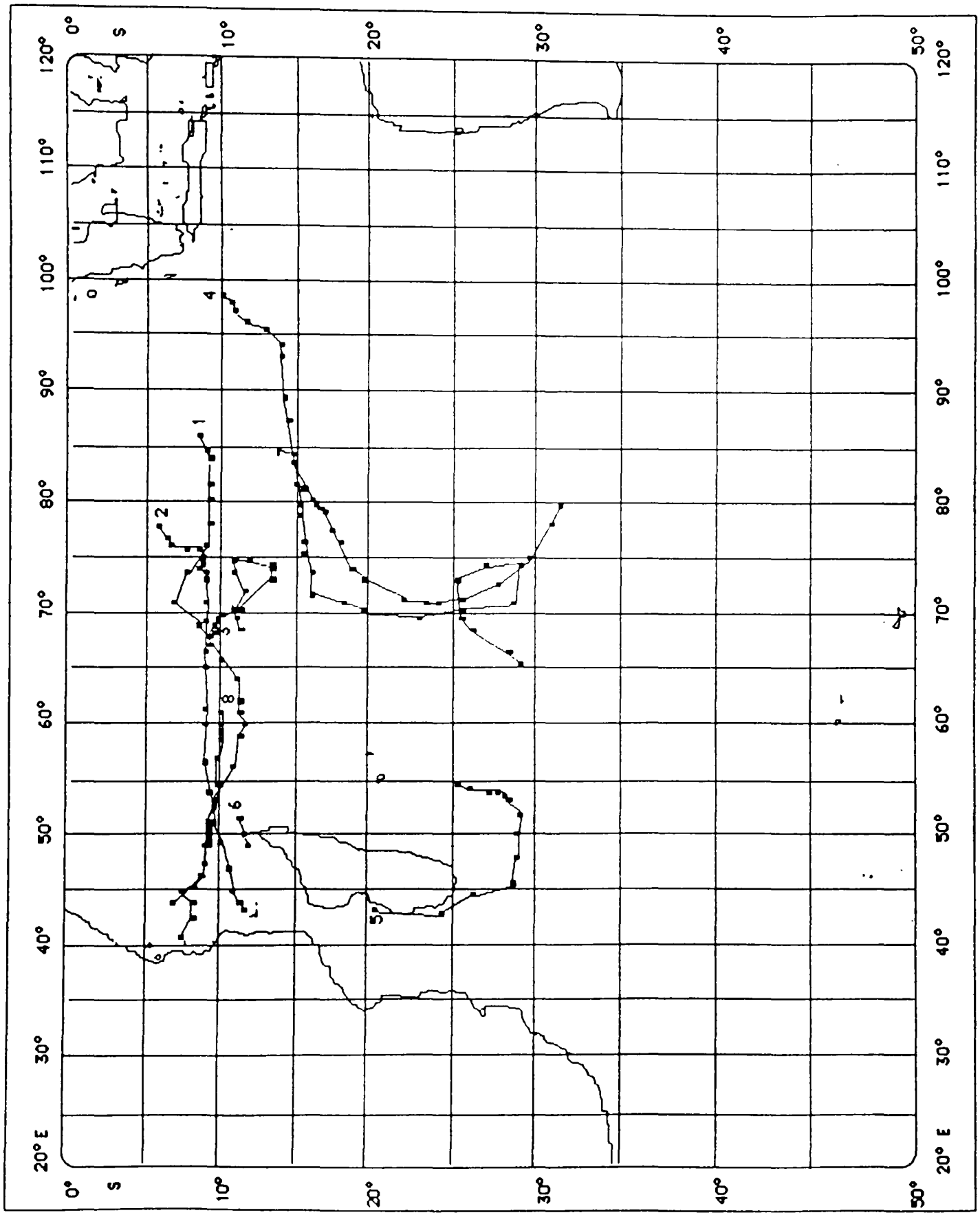

Figure A.12. Tropical cyclone tracks for season 1973-74.

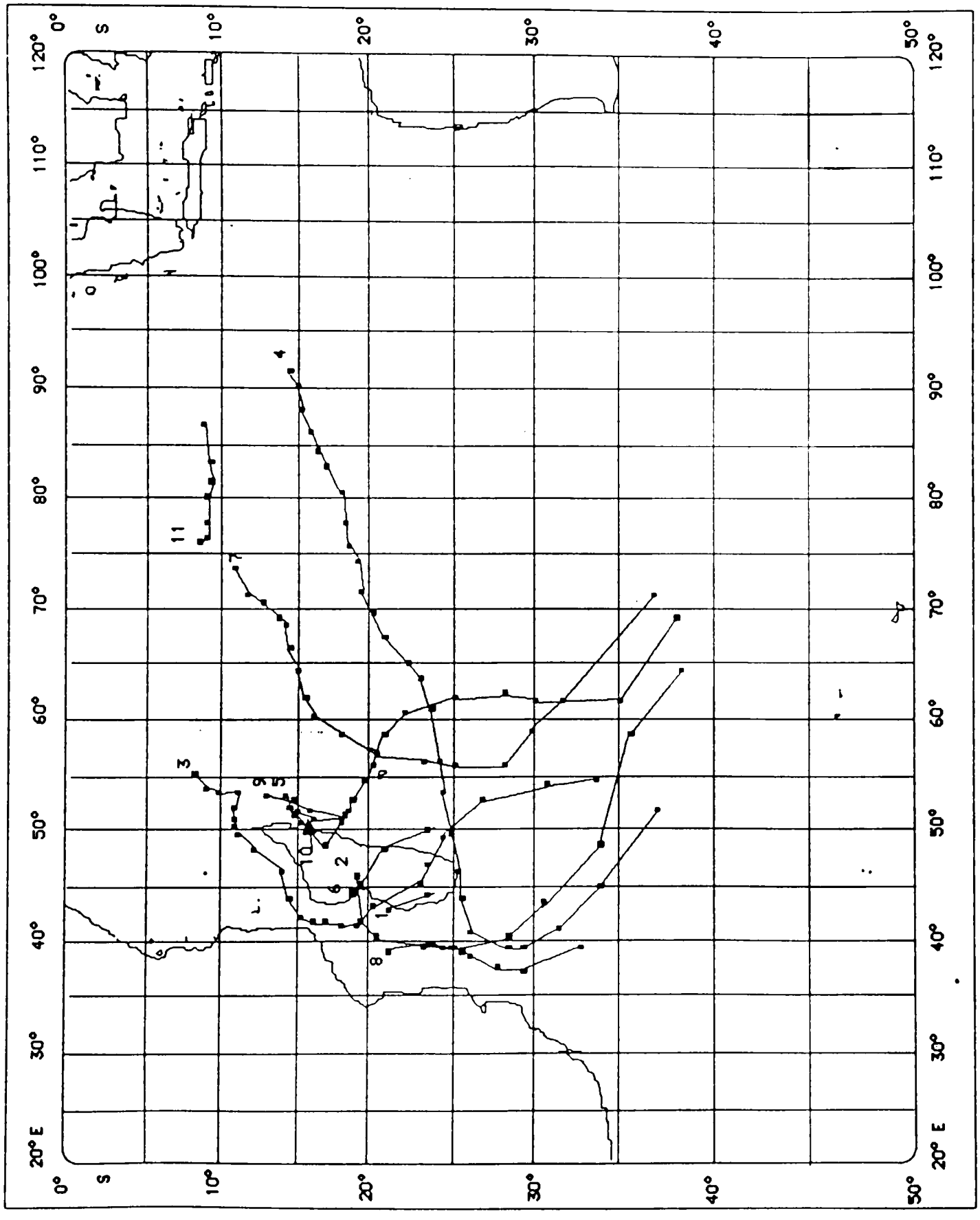

Figure A.13. Tropical cyclone tracks for season 1974-75.

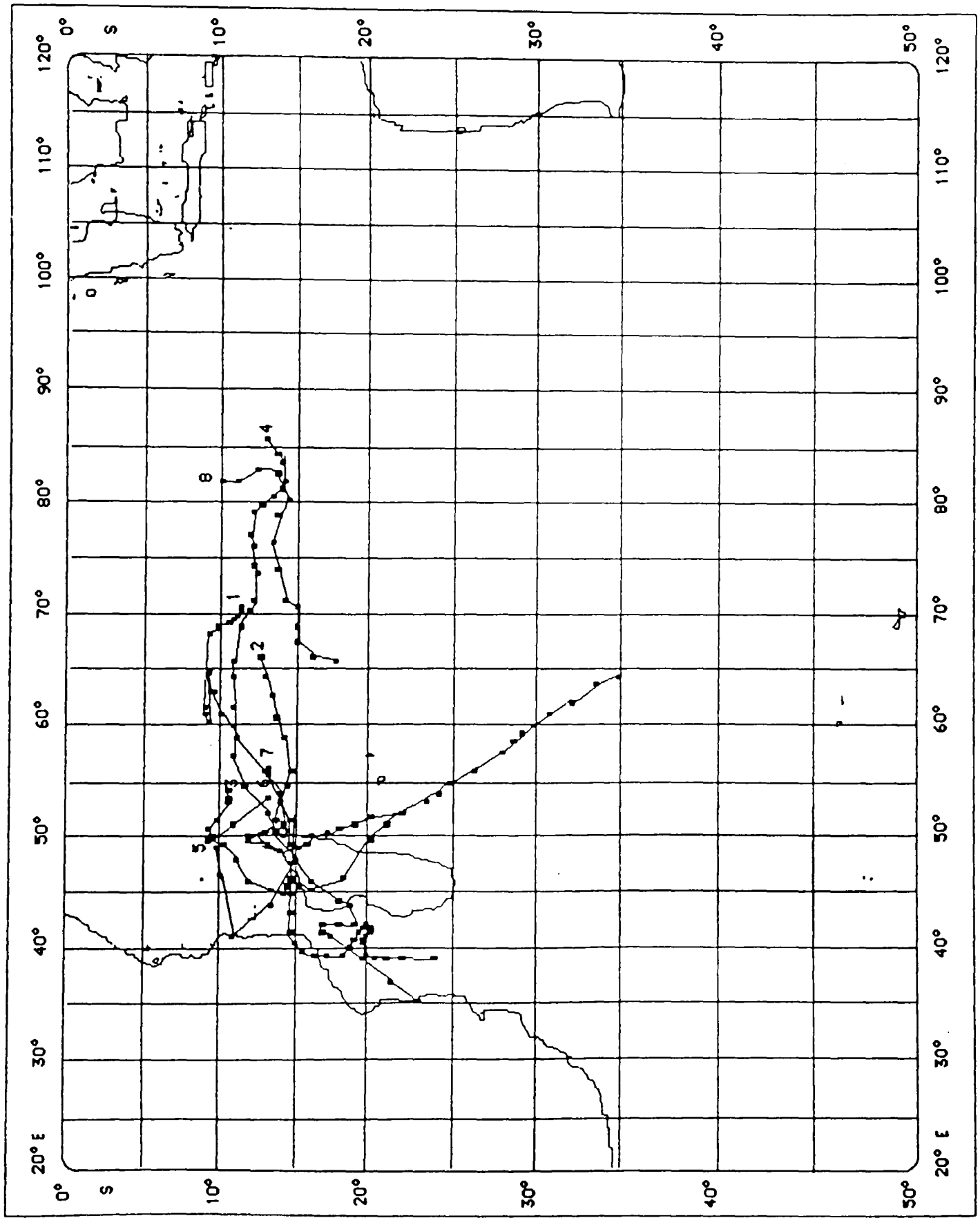

Figure A.14. Tropical cyclone tracks for season 1975-76.

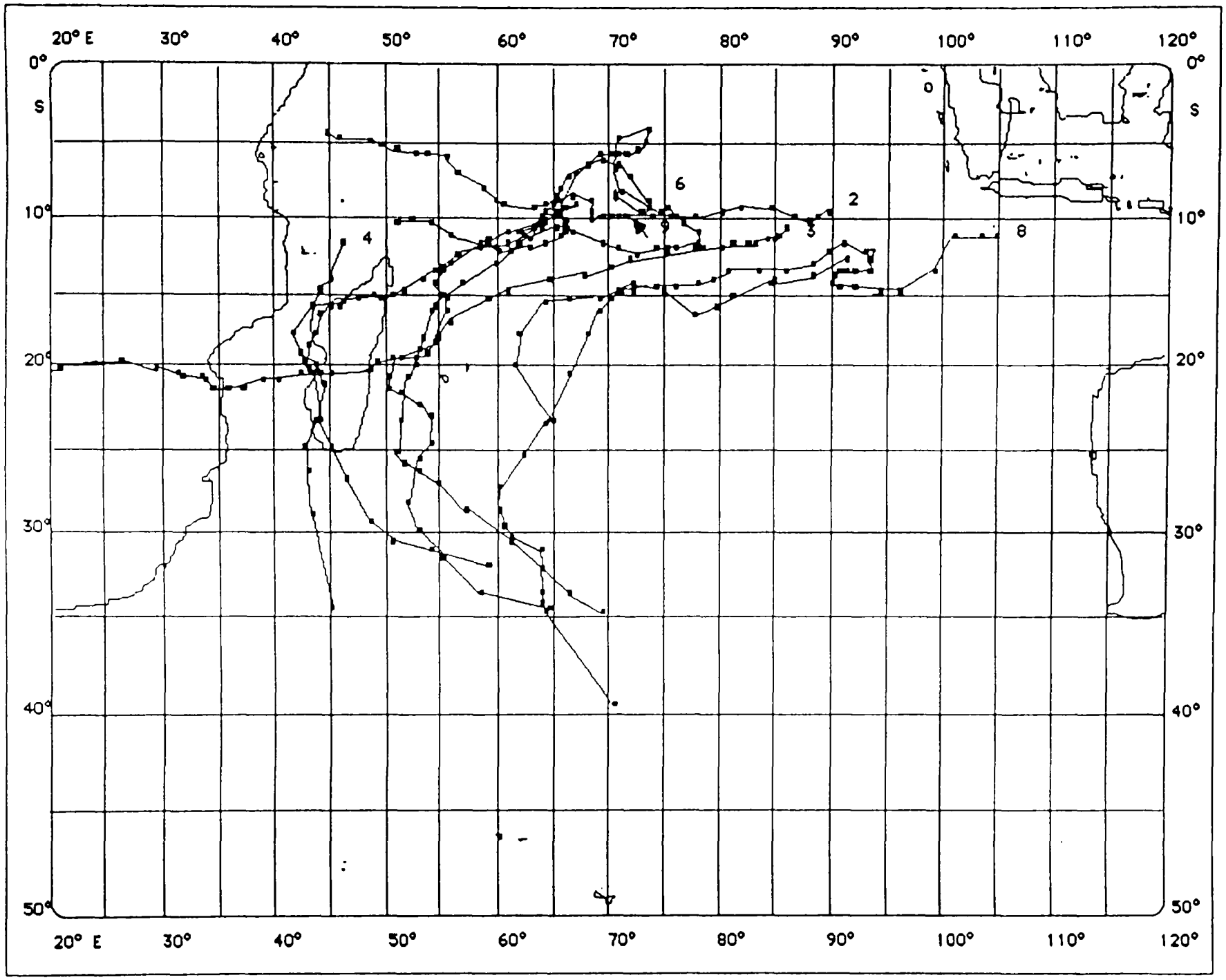

Figure A.15. Tropical cyclone tracks for season 1976-77.

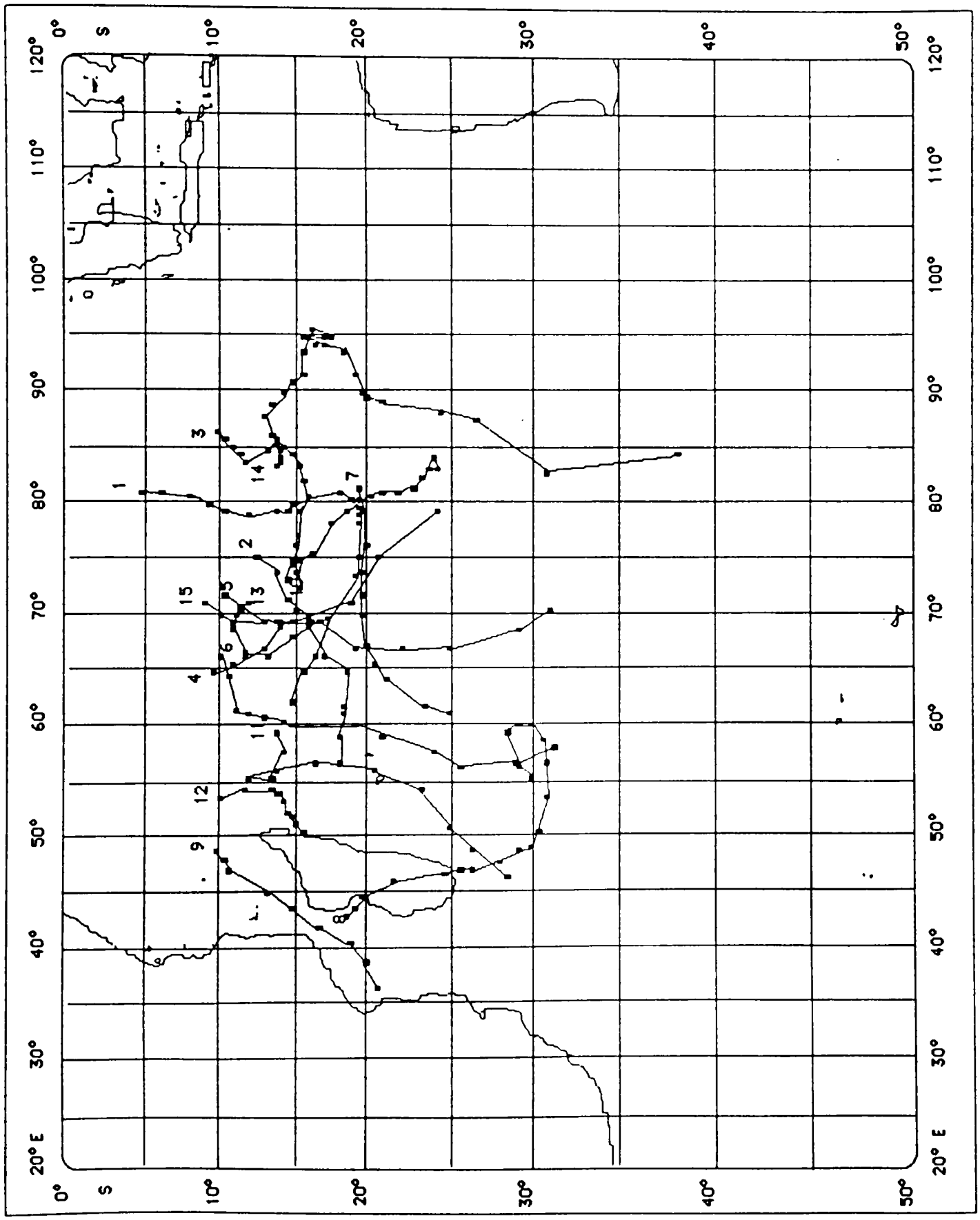

Figure A.16. Tropical cyclone tracks for season 1977-78.

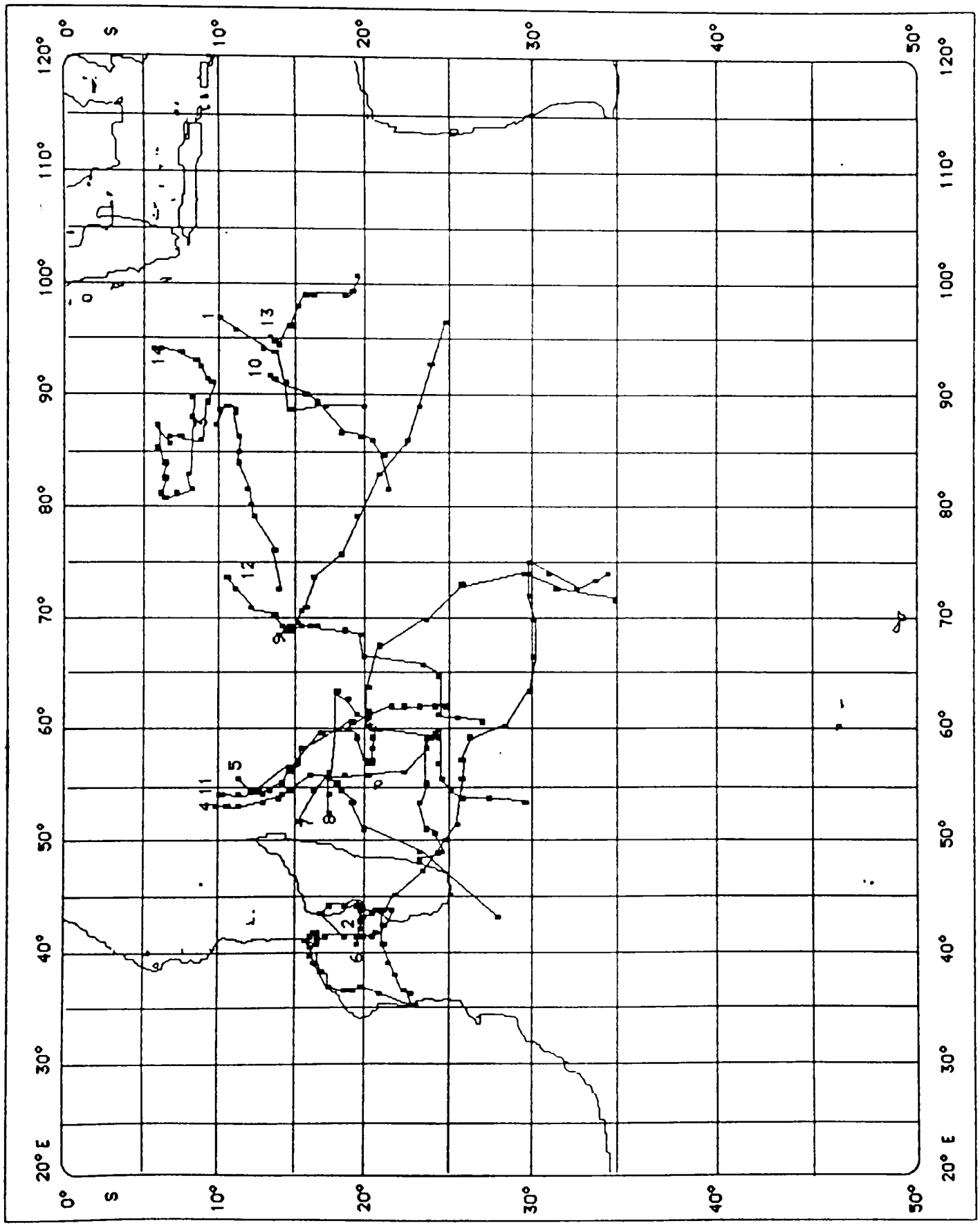

Figure A.17. Tropical cyclone tracks for season 1978-79.

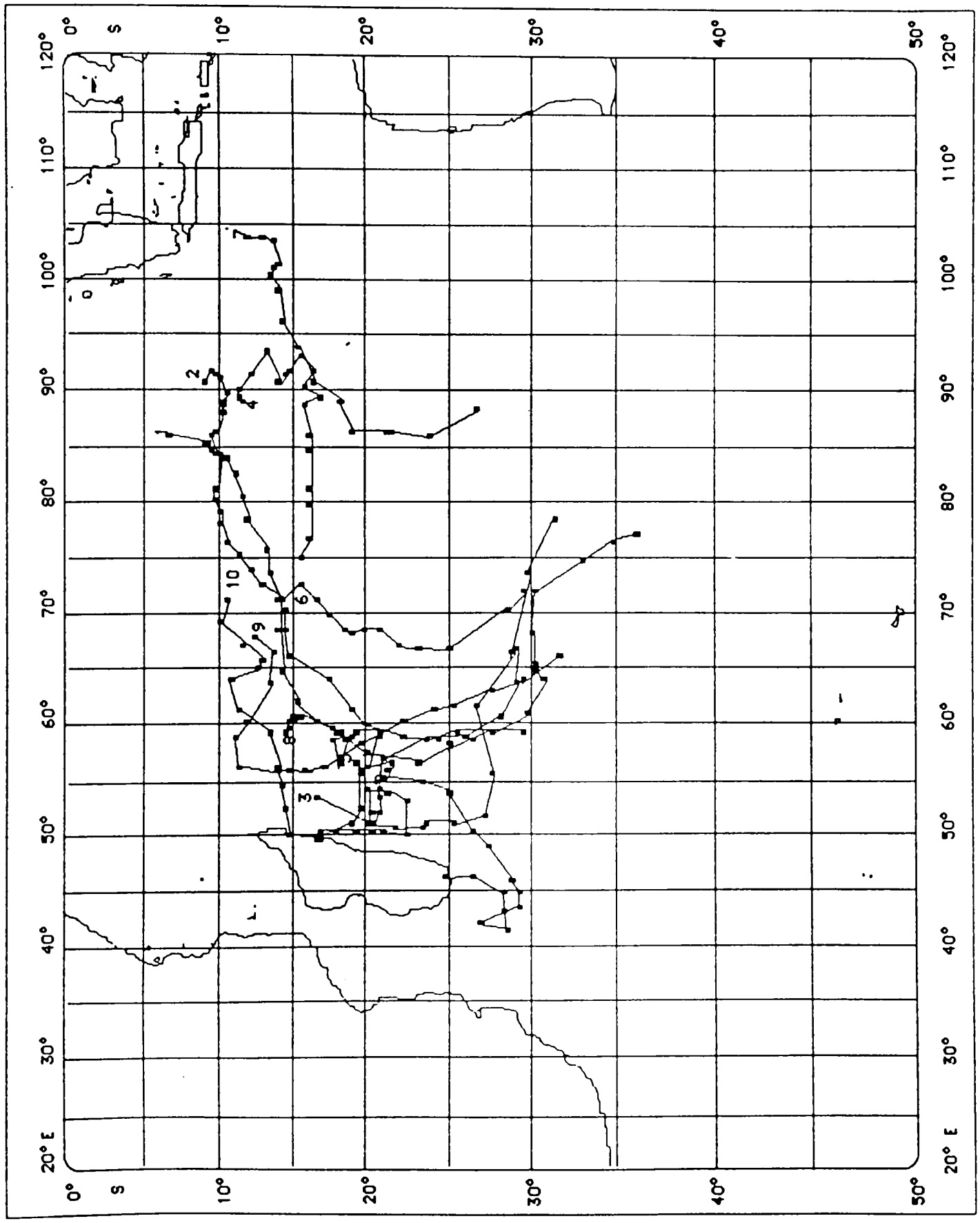

Figure A.18. Tropical cyclone tracks for season 1979-80.

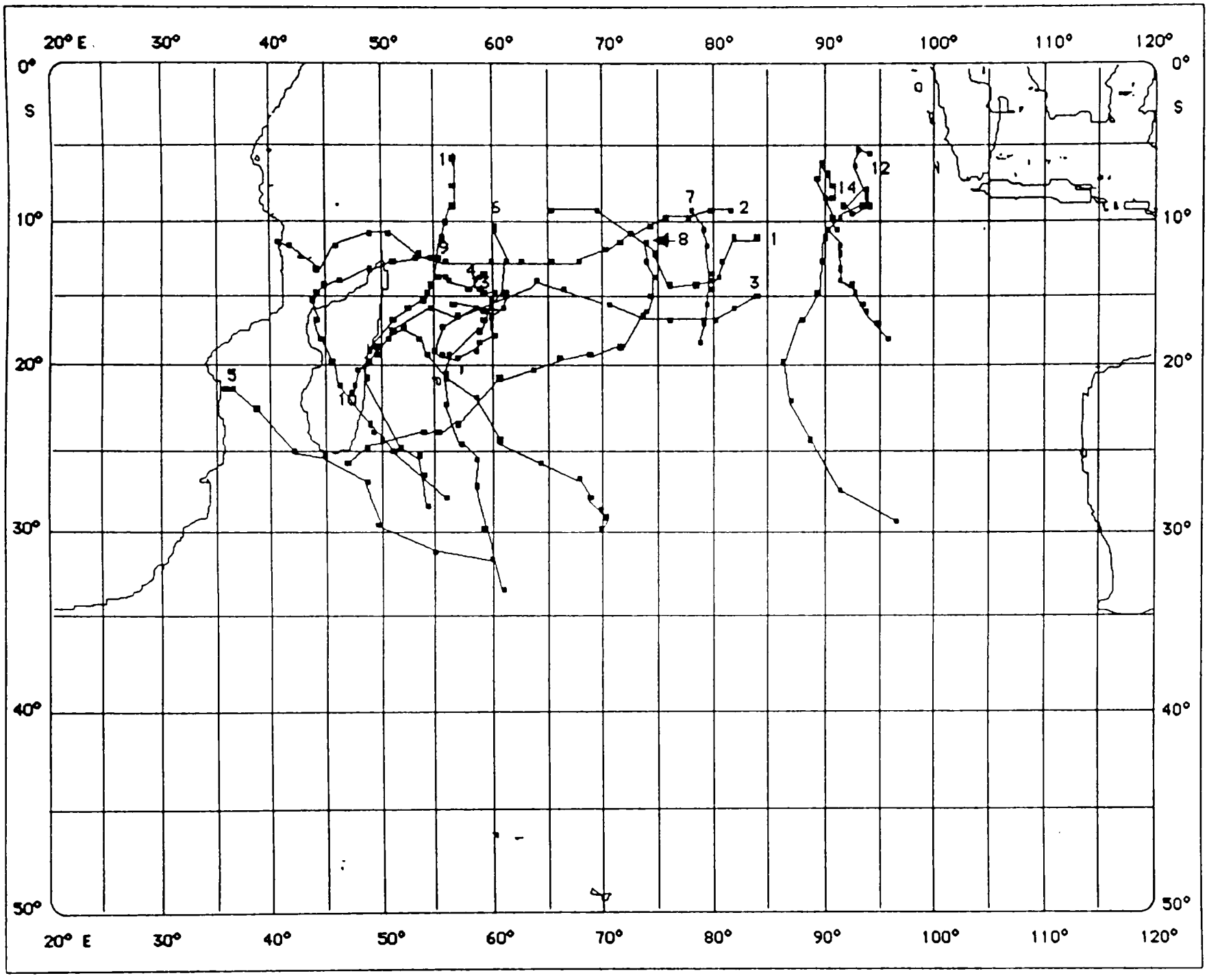

Figure A.19. Tropical cyclone tracks for season 1980-81.

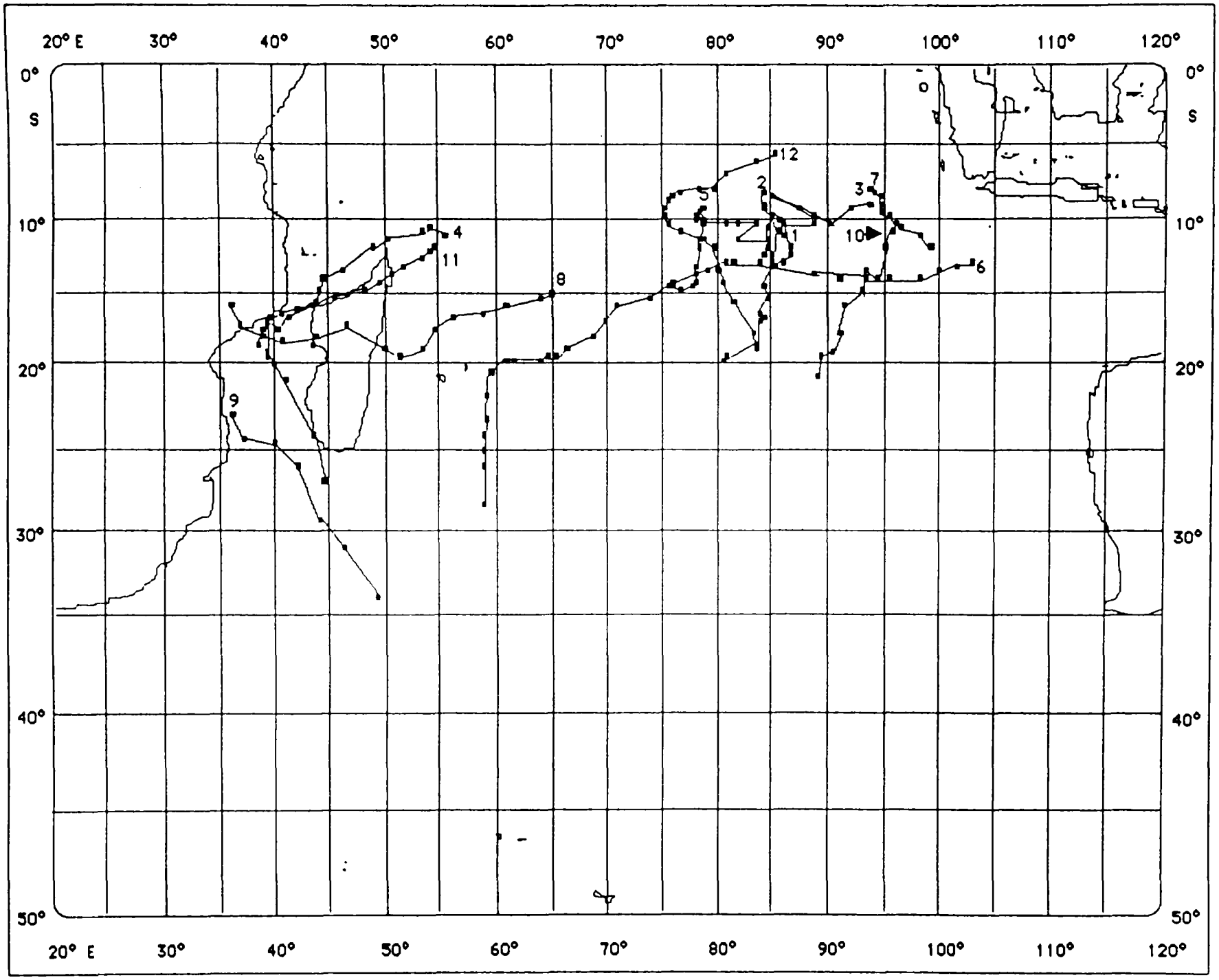

Figure A.20. Tropical cyclone tracks for season 1981-82.

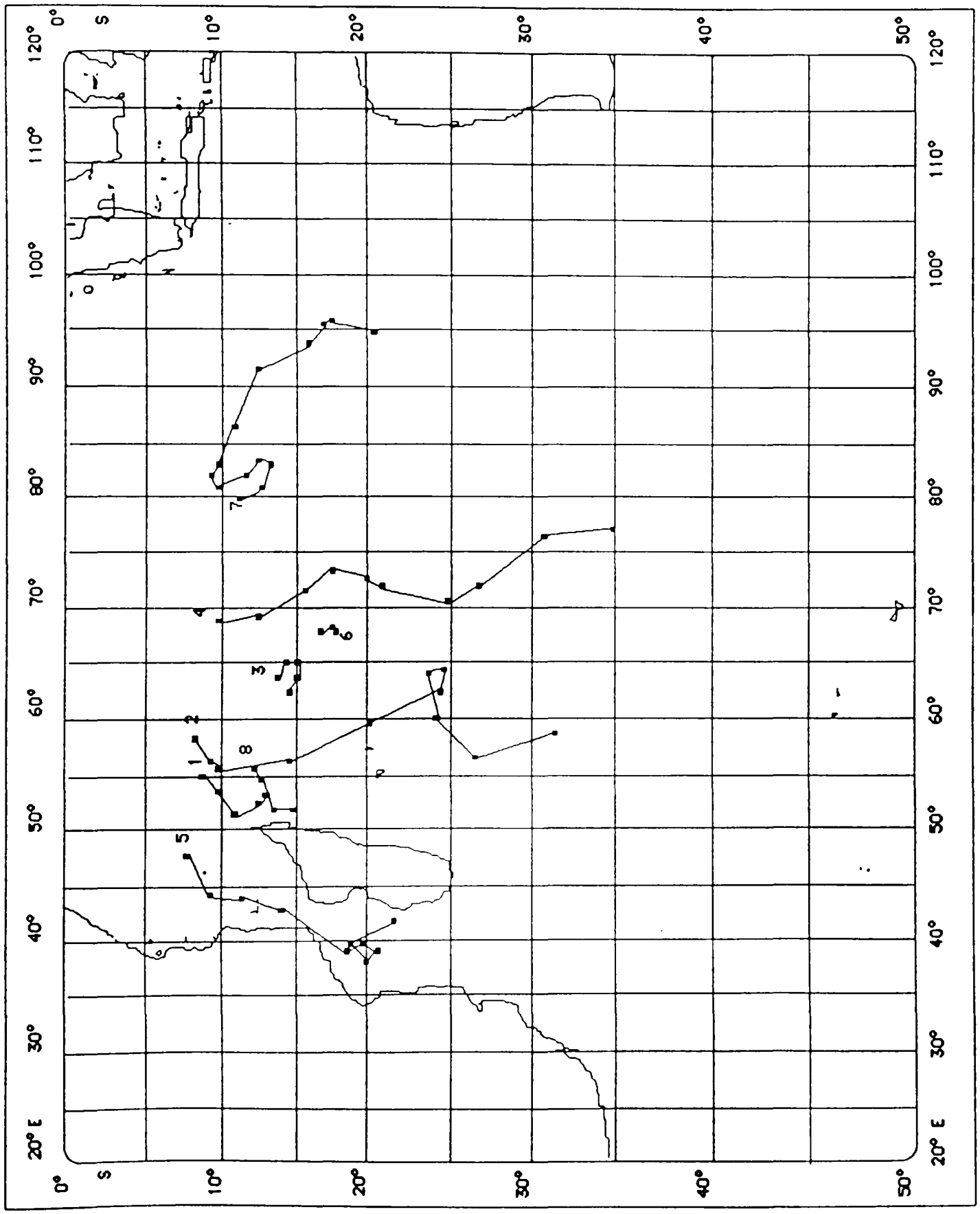

Figure A.21. Tropical cyclone tracks for season 1982-83.

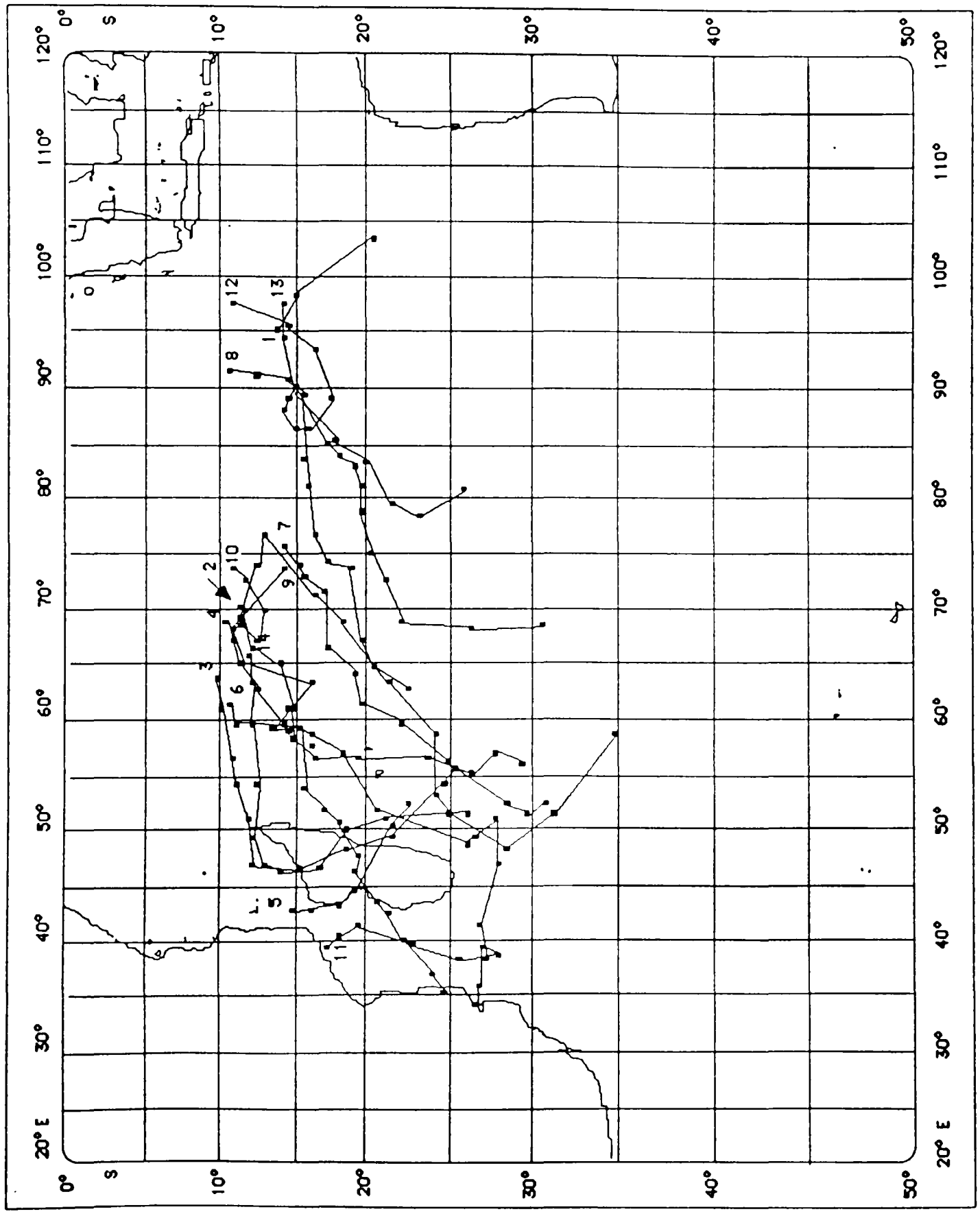

Figure A.22. Tropical cyclone tracks for season 1983-84.

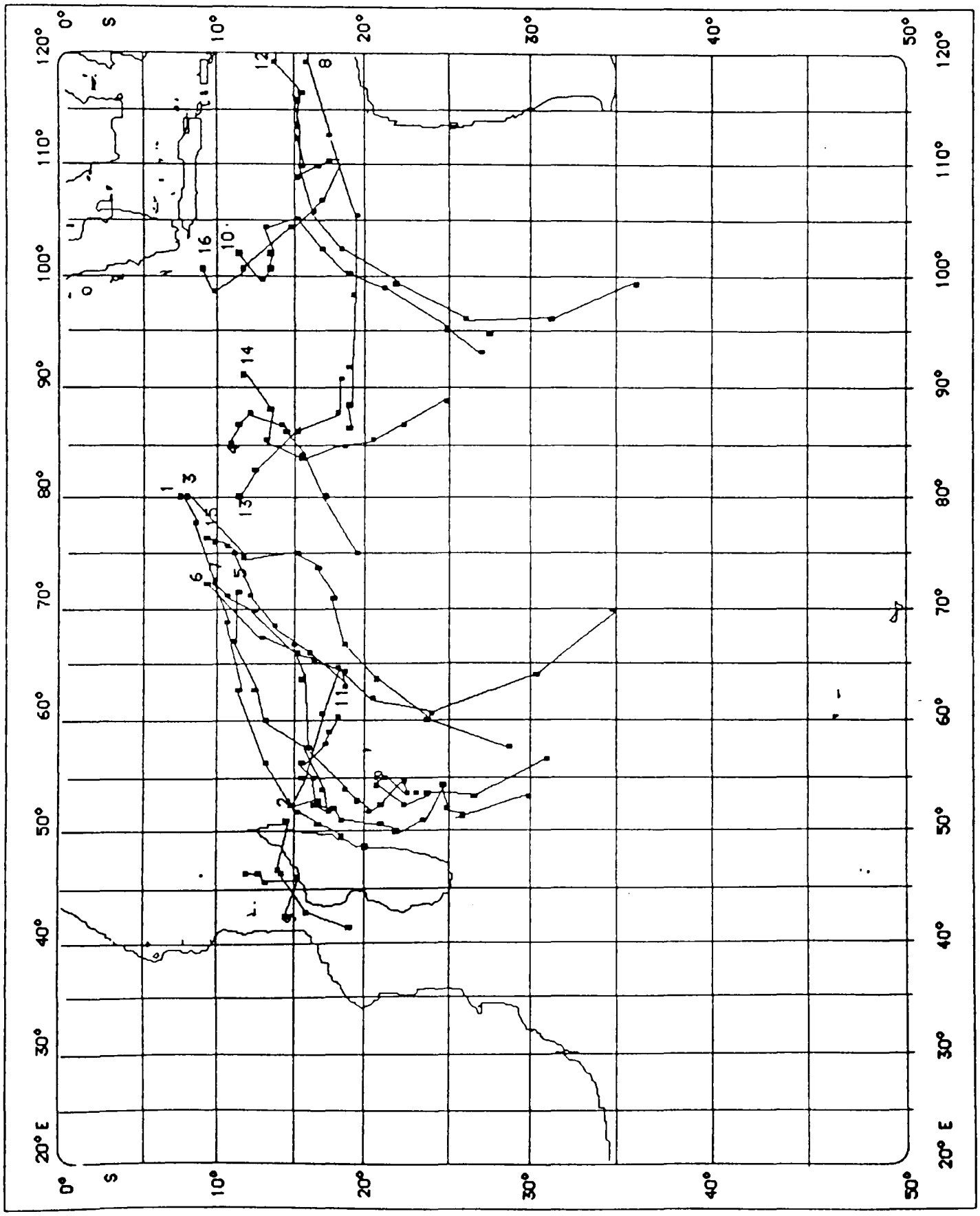

Figure A.23. Tropical cyclone tracks for season 1984-85.

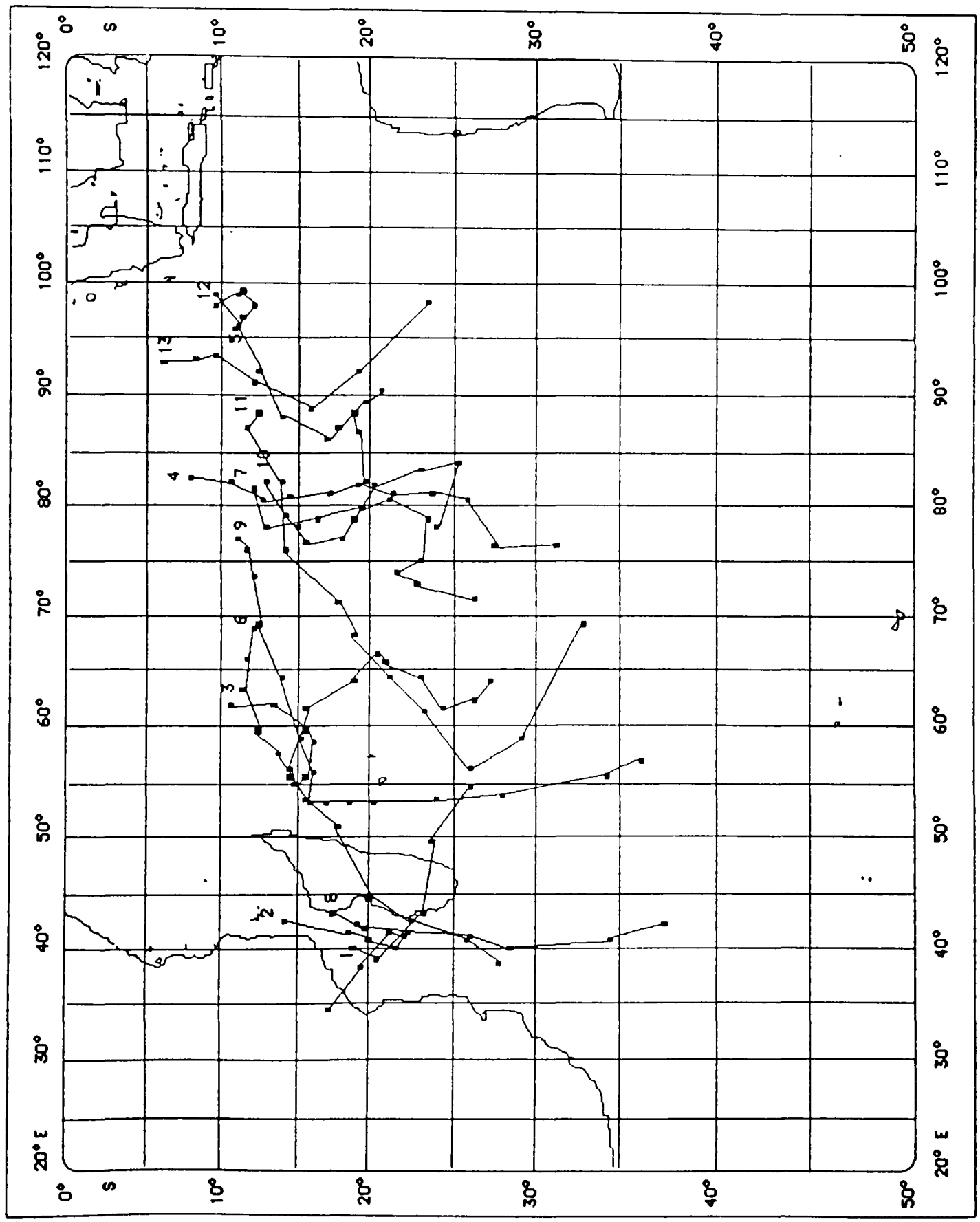

Figure A.24. Tropical cyclone tracks for season 1985-86.

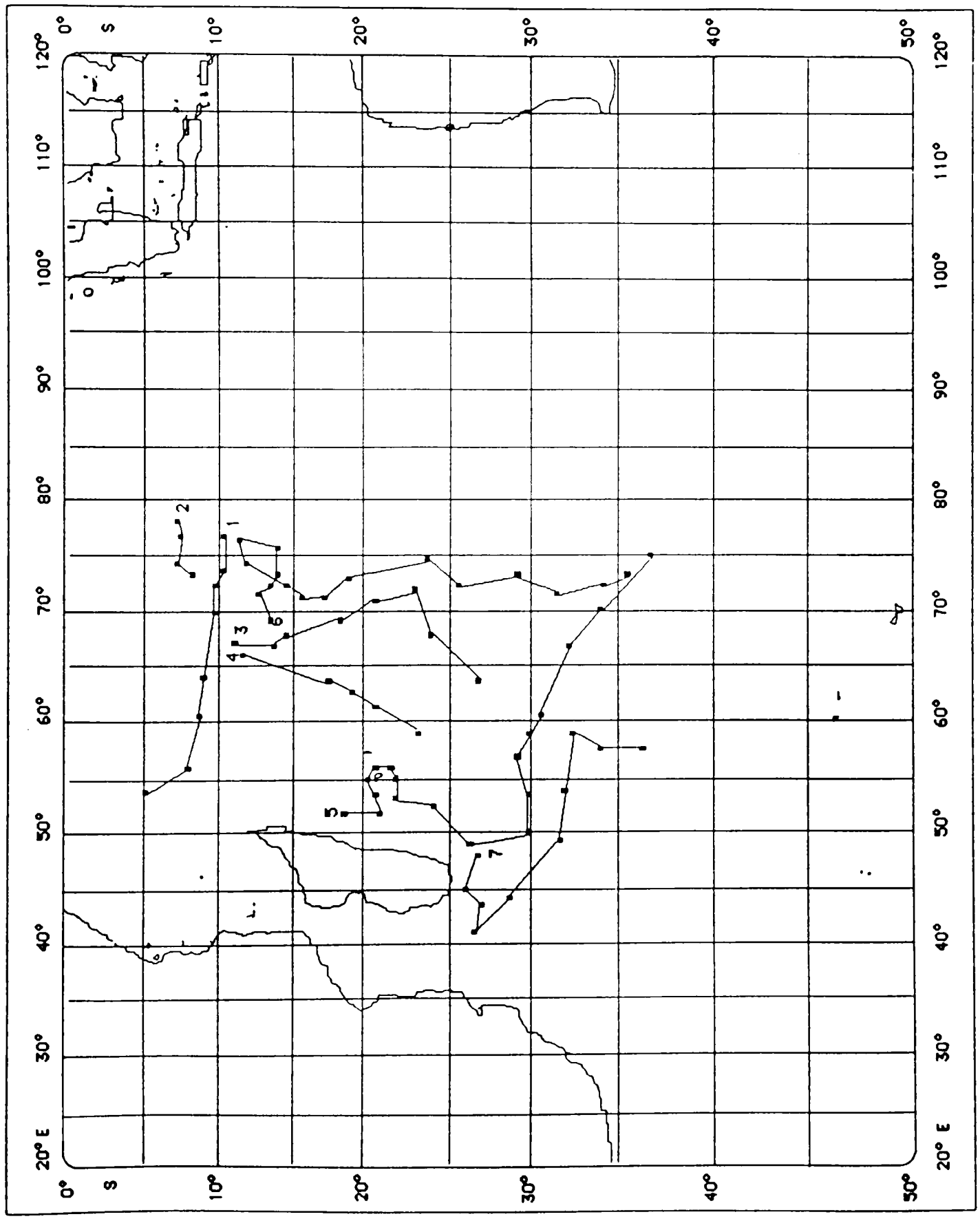

Figure A.25. Tropical cyclone tracks for season 1986-87.

APPENDIX B

TRANSLATION VECTORS FOR EACH MONTH OF THE YEAR

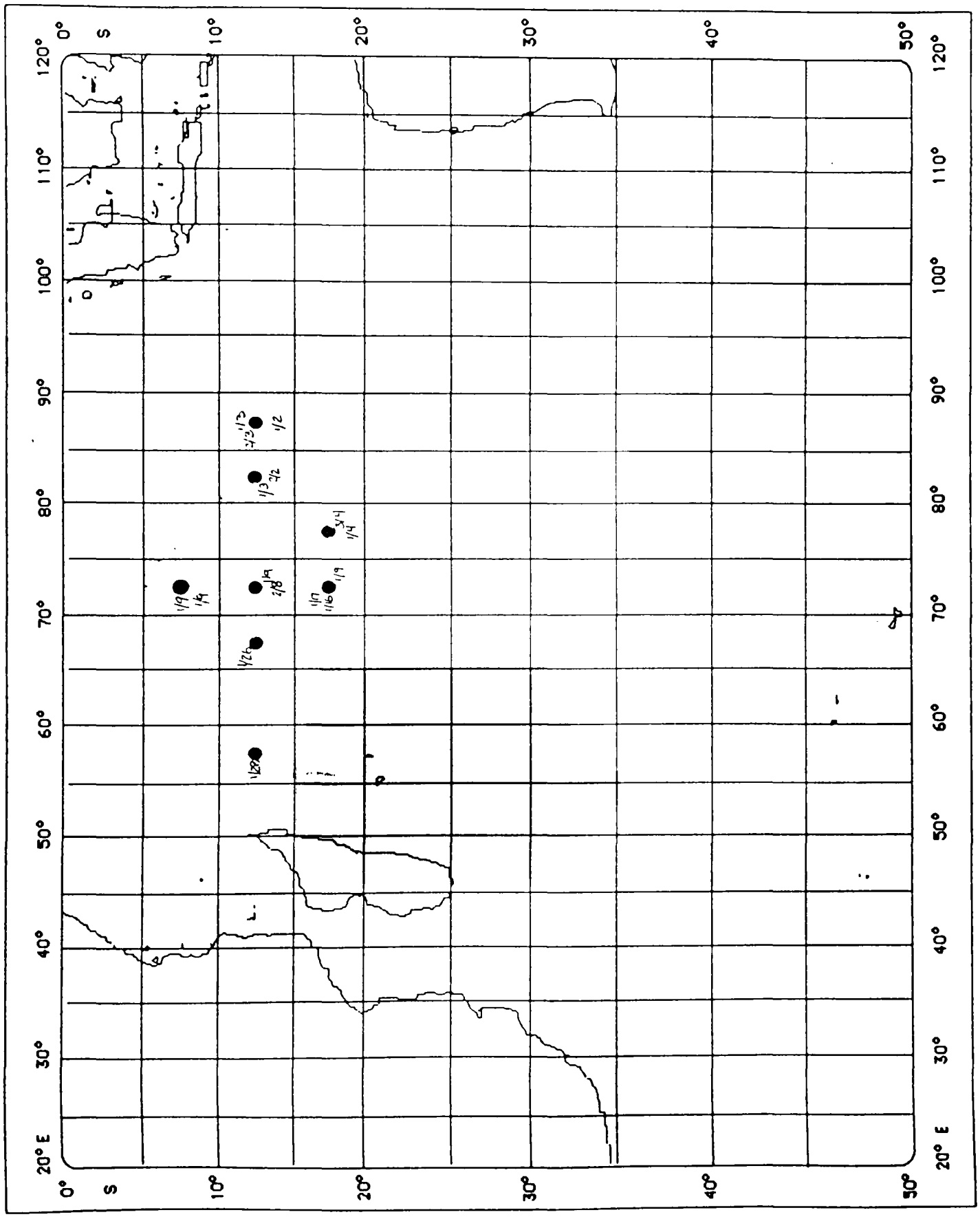

Figure B.1. Translation vectors for the month of July.

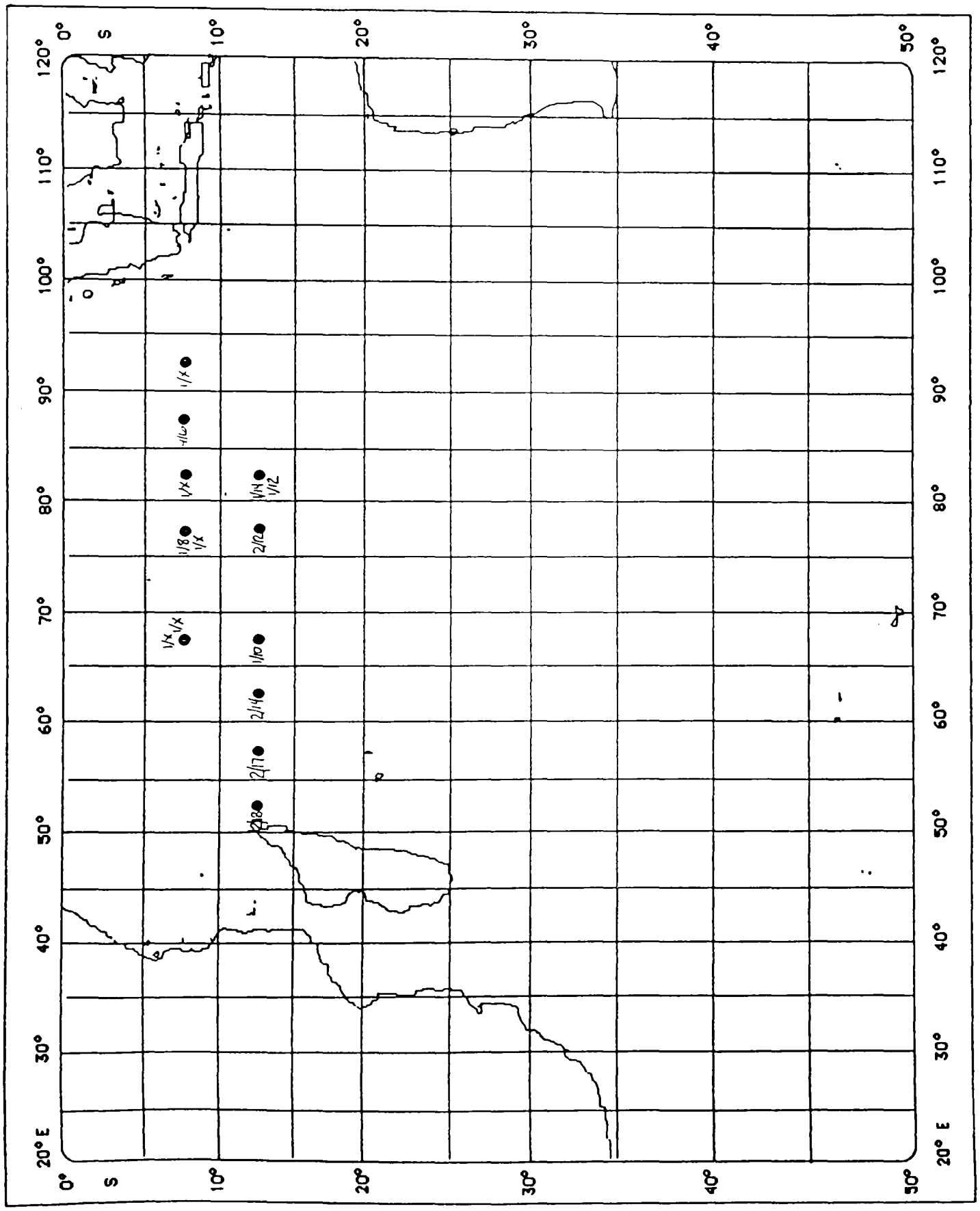

Figure B.2. Translation vectors for the month of August.

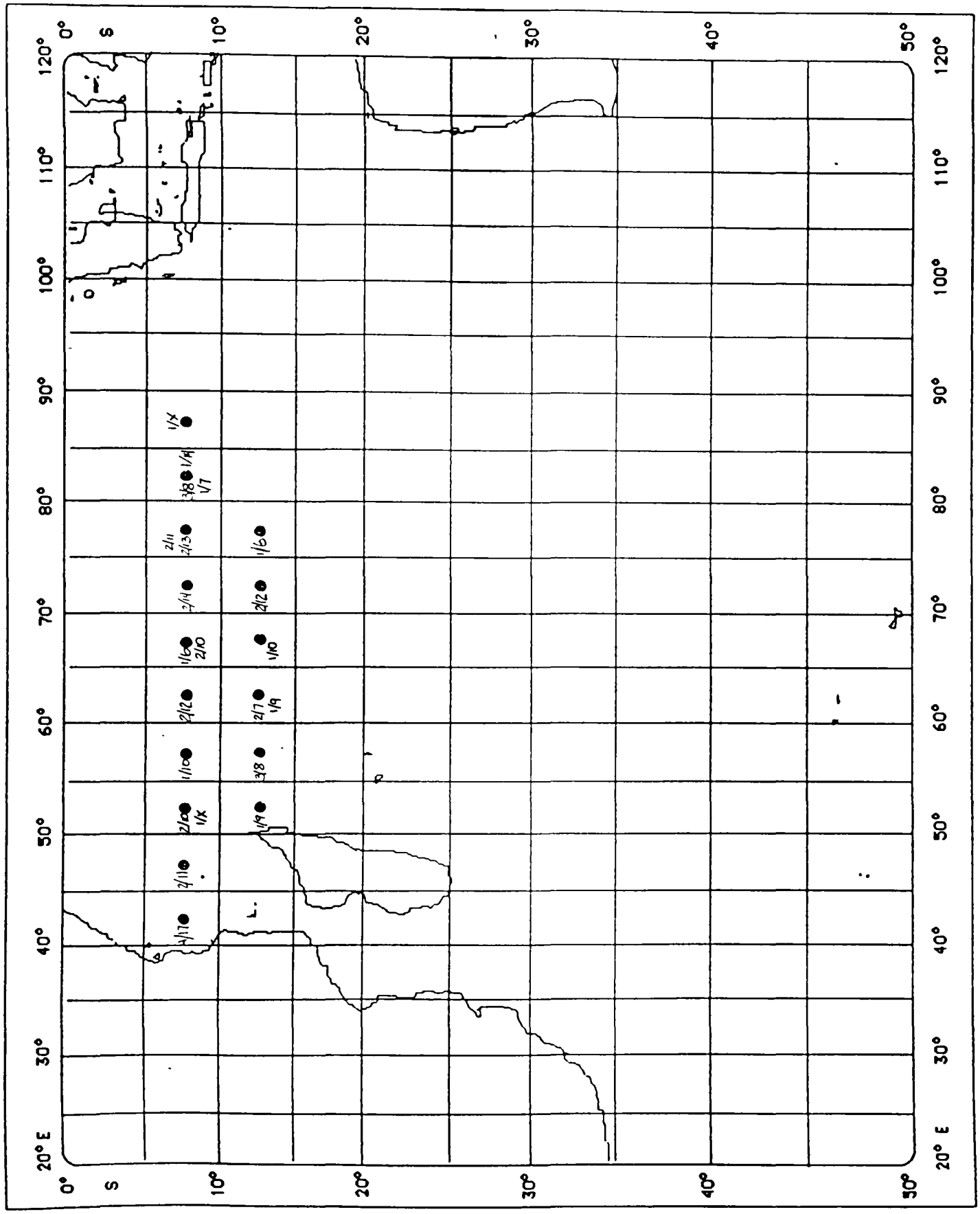

Figure B.3. Translation vectors for the month of September.

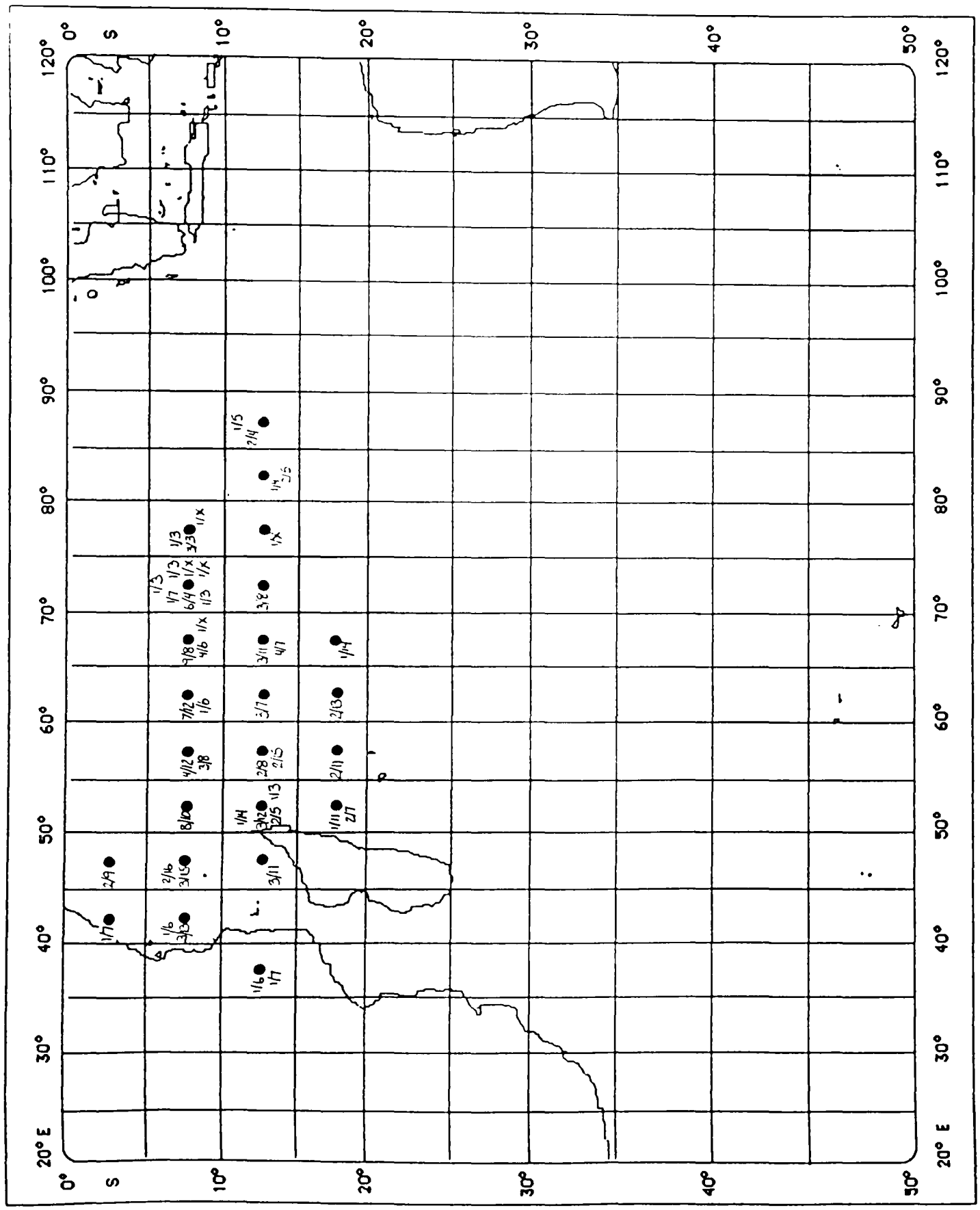

Figure B.4. Translation vectors for the month of October.

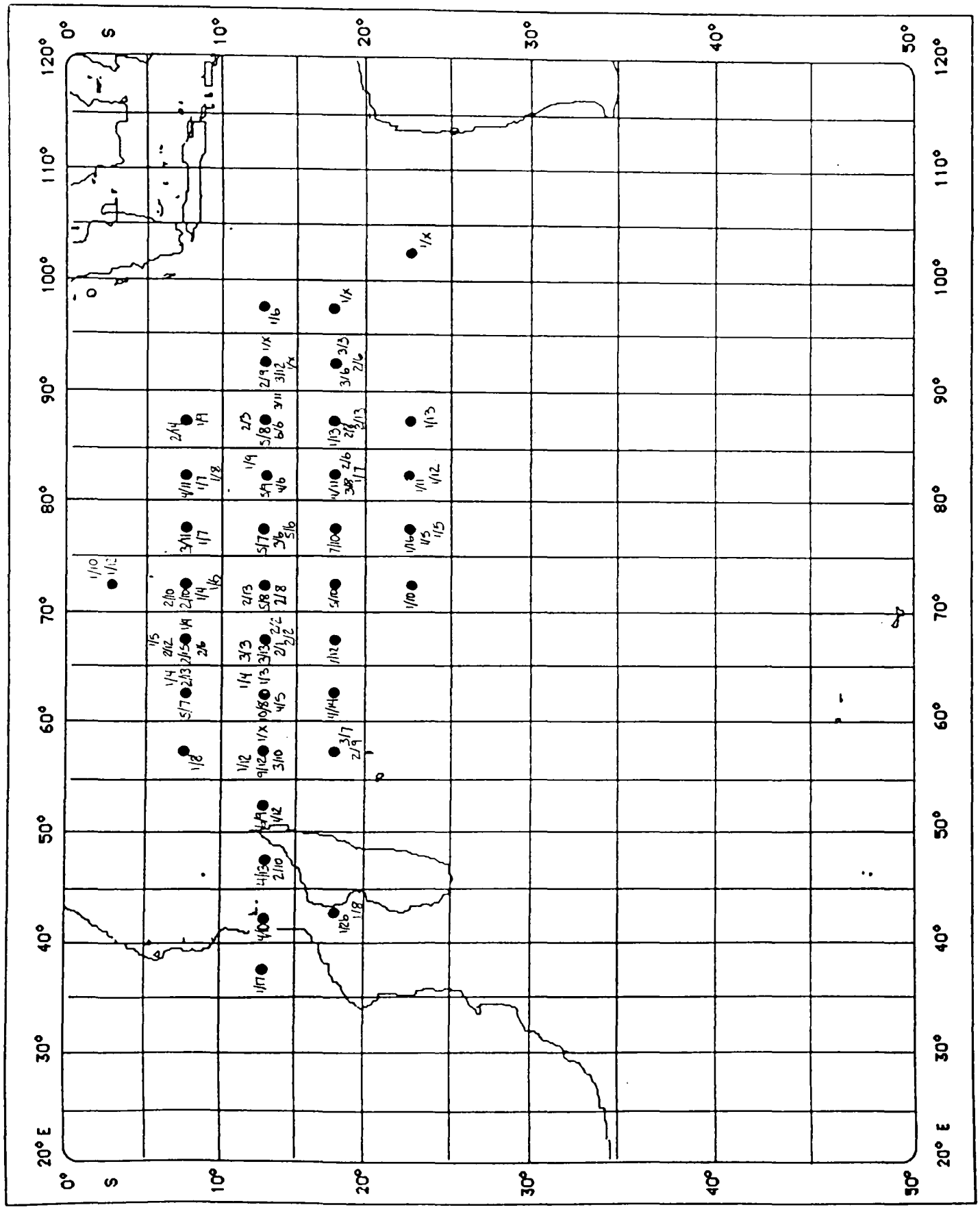

Figure B.5. Translation vectors for the month of November.

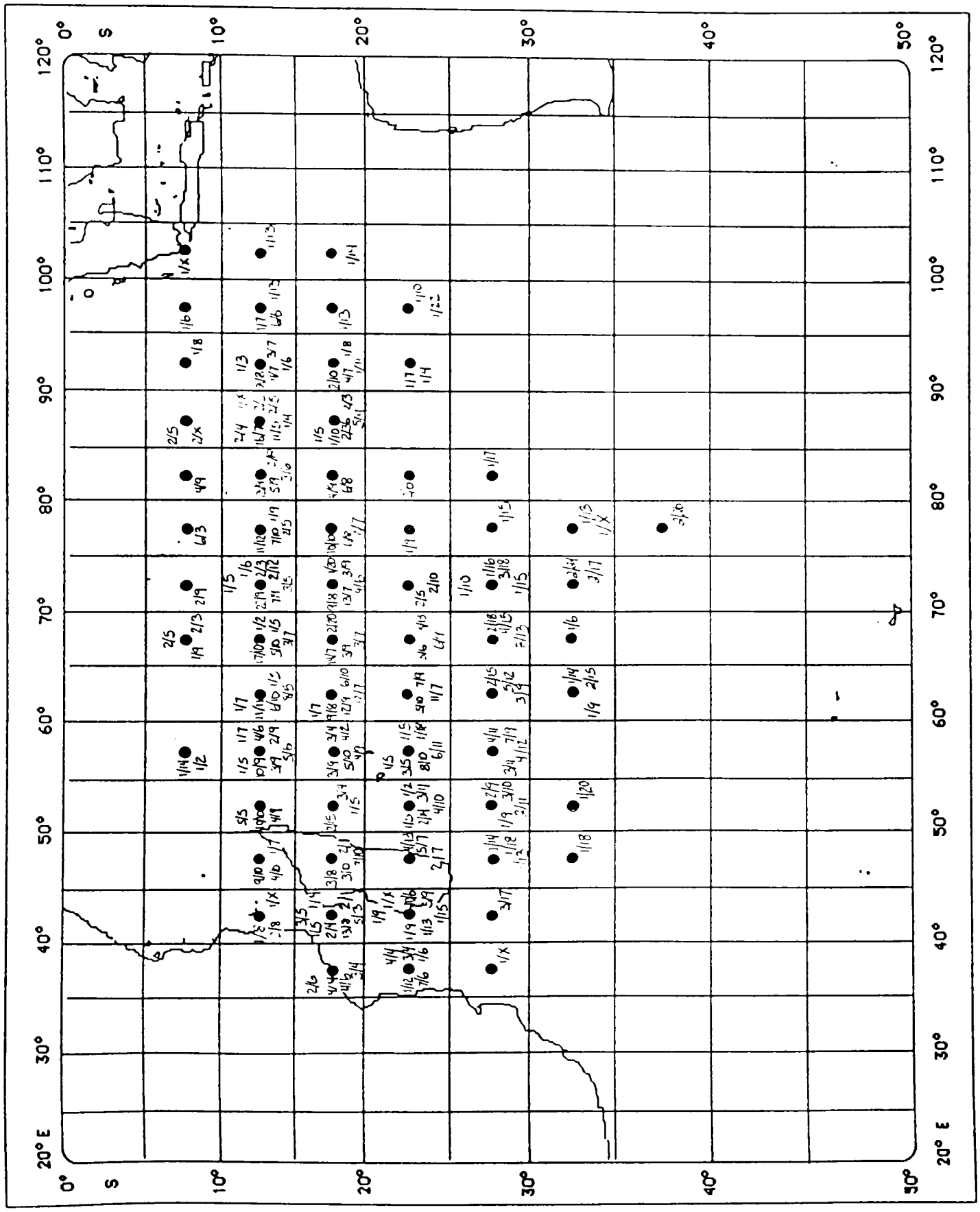

Figure B.6. Translation vectors for the month of December.

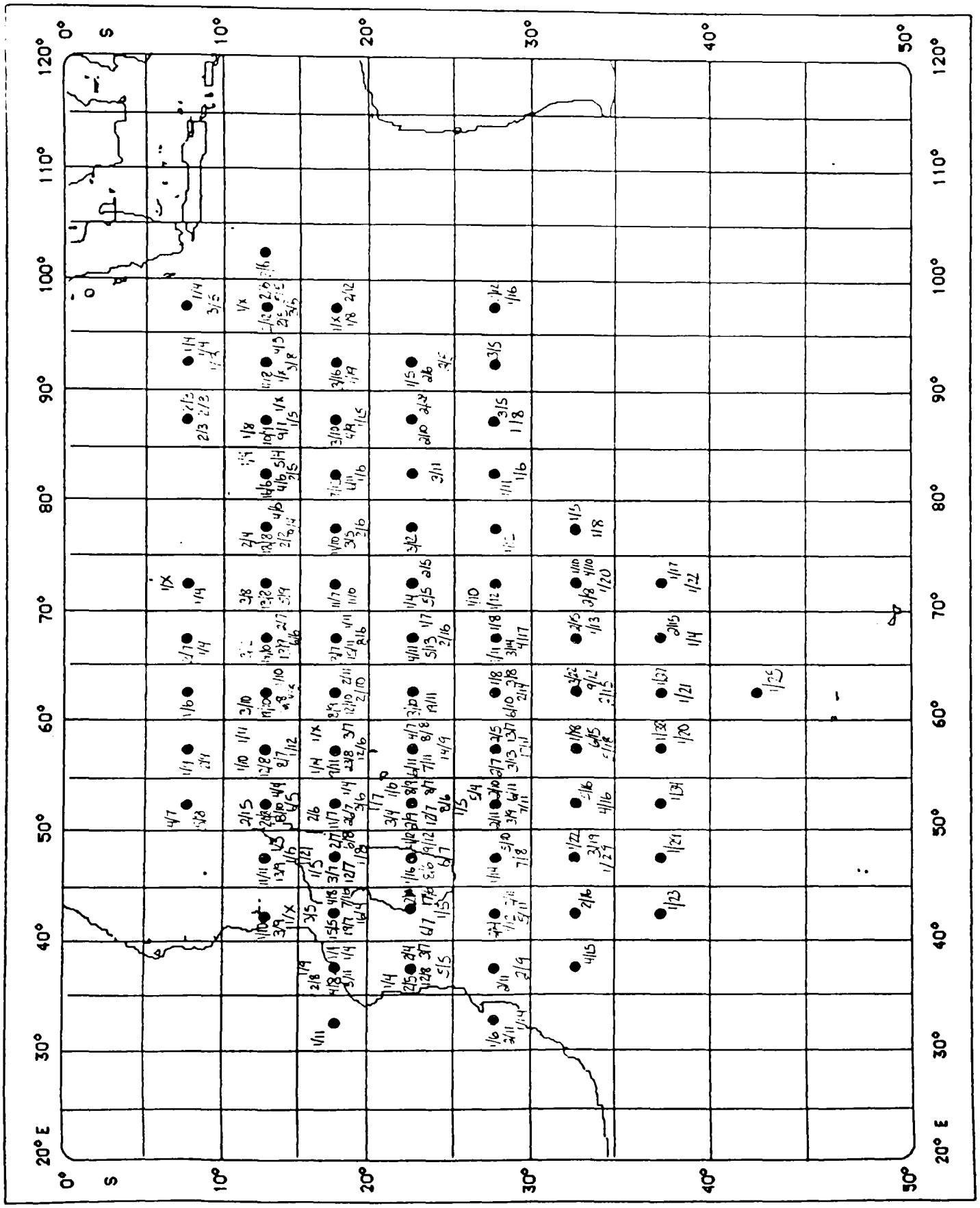

Figure B.7. Translation vectors for the month of January.

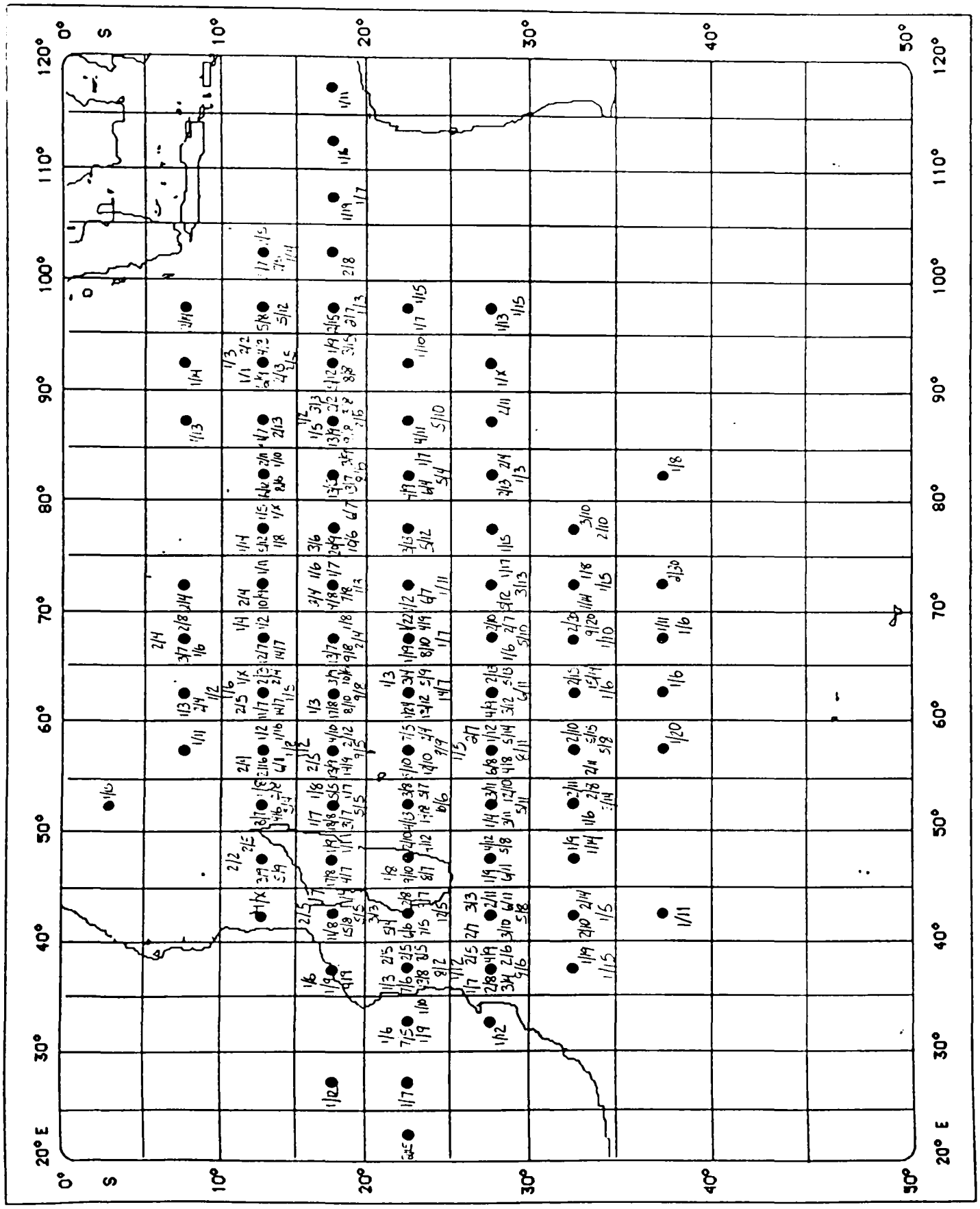

Figure B.8. Translation vectors for the month of February.

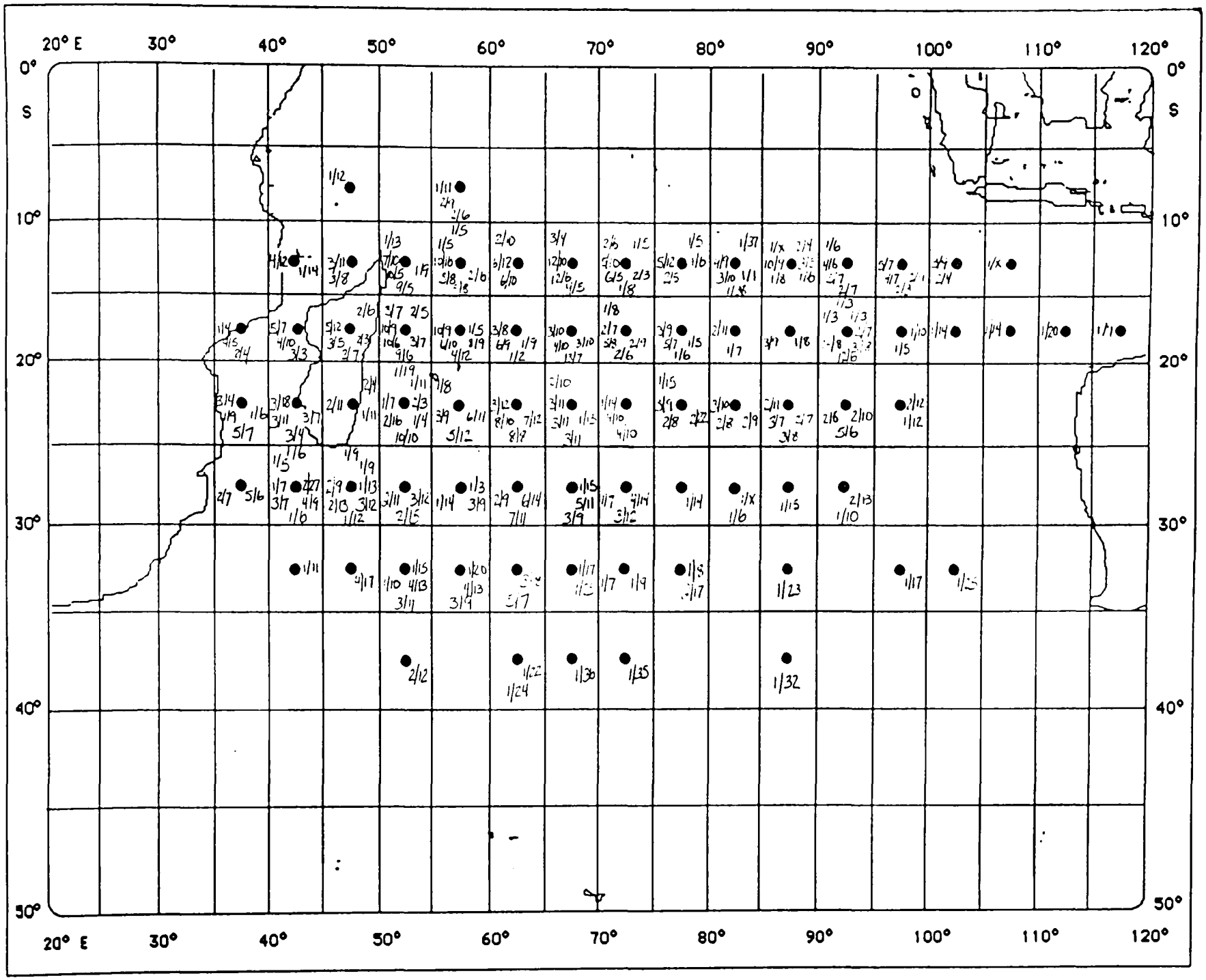

Figure B.9. Translation vectors for the month of March.

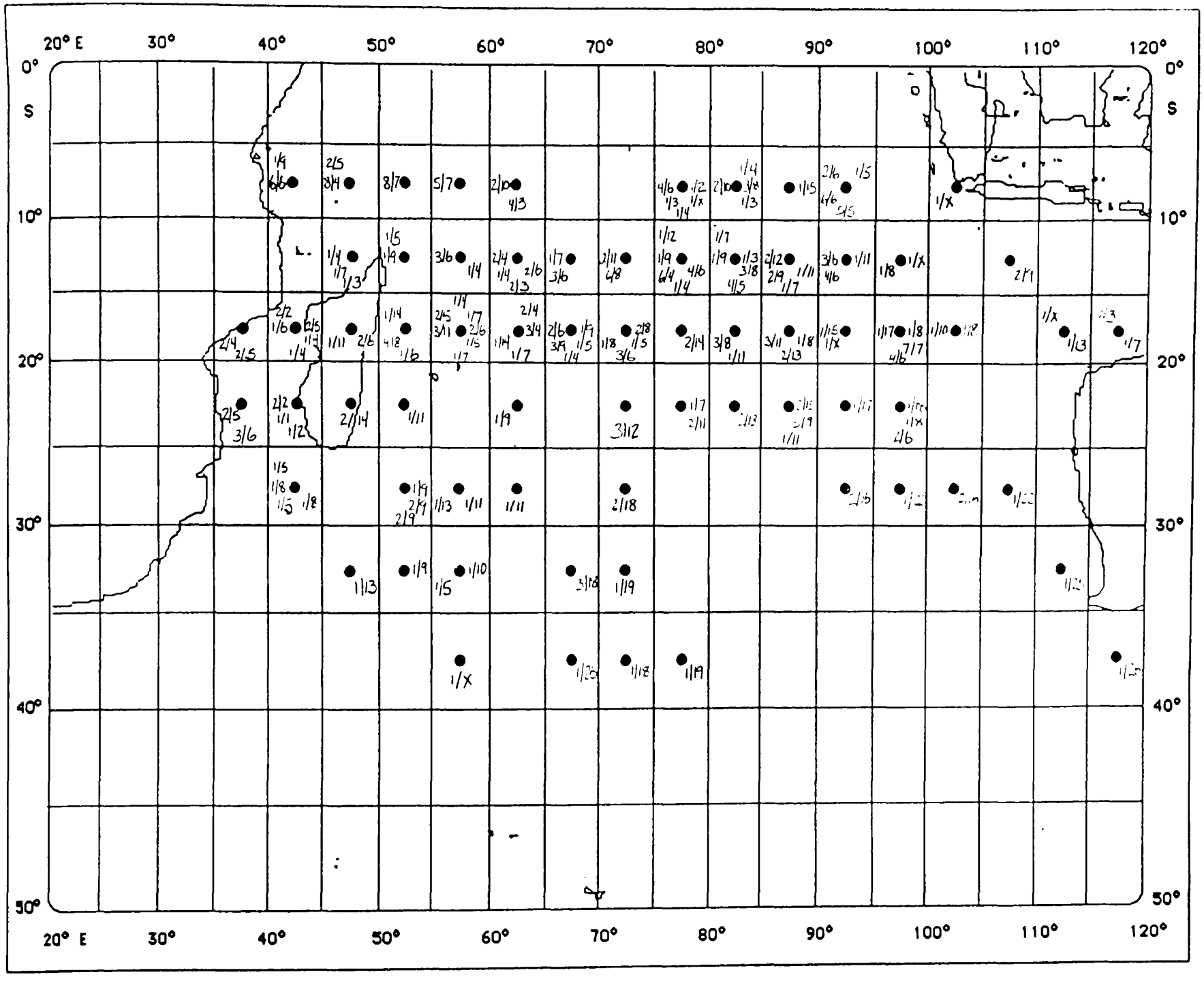

Figure B.10. Translation vectors for the month of April.

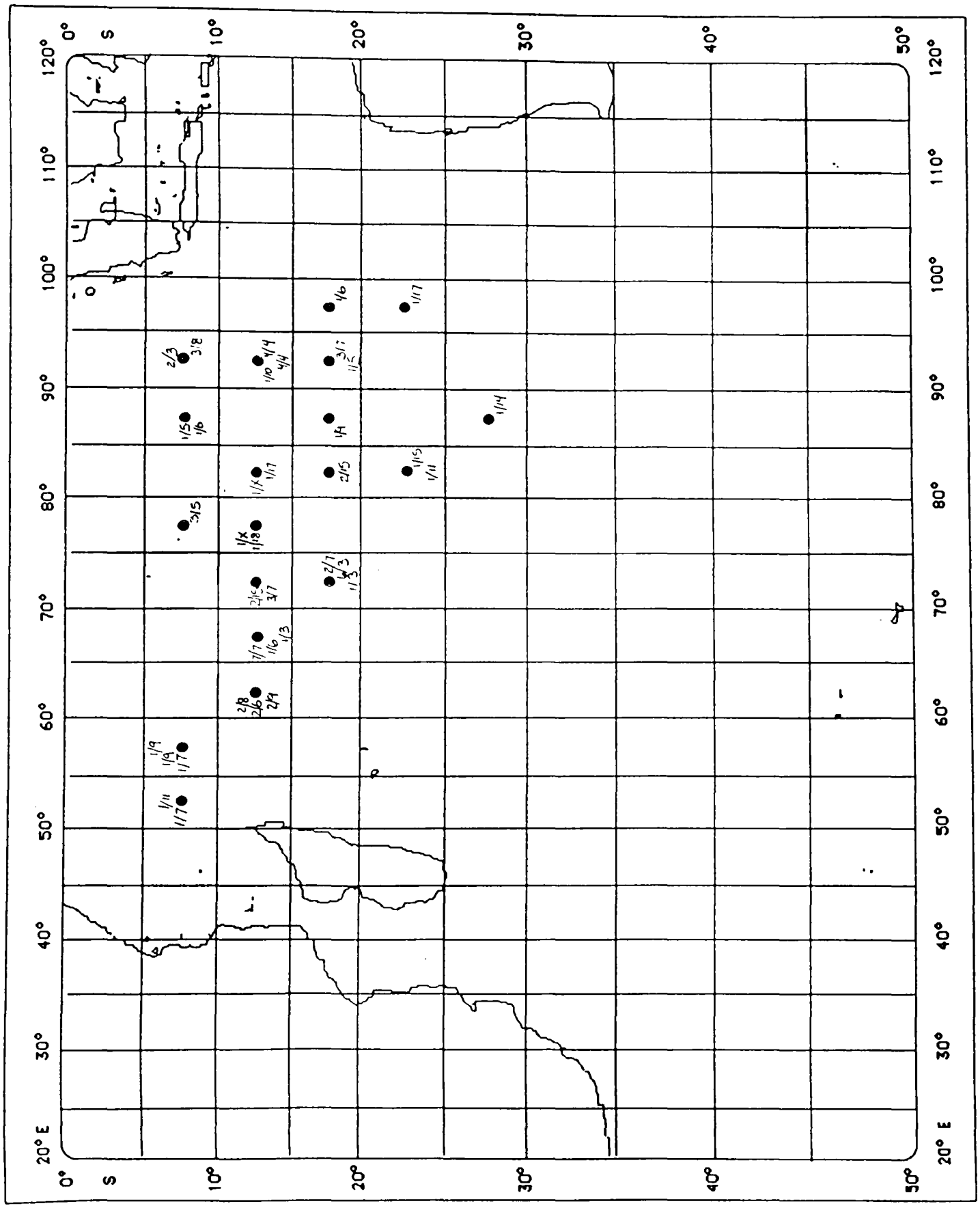

Figure B.11. Translation v

on vectors for the month of May.

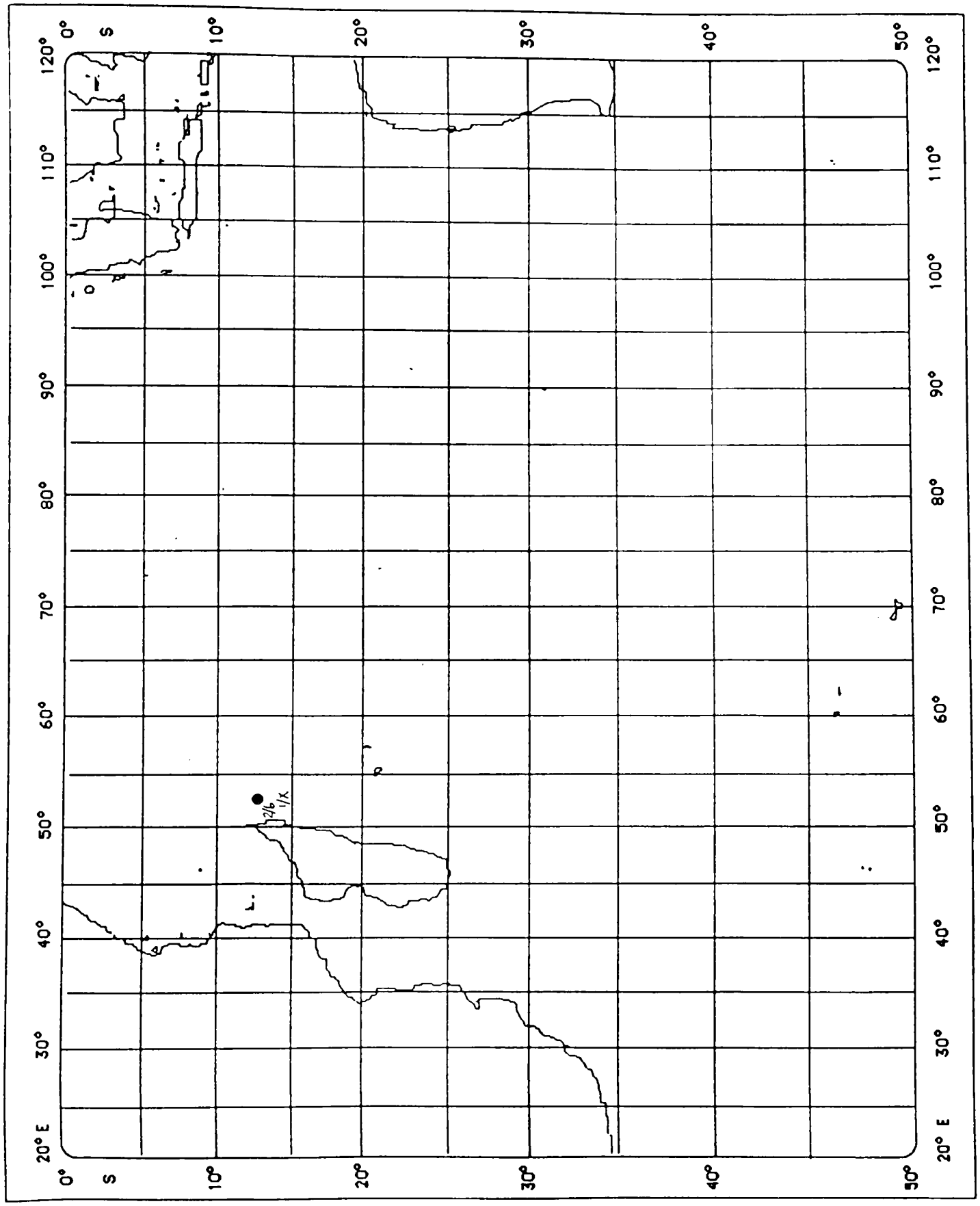

Figure B.12. Translation vectors for the month of June.